Identification and classification of microorganisms based on their fatty acid profiles

Ph.D. dissertation

Huỳnh Thư

Supervisors:
Dr. András Szekeres, senior research fellow
Dr. György Sipos, professor

Doctoral School of Biology
Department of Microbiology
Faculty of Science and Informatics
University of Szeged

2022

Szeged

1. TABLE OF CONTENTS

2. LIST OF ABBREVIATIONS

ACC	acetyl-CoA carboxylase
ACP	acyl carrier protein
AR	antibiotic resistance
AR/HT	area/height ratio
AT	malonyl/acetyl transacylase
ATCC	American Type Culture Collection
BGSC	Bacillus Genetic Stock Center, The Ohio State University, USA
CAS	Chromatographic Analysis System
CDC	Centers for Disease Control and Prevention
DH	dehydratase
DSMZ	German Collection of Microorganisms and Cell Cultures
ECL	equivalent chain length
ED	Euclidean distance
ER	enoyl-reductase
FA	fatty acid
FAME	fatty acid methyl ester
FAS	fatty acid synthase
FID	flame ionization detector
FMN	flavin mononucleotide
FZB	FZB Biotechnik GmbH/ ABiTEP, Berlin
GC	gas chromatography
gyrA	the partial sequences of the genes encoding the subunit A protein of DNA gyrase
KR	ketoreductase
KS	ketosynthase
LAMP	loop-mediated isothermal amplification
LMG	Belgian Coordinated Collections of Microorganisms / LMG Bacteria Collection, Laboratorium voor Microbiologie, Universiteit Gent, Belgium
LPS	lipopolysaccharide
MALDI-TOF	matrix-assisted laser desorption ionization time-of-flight
MEA	malt extract agar
MIDI	MIDI, Inc., Newark, DE, USA
MIS	The MIDI Sherlock® Microbial Identification System
MMC	Montefiore Medical Center

MPT	malonyl/palmitoyl-transacylase
MS	mass spectrometry
MTBE	methyl tert-butyl ether
MUFA	monounsaturated fatty acids
PC	principal component
PCR	polymerase chain reaction
PDA	potato dextrose agar
PGPR	plant growth-promoting rhizobacteria
PPT	phosphopantetheine transferase
PUFA	polyunsaturated fatty acids
QC	quality control
rpoB	the partial sequences of the genes encoding the RNA polymerase beta-subunit
RS	Roth and Show agar
Rt	retention time
SD	standard deviation
SDA	Sabouraud dextrose agar
SFA	saturated fatty acids
SI	similarity index
SZMC	the Szeged Microbiological Collection
TSBA	trypticase soy broth agar
UFA	unsaturated fatty acids

3. INTRODUCTION

In our study, the Sherlock Chromatographic Analysis System (CAS) method using signaling fatty acids (FAs) of 9–24 carbons in length and automated gas chromatography (GC) analysis were developed for certain microorganisms to perform routinely, user-friendly, and fast-automated identification as a taxonomic method. The Sherlock CAS was developed by MIDI with several available Sherlock methods and libraries for microbial identification, but it can be used also for research purposes due to its expandability and flexibility.

Several *Bacillus* species are involved in Sherlock CAS and can be identified using method RTSBA6 and library RTSBA6. During our examinations, 107 isolates were identified out of 128 *Bacillus* strains including 4 strains as *B. atrophaeus*, 6 strains as *B. cereus*, 27 strains as *B. licheniformis*, 39 strains as *B. megaterium*, 4 strains as *B. pumilus*, 5 strains as *B. simplex*, and 18 strains as *B. subtilis*. Next, the identity of the unknown *Bacillus* strains was revealed using the partial sequences of the genes encoding the subunit A protein of DNA gyrase (*gyrA*) and the RNA polymerase beta-subunit (*rpoB*) as *B. endophyticus* (1 strain) and *B. velezensis* (20 strains). Then the fatty acid methyl ester (FAME) profiles of *B. endophyticus* and *B. velezensis* were analyzed and applied as samples (n=3) to develop a new library also containing the representative profiles of these species. Furthermore, the new library was successfully applied for the differentiation between the closely related *B. velezensis* and *B. amyloliquefaciens* species.

Furthermore, a MIDI yeast method was applied to identify yeast species using commercially available libraries. However, these chemotaxonomical libraries have not contained the recently described *Candida auris* species, yet. Thus, using the collection of isolates belonging to this species, a novel library was built for their identification. As a result, the developed method can be applied to classify *C. auris* at both species and clades levels.

There had been no fatty acid-based method and library available regarding *Armillaria* species. Thus, we carried out optimizations on the cultivation conditions, on sample pretreatment steps and then developed a method and a library to the identification of *Armillaria* species, which can classify *Armillaria* isolates at the species level.

By taking advantage of the current knowledge regarding biomarkers, the FA-based identification proved to be applicable for the taxonomic classification and differentiation among microorganisms, even among closely related species. Our study provided a cost-effective, reliable, and fast-automated method for microbial identification.

4. LITERATURE BACKGROUND

4.1. Fatty acid in organisms

Organisms synthesize diverse structural, storage, and signaling fatty acids (FAs) regarding to bio-functions such as building blocks of complex lipids, energy reservoirs, and signaling molecules (Pan, Hu and Yu, 2018). FA profiles are diverse and specific among species and may reflect differences in the biological mechanisms (Rock and Jackowski, 2002; Cronan and Thomas, 2009; De Carvalho and Caramujo, 2018).

4.2.1. Types of fatty acids

A wide range of straight, saturated, unsaturated, branched, hydroxyl, cyclopropane, ω-cyclic, dicarboxylic, and ladderane FAs with chains from 4 to 36 carbon atoms were described (Figure 1) (Cronan and Thomas, 2009; da Costa *et al.*, 2011; Stillwell, 2013). Due to the biosynthesis extended from 2-carbon acetyl-unit cycles, odd-chain FAs are far less abundant compared to even-chains in nature (Stillwell, 2013; Beld *et al.*, 2016).

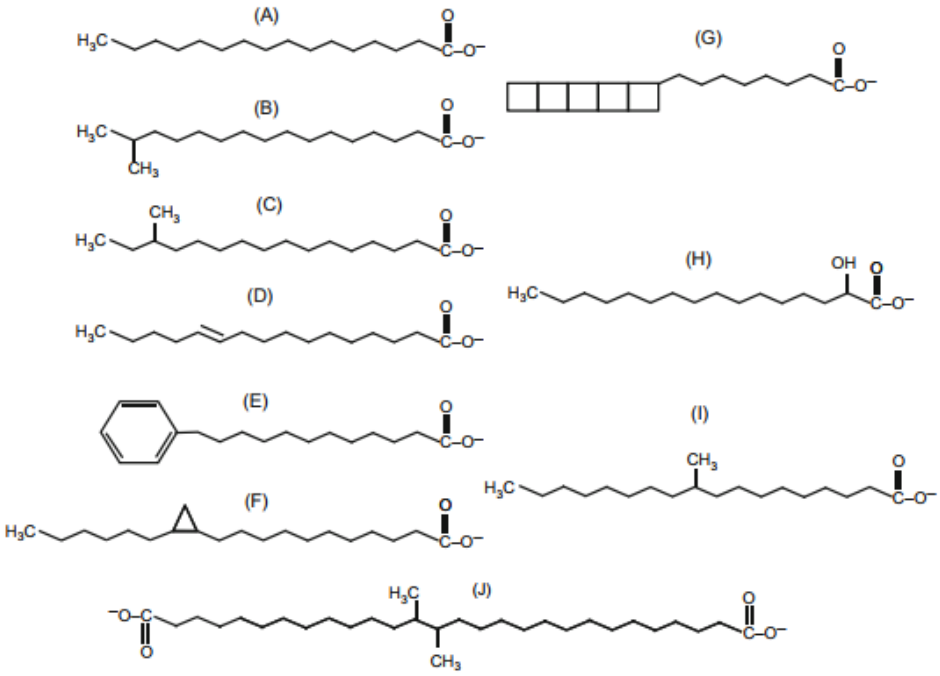

Figure 1. Main types of FAs. (A) straight-chain FA; (B) iso-branched FA; (C) anteiso-branched FA; (D) straight-chain UFA; (E) cyclohexyl FA; (F) cyclopropane FA; (G) ladderane FA; (H) 2-hydroxyl FA; (I) internally branched FA; (J) dicarboxylic FA (da Costa *et al.*, 2011).

Prokaryotes and eukaryotes share similarities to most FAs, except that prokaryotic FAs tend to be slightly shorter and more branched, have different double-bond positions in monoenoic C18 acids, and lack polyunsaturated fatty acids (PUFAs) (Cronan and Thomas, 2009).

4.2.1.1. Straight-chain saturated fatty acid

FAs without double bonds are saturated FAs (SFAs), which are prevented from hydrogenation, halogenation and oxidation (Stillwell, 2013). SFAs are called with the same number of saturated hydrocarbons. For example, the C16:0 represents the palmitic acid with the letter "C" as carbons and the number "16" as the number of carbons in the compound (Stillwell, 2013). SFAs are the primary components of most phospholipids and storage lipids. Short-chain FAs are moderately toxic to microbes, while long-chain FAs like palmitic acid (C16:0) inhibit methanogenesis (Geiger, 2019). The palmitic and myristic acids in eukaryotic cells like yeasts are utilized in directing proteins to and from membranes and organelles by attaching or removing cysteine or glycine residues (Geiger, 2019).

FAs with less than 12 carbon in length have been detected in small amounts including formic (C1:0), acetic (C2:0), propionic (C3:0), butyric (C4:0), valeric (C5:0), caproic (C6:0), enanthic (C7:0), caprylic (C8:0), pelargonic (C9:0) and capric (C10:0) acids. In comparison, the longer FAs constitute a much larger proportion such as lauric (C12:0), myristic (C14:0), palmitic (C16:0), stearic (C18:0), arachidic (C20:0), behenic (C22:0), lignoceric (C24:0), cerotic (C26:0) and montanic (C28:0) acids. No straight-chain SFA longer than C28:0 such as melissic (C30:0), lacceric (C32:0), psyllic (C33:0) and geddic (C34:0) acids have been reported other than in the mycobacteria (O'Leary, 1962; Geiger, 2019).

4.2.1.2. Unsaturated fatty acid

FAs with carbon–carbon double bonds are classified as unsaturated FAs (UFA). UFAs containing a single double bond belong to the monoenoic or monounsaturated FA (MUFA), and containing more than one double bond are revealed as polyenoic or polyunsaturated FA (PUFA) (Stillwell, 2013). There are two isomeric forms including *cis* (Z) and *trans* (E) forms. Most biological UFAs belongto *cis*-form, however, *trans*-forms are well-known as well. For example, bacterial membrane phospholipids contain *trans*-FAs (Geiger, 2019). The low melting point and susceptibility to oxidative degradation of UFAs are essential for a biochemical mechanism such as prevention of membrane oxidation, enhancement of membrane fluidity,

thermal adaptation, and cell growth-stimulating effects (O'Leary, 1962; Stillwell, 2013). Thus, microbes increase the amount of UFA at lower temperatures. However, *Vibrio* and *Colwellia* seem to isomerize *cis*- to *trans*-FAs at higher temperatures (from 5℃ to 20 ℃) (Geiger, 2019). Microbial FAS II produces UFA as major factor of membrane fluidity and function by introducing the *cis*- double bond into the growing acyl chain (Lu, Zhang and Rock, 2004). In addition, PUFAs such as linoleic acid and α-linolenic acid play an important multifunctional role in human nutrition/diet and food science (Geiger, 2019).

Table 1. Nomenclatures of some MUFAs (Geiger, 2019)

Carbon number	Position of unsaturation	Common name
C10	*cis* 10:1, ω1	Caproleic
	cis 10:1, ω6	Obtusilic
C12	*cis* 12:1, ω3	Lauroleic
	cis 12:1, ω7	Denticetic
	cis 12:1, ω8	Linderic
C14	*cis* 14:1, ω5	Myristoleic
	cis 14:1, ω9	Physeteric
C16	*cis* 16:1, ω7	Palmitoleic
	*trans*16:1, ω7	Palmitelaidic
C18	*cis* 18:1, ω7	Asclepic
	trans 18:1, ω7	Vaccenic
	cis 18:1, ω9	Oleic
	trans 18:1, ω9	Elaidic
	cis 18:1, ω12	Petroselinic
	trans 18:1, ω12	Petroselaidic
	cis,*cis*-5,11-octadecadienoic ω7	Ephedric
	cis,*cis*-6,11-octadecadienoic ω7	Cilienic
	cis,*cis*-9,12-octadecadienoic ω6	Linoleic
	trans,*trans*,*cis*-5,9,12-octadecatrienoic ω6	Columbinic
	cis,*cis*,*trans*-8,10,12-octadecatrienoic ω6	α-Calendic
	all-*cis*-8,10,12-octadecatrienoic ω6	β-Calendic
	trans,*cis*,*trans*-8,10,12-octadecatrienoic ω6	Jacaric
	trans,*cis*,*trans*-9,11,13-octadecatrienoic ω5	Punicic
	cis,*trans*,*trans*-9,11,13-octadecatrienoic ω5	α-eleostearic
	all-*trans*-9,11,13-octadecatrienoic ω5	β-eleostearic
	trans,*trans*,*cis*-9,11,13-octadecatrienoic ω5	Catalpic
	all-*cis*-5,9,12-octadecatrienoic ω6	Pinolenic
	all-*cis*-6,9,12-octadecatrienoic ω6	γ-Linolenic
	all-*cis*-9,12,15-octadecatrienoic ω3	α-Linolenic
	all-*trans*-9,12,15-octadecatrienoic ω3	α-Linolenelaidic
	cis,*cis*,*cis*,*trans*-8,10,12,14-octadecatetraenoic ω4	Ixoric
C20	*cis* 20:1, ω7	Paullinic
	cis 20:1, ω9	Gondoic
	cis 20:1, ω11	Gadoleic
C22	*cis* 22:1, ω9	Erucic
C24	*cis* 24:1, ω9	Nervonic aka selacholeic
C26	C26:1, ω9	Ximenic

4.2.1.3. Branched-chain fatty acid

Branched-chain FAs include iso-, anteiso-, and ω- alicyclic FAs with or without unsaturated and hydroxylated modification (Kaneda 1963, 1991). These FAs containing different acyl groups are produced from biosynthesis pathways for branched-chain amino acids, which produces short-chain branched acyl-CoAs as primers for FAS II in place of acetyl-CoA such as iso-butyric, iso-valeric, and 2-methylbutryric acids (Lu, Zhang and Rock, 2004).

4.2.1.4. Other substituted fatty acids

Hydroxy FAs contain hydroxyl functional groups (-OH) at varied positions. However, these are not common in microbial community (MIDI Inc., 2018).

The post-synthesized cyclopropanation can convert FAs to cyclopropane derivatives to protect the reactive double bond from adverse reactions during the stationary phase of bacterial growth. The process reveals a significant energy commitment by cells using S-adenosylmethionine (Rock, 2008).

Dimethyl acetal derivatives are present in anaerobic bacteria as analogs of the FAs. They arise from the ether-linked lipids in plasmalogens (MIDI Inc., 2018).

4.2.2. Fatty acid synthesis

The FA biosynthesis is an energy-intensive and vital mechanism of cell physiology (Rock and Jackowski, 2002). The FAs are synthesized from either exogenous sources or *de novo* synthesis. All higher organisms such as insects, mammals, and fungi possess an enormous integrated and multifunctional enzyme denominated type I fatty acid synthase (FAS I) system. Accordingly, fungi typically employ a fungal type-Ia FAS system (FAS Ia) while the FAS Ib regulates the FA synthesis in animals. Besides, the type II FAS system (FAS II) with a basic set of monofunctional enzymes appears in the majority of prokaryotes and the organelles of prokaryotic descent such as mitochondria and chloroplasts. However, the Gram-positive bacteria producing mycolic acid contain both FAS I with the ability to start *de novo* biosynthesis and an additional FAS II involved in the elongation of medium-chain FAs (Rock and Jackowski, 2002; Schweizer and Hofmann, 2004; Beld *et al.*, 2016; De Carvalho and Caramujo, 2018).

4.2.2.1. The type-Ia fatty acid synthesis

The FAS I is an iterative process with the activation of an acyl carrier protein (ACP) (Figure 2). The multifunctional enzyme complexes are highly integrated involving enormous catalytic reactions as discrete functional domains, either on a single polypeptide chain or two different multi-domain units. The FAS I may be subdivided according to functional domain organization or their subunit stoichiometry. Microbial FAS Ia is hexamers with domain sequences of ac(et)yltransferase (AC)- enoyl-reductase (ER)- dehydratase (DH)- malonyl/acetyl- or malonyl/palmitoyl-transacylase (AT, MPT)/ACP- ketoacyl reductase (KR)- ketoacyl synthase (KS) forming either $\alpha_6\beta_6$ (fungi) or α_6 (bacteria) oligomers (Schweizer and Hofmann, 2004; Geiger, 2019; Singh *et al.*, 2020).

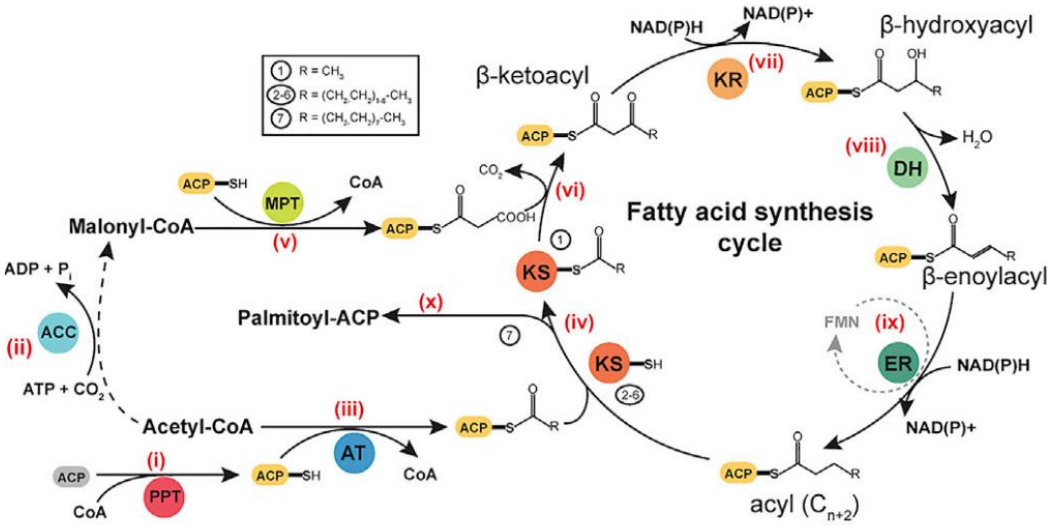

Figure 2. The FAS I biosynthesis cycle of FAs. (i) The iterative process requires the activation of ACP by phosphopantetheine transferase (PPT). (ii) Malonyl-CoA is synthesized from acetyl-CoA and CO_2 by acetyl-CoA carboxylase (ACC). (iii) The first two carbon atoms of the FA chain originating from acetyl-CoA are elongated using malonyl-CoA (v) through KS (iv and vi), KR (vii), DH (viii), and ER (ix) activities (Singh *et al.*, 2020).

The FAS I is initiated when AT/MPT transfers acetyl moiety of acetyl-CoA/ malonyl-moiety of malonyl-CoA to ACP, respectively, prior to transferring to the active cysteine site of the condensing KS. KS catalyzes the decarboxylative Claisen condensation of the acetyl and malonyl groups to yield a β-ketoacyl intermediate bound to the ACP. Subsequently, β-ketoacyl intermediate is modified following reduction of the β-keto- to the β-hydroxyacyl intermediate by the NADPH-dependent KR, dehydration of β-hydroxyacyl enzyme to 2,3-trans-enoate by

DH, and reduction of enoate to the saturated acyl-enzyme by an FMN-containing NADPH-dependent ER to result a fully saturated acyl intermediate elongated by two carbon atoms. Then, the intermediate is revealed as an initial substrate for the next cycle. The iterative elongation is terminated after seven or eight cycles by removing the product either by transesterification to an appropriate acceptor or hydrolyzing with palmitoyl transferase and thioesterase (Schweizer and Hofmann, 2004; Herbst, Townsend and Maier, 2018).

4.2.2.2. The type-II fatty acid synthesis

The FAS II is composed of a highly conserved collection of monofunctional enzymes for the initiation and elongation involving the condensation, dehydration, and reduction stepwise of acyl chains (Figure 3). The central feature is covalently connected with an acidic and low molecular weight protein ACP, which is responsible for all of the intermediates as thioesters (Lu, Zhang and Rock, 2004; Cronan and Thomas, 2009; Geiger, 2019).

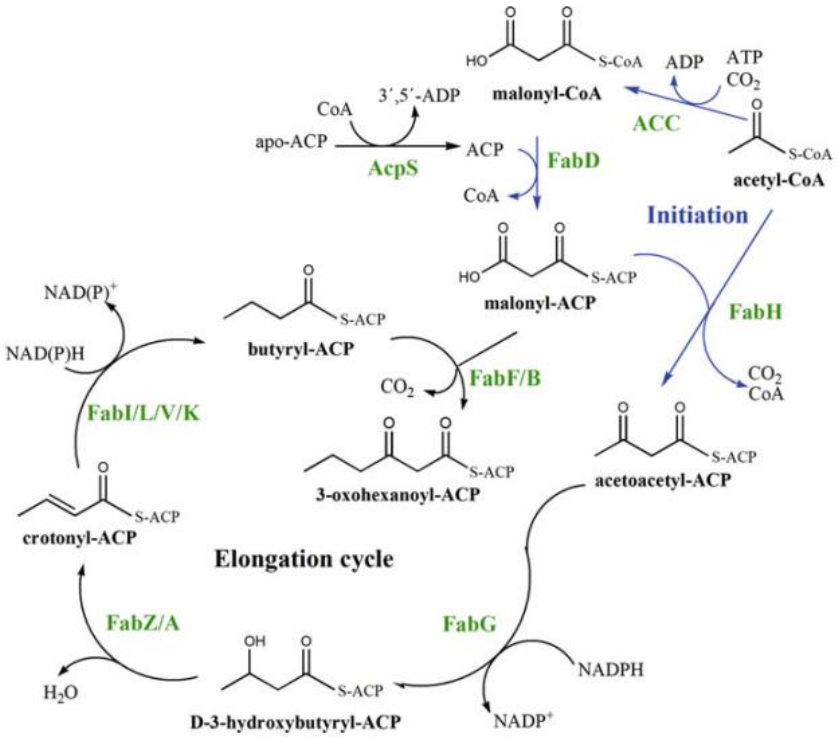

Figure 3. The FAS II biosynthesis pathway (Geiger, 2019).

The initiation step begins at the acetyl-CoA carboxylase with three known pathways (Rock and Jackowski, 2002; Lu, Zhang and Rock, 2004; Schujman and de Mendoza, 2008;

Cronan and Thomas, 2009). The pathway 1: The condensation of acetyl-CoA with malonyl-ACP is regulated by FabH (β-ketoacyl-ACP synthase III) to yield acetoacetyl-ACP (Figure 4). The pathway 2: The acetate moiety is transferred from acetyl-CoA to acetyl-ACP by FabH. Subsequently, the acetyl-ACP is condensed with malonyl-ACP by FabB (synthase I) or altered by FabF (synthase II). The pathway 3: The decarboxylation of malonyl-ACP is catalyzed by FabH, FabB or FabF to form acetyl-ACP followed by subsequent condensation with malonyl-ACP.

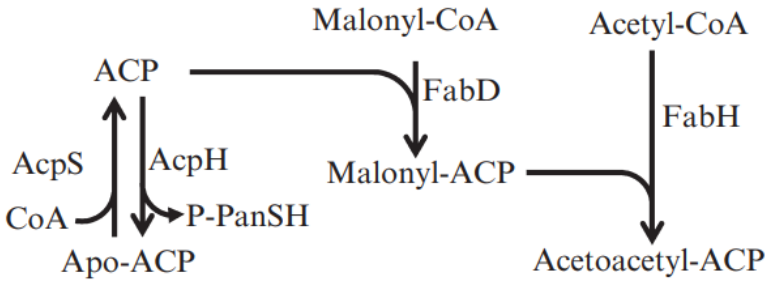

Figure 4. The initiation of FAS II pathway in *E. coli* (Cronan and Thomas, 2009).

The elongation cycle is initiated by the Claisen condensation of malonyl-ACP with acetyl-CoA regulated by a β-ketoacyl-ACP synthase (FabB and FabF) to form β-keto-butyryl-ACP (Figure 5).

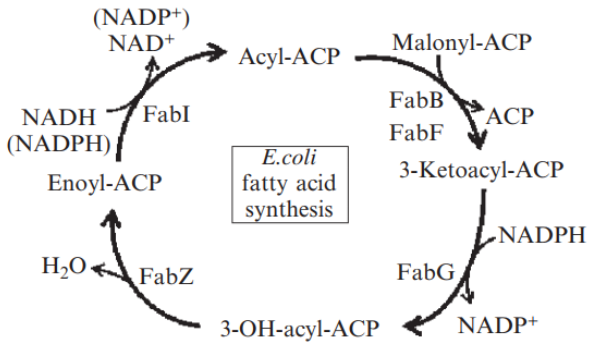

Figure 5. The reactions of FA elongation cycle in FAS II (Cronan and Thomas, 2009).

Each cycle involves a condensation, a first reduction, a dehydration, and a second reduction step that elongates the fatty acyl-ACP by two carbon units until a 16/18- carbon chain SFA. The first step is initiated by NADPH-dependent reduction of β-ketoacyl-ACP to β-hydroxyacyl-ACP by β-ketoacyl-ACP reductase (FabG), followed by the dehydration of the β-

oxoacyl-ACP to yield trans-2-enoyl-ACP catalyzed by either β-hydroxydecanoyl-ACP dehydratase/isomerase (FabA) or β-hydroxyacyl-ACP dehydratase (FabZ). The final step is the NAD(P)H-dependent reduction of the double bond in the trans-2-enoyl-ACP intermediate by an enoyl-ACP reductase (enoyl-ACP reductase I (FabI), enoyl-ACP reductase II (FabK), or enoyl-ACP reductase III (FabL)) to form an acyl-ACP, which can serve as a substrate for next elongation step or transfer into complex lipids if containing sufficient chain length. Either FabB or FabF can catalyze the next elongation cycles by condensation of malonyl-ACP with the acyl-ACP (Rock and Jackowski, 2002; Lu, Zhang and Rock, 2004; Cronan and Thomas, 2009; De Carvalho and Caramujo, 2018; Geiger, 2019).

Each isozyme plays unique roles based on substrates in the pathway. Most bacteria contain two β-ketoacyl-ACP synthases and two β-hydroxyacyl-ACP dehydratases. Besides, three β-ketoacyl-ACP synthases can be utilized for synthesizing branched-chain FAs. The scheme terminates in transferring the acyl chains of the acyl-ACP products to a glycerol-based backbone molecule by various acyltransferase systems (Lu, Zhang and Rock, 2004; Cronan and Thomas, 2009).

4.2.3. Fatty acids as biomarkers

The FAS II pathway is conserved in microbes, but different substrate specificity of enzymes leads to the diverse FAs in distinct genera. In addition, genomic analyses in bacteria have shown the lack of a homolog of the *plsB* gene (regarding a membrane-bound glycerol-phosphate acyltransferase at the first position), suggesting that an alternative biochemical step occurs for the attachment of the first FA (Schujman and de Mendoza, 2008). Thus, bacteria possess genetically conserved in different ecological niches during long periods (Kunitsky, Gerard and Sasser, 2006) and alternative mechanisms for FA biosynthesis and regulation (Schujman and de Mendoza, 2008).

The bacterial FAS system lacks polyunsaturation, makes branched chains, and has different double-bond positions at monoenoic C18 acids causing shorter FA chains (Cronan and Thomas, 2009). However, some bacteria contain branched-chain FAs instead of β-hydroxyacyl acids (Cronan and Thomas, 2009). On the other hand, bacteria containing methyl-end desaturases for their *de novo* synthesis have been considered as natural ω3 long-chain (≥ 20 carbons) polyunsaturated FA producers (De Carvalho and Caramujo, 2018). The marine bacteria can produce long-chain PUFAs, while most of others cannot (De Carvalho and Caramujo, 2018). *Mycobacterium tuberculosis* possesses FAS II producing very-long-chain mycolic acids (Lu, Zhang and Rock, 2004; Váradi *et al.*, 2021). *Geodia hentscheli*, *G. parva*,

G. atlantica, *G. barretti*, and *Stelletta rhaphidiophora* from boreal and Arctic sponge in the North Atlantic Ocean contain particularly distinct FA compositions with high amounts of isomeric mixtures of mid- and branched-chain, long- and linear- chain, mid- and branched-UFAs with 24–28 carbons in length and typical unsaturation as chemotaxonomic and ecological biomarkers (de Kluijver *et al.*, 2021). Sulphate-reducing bacteria accumulate 17:1 ω8 and 17:1 ω5 as biomarkers (Willers, Jansen van Rensburg and Claassens, 2015). Besides, bacteria may produce membrane ether FAs and archaea may produce non-ether FAs (De Carvalho and Caramujo, 2018). Methyl-branched FAs have been revealed as biomarkers of Actinomycetes (Willers, Jansen van Rensburg and Claassens, 2015). *Streptomyces coelicolor* contains at least five different FabH enzymes for producing diverse unusual FAs (Beld *et al.*, 2016).

Moreover, Gram-positive, and Gram-negative bacteria show a marked difference in cell-wall FA content. Gram-negative cell walls, which be composed of lipoprotein and LPS complexes contain between 10 to 20% lipid, but those are a few in Gram-positive bacteria (O'Leary, 1962). Besides, FabH is related to straight-chain FAs in Gram-negative bacteria, but larger branched-chain FAs in Gram-positive bacteria are based on substrates (Li *et al.*, 2010). Thus, branched-chain FAs including iso- and anteiso- C15:0 and C17:0 along with C18:0 are predominant in many Gram-positive bacteria, while Gram-negative bacteria are significantly composed of straight-chain and hydroxy FAs (Kunitsky, Gerard and Sasser, 2006). As reported, the methyl-branched chain FAs were only detected in *B. subtilis* and not in *E. coli* or *Francisella novicida*. Conversely, 3-hydroxyl FA was only detected in *E. coli* and *F. novicida*, but not in *B. subtilis*. Besides, their saturated and unsaturated FAs were discriminated by chain lengths and distribution patterns. Consequently, branched-chain and hydroxyl FAs have been revealed as taxonomic indicators for the differentiation between Gram-negative and Gram-positive bacteria (Lu, Zhang and Rock, 2004; Li *et al.*, 2010). The presence of LPS, as well as hydroxy FAs, indicates Gram-negative bacteria whereas the absence of those indicates Gram-positive bacteria (Kunitsky, Gerard and Sasser, 2006).

On the other hand, FA profiles cannot be significantly applied as taxonomic biomarkers at the species level in eukaryotes. However, the particular FAs are often considered as characteristics of algal classes and some other organisms (De Carvalho and Caramujo, 2018). The alternative pathways with varied FA products were reported among different evolutionary microorganisms such as the facultatively anaerobic intestinal bacterium *E. coli*, photosynthetic freshwater cyanobacterium *Synechocystis*, photosynthetic green algae *Chlamydomonas reinhardtii*, and diatom *Thalassiosira pseudonana* (Beld *et al.*, 2016). The bacterium *E. coli*, green microalga *C. reinhardtii*, and diatom *T. pseudonana* can produce longer FAs from short-

chain precursors (C3 and C5), while cyanobacterium *Synechocystis* can incorporate and elongate longer chain FAs due to acyl–acyl carrier protein synthetase (AasS) activity (Beld *et al.*, 2016). The polyphyletic microbes as green microalgae accumulate C16-18 FAs, whereas heterokonts such as eustigmatophytes and diatoms contain C18 FAs as minor components that are largely replaced by C20 (or C22) FAs (Geiger, 2019). As regards, green algae and cyanobacteria producing more 18:3 ω3, whilst diatoms produced more 20:5 ω3 and 22:6 ω3 and also 16:2 ω4 and 16:3 ω4 (De Carvalho and Caramujo, 2014). The specific FAs were investigated in microalgae such as 18:5 ω3 in Dinophyceae and Haptophyta I; 16:2 ω4, 16:3 ω4, 16:4 ω1 and 20:5 ω3 in Bacillariophyceae; 16:3 ω3, 16:4 ω3, and 18:3 ω3 in Chlorophyta; a high proportion of 18:1 ω9 and 18:2 ω6 and lack of long-chain PUFAs in Cyanobacteria (De Carvalho and Caramujo, 2018). The freshwater heterotrophic protists contain high amounts of ω6 FAs, while marine ciliates and freshwater algivorous heterotrophic protists contain high levels of ω3 FAs (De Carvalho and Caramujo, 2018). *Mucor circinelloides* contains 15–36% of lipid with mostly long-chain FAs in its cell dry weight (Hussain *et al.*, 2020). The C15:0 iso and anteiso are significantly presented in Firmicutes and Actinobacteria but not present in either Proteobacteria or fungi and algae. Higher amounts of 18:1ω9c were detected in Ascomycetes and Zygomycetes while Basidiomycetes contain larger quantities of 18:2 ω6c (De Carvalho and Caramujo, 2014; Willers, Jansen van Rensburg and Claassens, 2015).

The diversity and specificity of FA and their ratios have been used to derive taxa compositions in prokaryotes or even in some eukaryotes. FAs can be used as chemotaxonomic biomarkers to distinguish many closely related species (O'Leary, 1962; da Costa *et al.*, 2011). The referenced biomarkers were revealed in Table S1 (Appendix). For illustration, *Bacillus* species shared the high rDNA similarity causing taxonomic problems, which can be solved by the application of FA profiles (De Carvalho and Caramujo, 2018). FA profiles and their relative proportion as taxa markers were investigated to understand the high diversity of the microbial community of Mediterranean temporary ponds (De Carvalho and Caramujo, 2014). By analyzing the ratio between fungal and bacterial FA biomarkers, that fluctuations in this ratio have been associated with environmental effects and shifts in soil microbial communities could be understandable. In addition, the ratio between Gram-positive bacteria and Gram-negative bacteria has been indicated by relative FA markers (Willers, Jansen van Rensburg and Claassens, 2015). The 16:1 ω5c has been revealed as biomarkers of arbuscular mycorrhizal fungi, while saprotrophic fungal biomarkers include 18:2 ω6c, 18:3 ω6c and 18:2 ω9c. The discrimination in the range of FA biomarkers has been employed to indicate saprotrophic and ectomycorrhizal fungi (Willers, Jansen van Rensburg and Claassens, 2015). Cyanobacteria and

diatoms use MUFAs such as16:1 ω7c, 18:1 ω7c, 18:1 ω9c, and PUFAs such as 18:2 ω6c, 18:3 ω6c, 16:2 ω4, 16:2 ω6, 16:2 ω7, 16:3 ω3, 16:3 ω4, 16:4 ω3, 16:4 ω1, 18:4 ω3, 18:5 ω3, 20:4 ω6, 20:5 ω3, 22:5 ω3, 22:6 ω3 as signature biomarkers (Willers, Jansen van Rensburg and Claassens, 2015).

Besides, oxygen supply, pH, growth conditions, the phase of growth, medium components, and relative proportions of nutrient substances present in the medium can affect FA composition (da Costa *et al.*, 2011; Bajerski, Wagner and Mangelsdorf, 2017). For example, supplementation with thia-FAs altered FA profiles in bacteria, cyanobacteria, green microalgae, and diatoms based on the location of the sulfur in the chain (Beld *et al.*, 2016). Several FA used as biomarkers of certain taxa may be investigated in other organisms. The cyclopropyl FA such as cyclo17:0 and cyclo19:0 interrelated to anaerobic bacteria can also be presented in older cells of Gram-negative bacteria, which can convert 16:1 ω7c and 18:1 ω7c to, respectively, cyclo17:0 and cyclo19:0 as shifting from exponential to stationary growth phase (De Carvalho and Caramujo, 2014, 2018). Thus, the optimized cultivation conditions have strengthened the accuracy of identification by cellular FA profiles (De Carvalho and Caramujo, 2018).

4.3. Introduction of the Sherlock system for microbial identification

The study was using the Sherlock Chromatographic Analysis System (CAS), developed and marketed by MIDI, Inc., Newark, DE, USA (MIDI) for analyzing whole-cell FAs (MIDI Inc., 2018). The method using FAs 9-24 carbons in length and automated GC analysis analyzes qualitatively and quantitatively whole-cell FAMEs. FA profiles were automatically assessed by GC including a comparison of the peak retention times (RT) and the equivalent chain length (ECL) of samples with those of known standards. For identification, FA profiles are compared to available libraries in the system. The Sherlock CAS can identify a wide range of microorganisms in many areas. The FAME profiles, which have allowed for the creation of very large microbial libraries are unique amongst microbes (MIDI Inc., 2018).

4.3.1. The Sherlock software and GC system

Gas chromatography (GC) consisting of a flow control section, a sample injection port, a column, a column oven, and a detector is widely used to analyze multi-components in samples. The GC method is revealed as a sensitive, rapid and precise, and good reproducible analysis in many fields (Tang and Row, 2013; Shimadzu, 2020; Sugita and Sato, 2021). A GC

system includes gas suppliers involving carrier gases, which is hydrogen (H_2) in the case of Sherlock CAS accommodating a constant flow rate to the sample, and a detector-supporting gas for the flame ionization detector (FID). The sample injection port introduces samples to the system. Part of the system is a capillary column, which is connected between the injection port and the detector to separate components of samples. The introduced samples instantaneously vaporize and flow through the column in the stationary phase with the carrier gas. At the end of the system, after the separation, the detector converts the sample components eluted from the column to electrical signals and sends them to a computer, which analyzes the signals. After the data processing, the analyzed compounds are identified qualitatively and quantitively.

Table 2. Sherlock libraries and methods (MIDI Inc., 2018)

Package	Library	Method(s)	Description
AEROBE	TSBA6	TSBA6	Aerobes, 28 °C, 24 hours, on TSBA
	RTSBA6	RTSBA6	
	ETSA1	ETSA1	Environmental aerobes, 30 °C, 24 hours, on TSA
	ITSA1	ITSA1	
	CLIN6	CLIN6	Clinical Aerobes, 35 °C, 24 hours, on Blood Agar, Chocolate, etc.
	RCLIN6	RCLIN6	
	EBA1	EBA1	
	IBA1	IBA1	
	BTR3	BTR3	Bioterrorism Clinical Aerobes, 35 °C, 24 hours, on Blood Agar, Chocolate, etc.
	RBTR3	RBTR3	
	M17H10	MYCO6 SMYCO6	Mycobacteria, 35 °C, 5-10% CO_2, on Middlebrook 7H10 Agar with OADC enrichment
	IMYC1	IMYC1	
	IR2A1	IR2A1	Water/stressed organisms, 30 °C, 24 hours, on R2A.
ANAEROBE	BHIBLA	ANAER6 SAENER6	Anaerobes, 35 °C, 48 hours, on BHIBLA plates in Gas Packs
	MOORE6	MOORE6 SMOORE6	VPI Broth-grown Anaerobe Library, 35 °C, in PYG Broth
YEAST	YST28	YEAST6 SYEAST6	Yeasts, 28 °C, 24 hours, SAB Dextrose Agar
	YSTCLN	YSTCLN6 SYSTCLN6	Yeasts, 28 °C, 24 hours, SAB Dextrose Agar
	ITY1	ITY1	Yeasts, 30 °C, 24 hours, TSA
	FUNGI	FUNGI6 SFUNGI6	Fungi, 28 °C, 2-5 days, in SAB Dextrose Broth, 150 RPM shake culture
	ACTIN1	ACTIN6 SACTIN6	Actinomycetes, 28 °C, 3-10 days, in TSB, 150 RPM shake culture
Fatty Acid Profiling		PLFAD2	Phospholipid Fatty Acids from soil (PLFA)
		MARINE1	Fatty acids from marine sources

The Sherlock CAS Software, qualified by MIDI, Inc., operated on Shimadzu's GC-2010/2030 platform together with Shimadzu's LabSolutions software. The composition of whole-cell FAs was determined by the Sherlock CAS Software ver. 6.4 (Microbial ID Inc., USA) operating through the LabSolution ver. 5.97 software (Shimadzu, Japan) on a Nexera

GC-2030 gas chromatograph (Shimadzu, Japan) equipped with an AOC-20i Plus autoinjector (Shimadzu, Japan) and a HP-Ultra 2, 25 m x 0.2 mm x 0.33 μm thickness fused silica capillary column (Agilent, USA).

4.3.2. Sherlock standard methods and libraries

The MIS established several databases for different types of organisms such as anaerobic bacteria, aerobic bacteria, and fungi (MIDI Inc., 2018). The current CAS libraries have over 1,800 species of bacteria, 200 species of yeasts, and 60 species of fungi. Each strain grown a certain medium and temperature possesses a unique FA profile allowing their identification (Table 2).

Each library entry is computer-generated from the well-characterized strains of each species or subspecies group of organisms with an appropriate method. Each method is generated involving analytical parameters for chromatographic analysis and calibration as well as the peak naming for individual FAs with Standard, Rapid (R), Sensitive (S), and Instant (I). Accordingly, Standard methods are the older form used by the Sherlock system for many years. Recent improvement in chromatographic equipment has allowed the development of R methods, which are equivalent in identification ability to standard method but run approximately three times faster and are twice as sensitive.

4.3.3. Overview of the Sherlock operation

The general Sherlock MIS procedure (MIDI Inc., 2018) contains (i) the cultivation of microbes on appropriate medium and incubation conditions, (ii) harvest and extraction of cell mass to collect whole-cell FAMEs, which (iii) are served as samples to the GC processing.

A batch of samples is run by the GC associated with calibration and QC. When a batch is started, the sample's method is downloaded to the LabSolutions software with GC parameters. Then, the automatic sampler commands the injector to inject a small portion of the extract into the GC, calibration is run at the beginning of the batch and at intervals throughout the batch. A capillary column installed in the GC oven separates FAME compositions through the column to the detector. The FID burns the FAMEs, creating proportional signals that are stored in LabSolutions. When the run is complete, the RT, response, and area/height ratio (AR/HT) of each peak are calculated by the LabSolutions software and transmitted to Sherlock for further processing. Peaks in the chromatogram are identified by fatty acid ECL value and name. When peak naming is complete, Sherlock searches the library associated with the method

to identify the microorganism. The library search uses both the peak name and the peak percent to match with known profiles stored in the library. Following the library search, the computer prints the Composition Report (Figure 6).

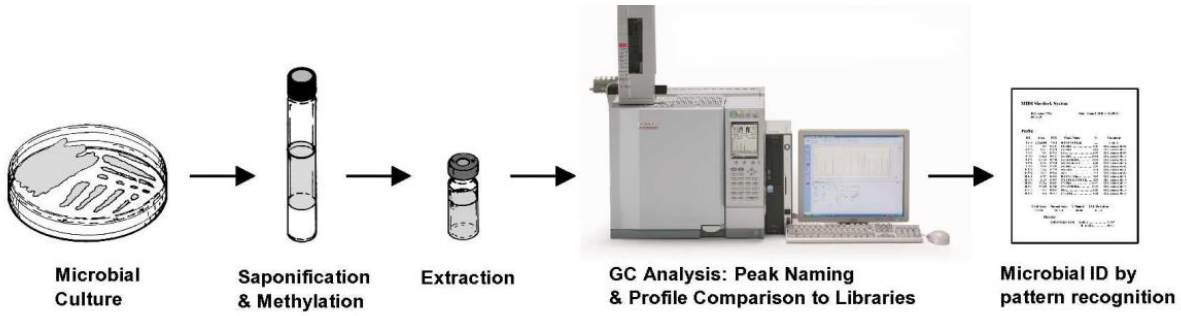

Figure 6. The Sherlock CAS process (Kunitsky, Gerard and Sasser, 2006).

4.3.4. Interpreting Sherlock reports

After being run and analyzed by Sherlock, the composition report which includes the peak naming, the library classification results, and the chromatogram is exported (MIDI Inc., 2018). Accordingly, the general sample information contains data location, batch, and operator information, as well as the creation date and time. Sample profile information contains the FA composition of the sample. This section also contains the summary area, which is useful to troubleshoot the system. Each peak from the chromatographic analysis is listed by RT, Response, AR/HT, and ECL. The Sherlock software compares the ECL of each peak in the analysis with the expected ECL of the FAs in the Peak Naming Table. The FA name is printed in the Peak Name column. Peaks that do not correspond to ECL values of known FA peaks are left unnamed and are not used in the library search. The Summary Section is useful to troubleshoot the system. The total area count (Total Response) of peaks eluting between C9:0 and C24:0 is related to the total extracted FAs. The total area of all named peaks (Total Named) is listed with the percentage named (Percent Named). After correcting each peak's area by the response factor and summing, the total amount (Total Amount) is listed. The error between the actual ECLs and the expected ECLs (ECL deviation) is a measure of the system's accuracy in naming peaks. The drift from the last calibration (Reference ECL shift) is a measure of chromatographic stability.

In addition, the library-matching lists are generated by comparing FA compositions to the Sherlock libraries. The FA composition can be matched with known organisms that are stored in the standard libraries. The standard library profiles have been carefully developed to

consider strain-to-strain and experimental variation. The Peak Naming Tables used are also designed with a built-in ability to recognize those FAs that may be related to other FAs in an extract. Thus, if one FA is a precursor of another FA, the software can account for a decrease in one and an increase in the other. The Sherlock library search report lists the most likely matches to the unknown composition and provides a SI for each match. Furthermore, the comparison chart is the graphical comparison of the sample to the library entry matches. This is the visual representation of the results of the library search given after the listings of the best possible matches and corresponding SI. All FAs found in the extract and the library entries are listed in elution order on the left side of the chart. A scale of percentages is printed across the bottom of the chart. For each FA, the bar represents a ± 2 standard deviation (SD) window around the entry mean. A sample chromatogram is generated as well. The chromatogram is a visual plot or trace of the electronic signal generated by FID as it burns the FAs eluting from the column. The raw data of the chromatogram is stored in a LabSolutions data file and can be reprinted if desired. In routine use of Sherlock, the chromatogram plotted by LabSolutions normally need not be evaluated. FAs in the sample are separated by the column and identified by the RT of each peak. RTs are measured to a resolution of 0.001 minutes (0.0001 minutes for rapid and instant methods).

4.3.5. Interpreting the library search

The library matches are listed in descending order of SI, with the highest SI match listed first (MIDI Inc., 2018). The technique used by the Sherlock system is based on SI ($0.0 \leq SI \leq 1.0$). The SI is a numerical value, which expresses how closely a FA composition compares with the mean of referenced FA composition created by the library entry listed as its match. The database search presents the best matches and associated SI. This value is a software-generated calculation of the distance, in multi-dimensional space, between the profile of the unknown and the mean profile of the closest library entry. As each FA varies from the mean percentage, the SI will decrease in proportion to the cumulative variance between the composition of the unknown and the library entry. The SI assumes that species of microorganisms have normal Gaussian distribution and that the mean of the population in any series of traits characterizes the group. Most of the population falls somewhere near the mean, but individuals will differ in composition and thus may show considerable variance from the mean. Another way of visualizing SI is by looking at the Gaussian distribution of the population. Samples with a $SI \geq 0.5$ and a separation ≥ 0.1 between the first and second choice are considered good library comparisons. If the SI is between 0.3 and 0.5 and well separated

from the second choice (> 0.1), it may be a good match, but an atypical strain. SI values ≤ 0.3 suggest that we do not have the species in the database, but the software will indicate the most closely related species (MIDI Inc., 2018).

4.4. Microorganism groups examined in this study

4.4.1. The *Bacillus* genus

The genus *Bacillus* belongs to the phylum Firmicutes, class Bacilli, order Bacillales, and family Bacillaceae. *Bacillus* is a large and heterogeneous group of aerobic or facultatively anaerobic group of Gram-positive, rod-shaped, endospore, low-GC-content bacteria (Jenson, 2014; Ehling-Schulz, Lereclus and Koehler, 2019). *Bacillus* species can be found in various environments with a wide range of conditions such as 20-50 ^{o}C growing temperature, neutral and acidophilic pH and high salt concentrations (Dahl, 1999). Such around 292 *Bacillus* species are widely distributed from food, soil, water, marine, animals, and plants (Jenson, 2014) and have been of industrial, clinical, and commercial interest. Their cell walls consist of peptidoglycan, a heteropolymer of glycan cross-linked by short peptides. The cell wall of *Bacillus* has often been a useful criterion in taxonomy because of its highly diverse peptidoglycan composition and structure (Dahl, 1999). Sporulation in *Bacillus* is induced by nutritional deprivation, or cell density and is affected by numerous factors such as temperature, pH, aeration, and availability of various nutrients when the cell culture reaches the stationary growth phase (Dahl, 1999; Jenson, 2014). The endospore formation relates to an energy-intensive pathway and the production of a complex morphological structure (Jenson, 2014).

Over the past six decades, *Bacillus* have received a great deal of attention due to the various discoveries made pertaining to their use in various sectors. *Bacillus* species are considered as important plant growth-promoting rhizobacteria (PGPR), producing a vast array of biologically active secondary metabolites that can potentially inhibit the growth of plant pathogens and deleterious rhizospheric microorganisms. As regards, *B. subtilis*, B. *amyloliquefaciens* and *B. velezensis* are recognized as biocontrol and plant growth-promoting agents (Reva *et al.*, 2004; Grady *et al.*, 2019). *B. thuringiensis*, *Paenibacillus popilliae*, *P. larvae*, *B. cereus*, *Lysinibacillus sphaericus*, and other related species have been used for microbial insect control (Jenson, 2014). Furthermore, *Bacillus* has been comparatively well exploited for various commercial applications ranging from the manufacture of enzymes (amylase, proteases, aminopeptidases, pectinolytic enzymes) to the production of antibiotics, biochemicals, and also applied in the textile industry (Jenson, 2014; Rabbee et al., 2019). *B. subtilis*, *B. clausii*, *B. cereus*, *B. coagulans*, and *B. licheniformis* have the obvious advantage

over potential probiotics in both animals and humans. Natto is a *B. subtilis*–fermented soybean product for which health benefits (Jenson, 2014). However, *B. cereus*, and *B. anthracis* are food spoilage agents which can survive in food processing (Ehling-Schulz, Lereclus and Koehler, 2019). Illness due to *B. pumilus*, *B. thuringiensis*, and *Brevibacillus brevis* had been reported (Jenson, 2014). *Bacillus* nutritional requirements, degradation and metabolism of nutrients, and the production of polymers are the cause of human foodborne pathogens and human illness as well (Ehling-Schulz, Lereclus and Koehler, 2019).

Besides, the *Bacillus* genera is a phylogenetically incoherent taxon and appears heterogeneous. As taxonomic attention, many distinct *Bacillus* species share high relatedness phenotypically and genotypically have been considered to be closely related. Thus, the classification of *Bacillus* species has received complicated issues (Xu and Côté, 2003; Bhandari *et al.*, 2013). By application of FA profiles, the taxonomic problems among *Bacillus* species can be solved (De Carvalho and Caramujo, 2018). As the aim of the current study, FA compositions in *Bacillus* have been considered.

4.4.2. The *Candida auris* species

C. auris (Ascomycota, Saccharomycetes, Saccharomycetales, Saccharomycetaceae, *Candida*) had been first identified from clinical specimens of the external ear canal at Tokyo Metropolitan Geriatric Hospital in 2009 (Satoh *et al.*, 2009). As an emerging multidrug-resistant pathogen, *C. auris* has been recognized as a cause of invasive candidiasis and healthcare outbreaks worldwide (Iguchi *et al.*, 2019; Kordalewska and Perlin, 2019) causing bloodstream infections as well as other invasive and superficial infections with a high mortality rate (30 - 60%) (Muñoz *et al.*, 2018). The serious global threat has often been isolated from the blood, urine, sputum, ear discharge, cerebrospinal fluid, bronchoalveolar lavage fluid, endotracheal aspirate, abdominal drain fluid, serous fluid, peritoneal fluid, ocular secretion, jejunal biopsy and soft tissue (Centers for Disease Control and Prevention, 2019; Iguchi *et al.*, 2019; Kordalewska and Perlin, 2019). As regards the notable antifungals resistance, *C. auris* have had a higher prevalence than other *Candida* species (Iguchi *et al.*, 2019), especially, some *C. auris* have been resistant to all three main classes of antifungal medications with limited treatment options (Muñoz *et al.*, 2018; Centers for Disease Control and Prevention, 2019). Given the emergence of *C. auris*, the US Centers for Disease Control and Prevention (CDC) suggested the tentative minimum inhibitory concentration (MIC) breakpoints as follows: fluconazole ≥ 32 μg/ml, amphotericin B ≥ 2 μg/ml, anidulafungin ≥ 4 μg/ml, caspofungin ≥ 2

μg/ml and micafungin ≥ 4 μg/ml (Centers for Disease Control and Prevention, 2020a). Furthermore, CDC has issued many clinical alerts about invasive *C. auris* infections and outbreaks (Centers for Disease Control and Prevention, 2019).

Efforts to control *C. auris* invasion have posed multiple challenges including frequent misidentification by diagnostic platforms, a poor understanding of resistance to antifungal drugs and disinfectants, and a high tendency to contaminate health care environments, which results in transmission of clonal *C. auris* isolates (Kordalewska and Perlin, 2019). The worldwide emergence of *C. auris* colonization and infection are arduous issues, which should be prevented by early detection and identification. However, the accurate identification of *C. auris* can be problematic especially when relying on conventional methods (Muñoz *et al.*, 2018; Iguchi *et al.*, 2019; Kordalewska and Perlin, 2019). Accordingly, *C. auris* may be misidentified as *C. famata*, *C. guilliermondii*, *C. lusitaniae*, *C. parapsilosis*, *C. intermedia*, *C. catenulata*, *C. haemulonii*, *C. sake*, *C. duobushaemulonii*, *Rhodotorula glutinis*, and *Saccharomyces kluyveri* (Caceres *et al.*, 2019; Kordalewska and Perlin, 2019; Centers for Disease Control and Prevention, 2020b). Currently, some diagnostic methods such as polymerase chain reaction (PCR), mass spectrometry (MS), matrix-assisted laser desorption ionization time-of-flight (MALDI-TOF), loop-mediated isothermal amplification (LAMP), and T2 magnetic resonance have been applied (Iguchi *et al.*, 2019).

Challenges in *C. auris* identification emphasize the importance of developing more accurate and routine methods to facilitate pathogenic management, improve infection control as well as reduce potential transmission. Whole-cell FA compositions had been investigated as yeast biomarkers in several publications (Peltroche-Llacsahuanga *et al.*, 2000; Patel, Tipre and Dave, 2009), however, this is the first investigation of whole-cell FA components in *C. auris*, comprehensively.

4.4.3. The *Armillaria* genus

Armillaria (Basidiomycota, Agaricales, Physalacriaceae) including 41 morphological species is considered a globally distributed pathogen to forest trees (Coetzee *et al.*, 2011; Koch *et al.*, 2017). *Armillaria* is spread by both wind-dispersed basidiospores and rhizomorphs (Koch et al., 2017; Yafetto et al., 2009). The temperatures between 10 and 31 ℃, with an optimum between 20 and 22 ℃ are favourable in the life cycle of *Armillaria*. The life cycle of *Armillaria* is characterized by varied gametogenesis cycles (mono-, di-, eukaryotic), varied phases in ecological status (pathogenic, saprotrophic, orchid-like symbiotic), varied methods of infection

(basidiospores, mycelium, rhizomorphs), and varied host reactions (tissue compartmentalization, resin outflow, host dying, wood decay) (Kubiak *et al.*, 2017). The majority of these species have a tetrapolar heterothallic mating system and only a few species are homothallic. *Armillaria* species are unique in that their vegetative state is diploid rather than dikaryotic (Baumgartner, Coetzee and Hoffmeister, 2011).

Accordingly, *Armillaria* species are known primarily as pathogens of a broad range of mostly woody, dicotyledonous hosts (Figure 7). The *Armillaria*-root-rot disease, a destructive white-rot symptom on woody trees, causes devastating forest damage and immense economic losses (Coetzee *et al.*, 2011; Drakulic *et al.*, 2017; Kubiak *et al.*, 2017). They attack fruit and nut crops, timber trees and ornamentals in boreal, temperate, and tropical regions of the world. Furthermore, *Armillaria* is a facultative necrotroph which colonizes living roots, kills root tissue, and then utilizes the dead tissue as its source of nutrition. After the plant dies, *Armillaria* persists as a saprophytic white-rotter on infected portions of the root system. Then, mycelium surviving saprophytically in woody residual roots can remain buried in the soil and serves as inoculum for infection of the next crop. Therefore, the genus is best known for its economic burden (Baumgartner, Coetzee and Hoffmeister, 2011).

Figure 7. Characteristic signs of *Armillaria* root rot. Young rhizomorphs (*A. ectypa*, left), fruiting bodies and the decay caused by *Armillaria* (*A. ostoyae*, middle) and the spread of fungal mycelium under the bark (*A. ostoyae*, right) of a conifer (Sipos, Anderson and Nagy, 2018).

Besides, *Armillaria*, playing the hosting role in the plant, have been identified as symbionts of orchids *Galeola* and *Gastrodia*. The mycorrhizal relationship is known as “myco-

heterotrophy" (Baumgartner, Coetzee and Hoffmeister, 2011). In this case, the orchid lacks chlorophyll, is not a source of nutrition for *Armillaria* and it takes carbon from the *Armillaria* mycelium. Instead, *Armillaria* may gain its nutrition from a second host plant, with which it remains connected via rhizomorphs and has a typical pathogenic relationship (Baumgartner, Coetzee and Hoffmeister, 2011). Similar contrasting roles as either parasite or host are revealed by *Armillaria* in symbioses with other fungi. *Armillaria* is parasitized by *Entoloma abortivum*, which causes misshapen *Armillaria* fruiting bodies. In contrast, *Armillaria* is thought to be a mycoparasite of *Wynnea* (Baumgartner, Coetzee and Hoffmeister, 2011).

On the other hand, some *Armillaria* species are edible and beneficial. The honey mushroom *A. mellea* was indicated to be rich in carbohydrates, ash, fat, proteins and organic acids (Kostić *et al.*, 2017). The bioactive protoilludene-type aryl esters, mycelium polysaccharides and armillarikin synthesized by *Armillaria* show potential for the development of novel medicine (Chen, Chen and Huang, 2016; An *et al.*, 2017; Engels *et al.*, 2021). Therefore, *Armillaria* was considered as a bioactivity-promising source as well such as antimicrobial and antioxidant (Kostić *et al.*, 2017), endo-β-1,4-glucanase (Jagtap *et al.*, 2014), neuroprotective (An *et al.*, 2017) and apoptosis- induced (Chen, Chen and Huang, 2016) properties. Due to interesting characteristics, a comprehensive understanding of *Armillaria* features should be investigated.

As the aim of the current study, FAs, important constituents of *Armillaria*, are considered. *Armillaria* contained simultaneously SFA and UFA with predominant UFA contents (Jing *et al.*, 2012; Çayan *et al.*, 2017; Kostić *et al.*, 2017). Limited information on *Armillaria* cellular FA composition was reported, recently. *A. luteo-virens* was revealed to accumulate linoleic (47.14%), oleic (22.15%), palmitic (8.29%), and stearic (3.00%) acids as major FAs. The UFA in wild *A. luteo-virens* was higher than the cultivated species including *Flammulina velutiper*, *Pleurotus eryngii*, *Copyinds comatus*, and *Agrocybe aegerita* (Jing *et al.*, 2012). *A. tabescens* contained 31.90% of SFA and 68.05% of UFA. Major FA components were linoleic (27.64%), oleic (35.92%), palmitic (19.40%), stearic (5.37%), palmitoleic (4.49%), lignoceric (3.56%) acids (Çayan *et al.*, 2017). Twenty-five FAs with the prevalence of linoleic (63.80%), oleic (15.47%), and palmitic (12.63%) acids were investigated in *A. mellea* (Kostić *et al.*, 2017). They consisted of 16–18 FAs ranging from 12–24 carbons in length generated from cultures of *A. tabescens*, *A. mellea*, and *A. gallica* suggesting that FAME profiling is sufficiently robust for species differentiation (Cox, Scherm and Riley, 2006). These scientific shreds of evidence showed typical and diverse FA components opening the potential of FAME profiles in *Armillaria* identification.

5. OBJECTIVES

The aim of this study was to reveal the possibility of using the cellular FAs as a taxonomic and diagnostic tool with the application of Sherlock CAS to certain groups of microorganisms where the previously applied identification was problematic. The development of Sherlock CAS has possibly become to perform cost-effective, sensitive, reliable, and rapid analyses in routine with a small amount of cell mass.

By considering these main objectives, our study was:

- The identification of environmental *Bacillus* isolates using a commercially available method,
- Development of a new library for the unidentified *Bacillus* strains,
- Generation of a new library to identify the clinically important *C. auris* species,
- Optimization of cultivation conditions, separation method, and identification library within the Sherlock CAS for *Armillaria* species.

6. MATERIALS AND METHODS

6.1. Strains used in this study

6.1.1. *Bacillus* strains

The *Bacillus* type-strains including ATCC 6633, DSM 7^T, DSM 1061^T and DSM 23117^T were obtained from the ATCC and DSMZ. The isolated *Bacillus* strains were deposited in the Szeged Microbiological Collection (SZMC, http://szmc.hu) of Department of Microbiology, University of Szeged, Hungary (Table S2).

6.1.2. *Candida* strains

Table S3 shows strains of *C. auris* used in this study. The information followed "*Candida auris* Panel" offered by CDC & FDA Antibiotic Resistance (AR) Isolate Bank, which contains *C. auris* isolates from all clades (Centers for Disease Control and Prevention, 2021). Besides, MMC-1 and MMC-2 were provided by Montefiore Medical Center (MMC, Bronx, NY) (Zamith-Miranda *et al.*, 2019).

6.1.3. *Armillaria* strains

The *Armillaria* isolates were deposited in SZMC (Table S4) (Chen et al., 2019).

6.2. Cultivation conditions

6.2.1. Cultivation method for *Bacillus* and *Candida* strains

The *Bacillus* strains were isolated according to the Vágvölgyi et al. by Mónika Vörös and Orsolya Kedves (Vágvölgyi *et al.*, 2013). Before the FA profiling, the bacteria were inoculated with the quadrant streaking method on TSBA (Becton, Dickinson and Company, Sparks, NV, USA) at 28 ℃ for 24 ± 2 hours.

The *C. auris* strains were inoculated with the quadrant streaking method on SDA (Becton, Dickinson and Company, Sparks, NV, USA) at 28 ℃ for 30 ± 2 hours before the FA profiling.

6.2.2. Cultivation method for *Armillaria* strains

Cultures were grown on potato dextrose agar (PDA, 200g/L potato infusion, 20g/L dextrose, 20g/L agar), malt extract agar (MEA, 30 g/L malt extract, 5 g/L peptone, 15 g/L agar), and Roth and Show agar (RS, 40 g/L malt extract, 20 g/L dextrose, 5 g/L peptone, 19 g/L agar) at 25 ℃ in dark for 30 days (Chen et al., 2019; Taipale et al., 2013). The growth diameter was measured every 7 days to demonstrate the most applicable medium.

Subsequently, cultures were grown in potato dextrose broth (PDB), malt extract broth (MEB), and Roth and Show broth (RSB) at 25 ℃ in dark for 30 days without shaking. The growth was observed every 5 days to demonstrate the most applicable medium and incubation time.

All cultivation was repeated three times. The data were presented as the mean of three replicates ± SD of mean.

6.3. Sample pretreatment

6.3.1. Sample pretreatment of *Bacillus* and *C. auris* strains

Sample processing was carried out according to the Sherlock^{TM} Operating CAS Manual (MIDI Inc., 2018). Briefly, 20–40 mg of cells were harvested and placed in a clean glass tube. Then, 1 mL of reagent 1 (45 g NaOH, 150 mL of methanol, and 150 mL of distilled water) was added to the sample and heated at 95–100 ℃ in a water bath. After 5 min, the sample was removed from the water bath, vortexed, and heated for an additional 25 min. The sample was mixed with 2 mL of reagent 2 (325 mL of 6.0 N HCl, 275 mL of methanol) and incubated at 80 ℃ in a water bath (Precision water bath NB-301, HandyLAB®System, N-BIOTEK, Bucheon-si, Korea) for 10 min. Subsequently, 1.25 mL of reagent 3 (200 mL of hexane, 200 mL of methyl tert-butyl ether) was added and the derivatized FAs were extracted for 10 min in a laboratory rotator (Rotator drive STR4 Stuart, Cole-Parmer^{TM}, Vernon Hills, IL, USA). The organic (upper) phase was recovered and washed with 3 mL of reagent 4 (10.8 g NaOH, 900 mL distilled water) for 5 min in a laboratory rotator. The resulting organic (upper) phase from the tube was transferred to a clean vial for GC analysis.

6.3.2 Sample pretreatment of *Armillaria* strains

Armillaria strains were cultivated in optimizing conditions. Cell mass was harvested, lyophilized, and stored at -20 ℃. For the extraction of the lyophilized mycelia, the instruction of MIDI (5.3.1) was followed, but certain elements of the sample pretreatment had to be

optimized. Initially, the effect of the lyophilized cell mass was examined by applying 50, 40, 30, 20, and 10 mg/mL concentrations. Then, the saponification time was altered from 30 min to 120 min in 30 min increments to detect an appropriate saponification time.

6.4. The Fatty Acid Methyl Ester (FAME) analysis

6.4.1. The FAME analysis of *Bacillus* strains

The MIDI Sherlock® Microbial Identification System (MIS, Microbial ID Inc., USA) was applied with the Sherlock CAS Software ver. 6.4 (Microbial ID Inc., USA) operating through the LabSolution ver. 5.97 software (Shimadzu, Japan) on a Nexera GC-2030 gas chromatograph (Shimadzu, Japan) equipped with an AOC-20i Plus autoinjector (Shimadzu, Japan) and a HP-Ultra 2, 25 m x 0.2 mm x 0.33 μm thickness fused silica capillary column (Agilent, USA). The whole-cell FAME profiles with database were analyzed by the standard method RTSBA6 and the standard library RTSBA6. The Library generation function of MIS Sherlock CommandCentre ver. 6.4 was applied to design a library RTSBA7 using the method RTSBA6. Injector and detector temperatures were 250 ℃ and 300 ℃, respectively. Carrier gas was hydrogen at a flow rate of 1.48 mL/min, while the detector gases were nitrogen (make up), oxygen, and hydrogen with the flows of 30, 30, and 350 mL/min, respectively. Samples were introduced in an injection volume of 2 μL in split mode with a 40:1 split ratio. The oven program started at 168.1 ℃, which ramped up to 291 ℃ with 28 ℃ per min, and then up to 300 ℃ with 60 ℃ per min, holding at this temperature for 1.50 min. The total column oven program time was 6.04 min. The 1300-C rapid calibration standard mix (Microbial ID Inc., Newark, DE, USA) was used for RT calibration and system suitability purposes as well as for the fine tuning of the pressure and temperature parameters at the system setup. The *B. subtilis* strain ATCC 6633 and pure hexane were considered as the quality control (QC) and the negative control, respectively.

6.4.2. The FAME analysis of *C. auris* strains

The whole-cell FAME profiles were analyzed by the method SYEAST6 and the standard library YST28 and YSTCLN using Sherlock CAS. The Library generation function of MIS Sherlock CommandCentre ver. 6.4 was applied to design new libraries of *C. auris* named CAN1 and CAN2. Injector and detector temperatures were 250 ℃ and 300 ℃, respectively. Carrier gas was hydrogen at a flow rate of 0.42 mL/min, while the detector gases were nitrogen

(make up), oxygen, and hydrogen with the flows of 30 mL/min, 30 mL/min and 350 mL/min, respectively. The injection volume was 2 µL, which was introduced in split mode with 45:1 split ratio. The oven program started at 170 °C, which ramped up to 260 °C with 5 °C per min, and then up to 300 °C with 60 °C per min holding at this temperature for 2 min. The total column oven program time was 20.67 minutes. The 1300-C rapid calibration standard mix (Microbial ID Inc., United States) was used for RT calibration, QC and system suitability purposes. The *C. albicans* ATCC 14053 and pure hexane were considered as the positive and negative control, respectively.

6.4.3. The FAME analysis of *Armillaria* strains

The Method and Library generation function of MIS Sherlock CommandCentre ver. 6.4 was applied to develop the new method ARMI and library ARMI. The temperature and pressure program selected as a trade-off between the resolution of calibrating the calibration standard mixture. The new method and new library were created concerning FAME profiling results of various *Armillaria* species (n = 70).

Injector and detector temperatures were 250 ℃ and 300 ℃, respectively. The carrier gas was hydrogen at a flow rate of 1.25 mL/min, while the detector gases were nitrogen (make up), oxygen, and hydrogen with the following flow of 30 mL/min, 30 mL/min, and 350 mL/min, respectively. The injection volume was 2.0 µL, which was introduced in split mode with 30:1 split ratio. The oven program started at 190 °C, which ramped up to 285 °C with 5 °C per min, and then up to 300 °C with 60 °C per min holding at this temperature for 1.25 min. The total column oven program time was 11 minutes. The 1208-C calibration standard mix (Microbial ID Inc., United States) was used for RT calibration, QC, and system suitability purposes.

6.5. New Library generation

To develop a new library, each sizable set of respective strains was identified and refreshed in an appropriate cultured condition. Their whole-cell FAMEs were extracted and analyzed using the appropriate MIS method. New entries were added by a statistical summary of a set of related samples. Each set of whole-cell FAME profiles was served as training files to a new library entry using the Library generation function of MIS Sherlock CommandCentre ver. 6.4. The performance of the newly created library was tested and verified using

visualization tools for library entries (MIDI Inc., 2018). Samples were analyzed and compared with both standard and newly created libraries for accurate identification.

6.6. *Bacillus* identification using molecular markers

Total cellular DNA was extracted by the E.Z.N.A.® Bacterial DNA Kit (Omega Bio-tek, Inc., Norcross, GA, USA) according to the manufacturer's instructions. Amplification of the *gyrA* gene (Vágvölgyi *et al.*, 2013) was performed in 50 µL reaction mixtures containing 10 pmol of each primer (gyrAF: CAGTCAGGAAATGCGTACGTCCTT; gyrAR: CAAGGTAATGCTCCAGGCATTGCT), 10 nmol dNTP mix, 2 µL template DNA, 5 µL 10× PCR buffer, 6 µL of 25 mM $MgCl_2$, and 1 U of Taq DNA polymerase (Thermo Fisher Scientific, Waltham, MA, USA). The PCR thermocycler (Doppio, VWR International GmbH, Darmstadt, Germany) was set to an initial denaturation step at 94 °C for 2 min, 30 cycles of denaturation at 94 °C for 30 s, annealing at 53 °C for 45 s, extension at 72 °C for 60 s, and a final extension at 72 °C for 5 min. The amplification of the *rpoB* gene (Stefanic and Mandic-Mulec, 2009) was conducted in 50 µL reaction mixtures containing 20 pmol of each primer (rpoBF: AGGTCAACTAGTTCAGTATGGACG; rpoBRO: GTCCTACATTGGCAAGATCGTATC), 10 nmol dNTP mix, 2 µL template DNA, 5 µL 10× PCR buffer, 6 µL of 25 mM $MgCl_2$, and 0.4 U of Taq DNA polymerase. The PCR cycling parameters included an initial denaturation step at 94 °C for 2 min, 30 cycles of denaturation at 94 °C for 30 s, annealing at 57 °C for 30 s, extension at 72 °C for 50 s, and a final extension at 72 °C for 5 min. Sequencing of the amplified DNA fragments was performed on an ABI 3730XL sequencer (Thermo Fisher Scientific, Waltham, MA, USA) with Sanger sequencing.

The sequences were analyzed using the Mega X software (Kumar S., Stecher G., Li M., Knyaz C., 2018). The NCBI Nucleotide BLAST similarity search was carried out at https://blast.ncbi.nlm.nih.gov/Blast.cgi. Alignments were performed by the MUSCLE algorithm. The phylogenetic tree was inferred using the Neighbour-Joining method (Saitou N. and Nei M., 1987) with 1000 bootstrap replicates. The evolutionary distances were computed using the Tamura-Nei method and the units of the number of base substitutions per site (Tamura K. and Nei M., 1993). The rate variation among sites was modeled with a gamma distribution (shape parameter = 0.5).

6.7. Statistical analysis

The MIS Sherlock CommandCentre ver. 6.4 was applied to install new methods and libraries as well as data analysis. The Dendrogram cluster analysis technique, using Euclidean Distance (ED) metric for determining the distance between individual FAs, produces unweighted pair matchings based on FA compositions. The results are displayed graphically to depict the relatedness between organisms. Besides, the 2-D Plot cluster analysis technique uses Principal Component (PC) analysis to separate groups of samples in n-dimensional space. All determinations were carried out at least three times (three separate samplings) and in triplicate. Values were averaged (mean) and reported along with the SD.

7. RESULTS AND DISCUSSION

7.1. Analysis of FA profiles in *Bacillus*

7.1.1. Identification of *Bacillus* sp. using Sherlock MIS

The taxonomic identification was carried out using FAME analysis. The *Bacillus* whole-cell FAME profiles were extracted and analyzed. The varied FA profiles can be applied as distinguishable biomarkers among other *Bacillus* species in agreement with previous reports (Roberts, Nakamura and Cohan, 1994; Perez *et al.*, 2017). The FAME-based identification has confirmed 107 of 128 (83.59%) strains as *B. amyloliquefacies, B. atrophaeus, B. cereus, B. licheniformis, B. megaterium, B. pumilus, B. simplex,* and *B. subtilis* (Table S2) using the standard library RTSBA6. As a result, the strains associated with *Bacillus* species were identified with high SI (SI > 0.5) and well-SI-separations (> 0.1). Accordingly, the lower ED reveals more related between comparisons, and ED < 10 indicates similar species (MIDI Inc., 2018). Besides, the 21 of 128 strains, which had not been identified using library RTSBA6 were served as samples to develop a new library RTSBA7.

7.1.2. Developing the new library RTSBA7

The current library RTSBA6 constructed by MIDI has contained 40 *Bacillus* species. There are a number of species that are not included in the available database. The unidentified *Bacillus* strains using library RTSBA6 and type strains (Table S2) were revealed as samples (n = 3) to develop the new library RTSBA7. As a confirmatory analysis, the partial sequences of the genes encoding the subunit A protein of DNA gyrase (*gyrA*) and the RNA polymerase beta-subunit (*rpoB*) were determined to identify the isolates. The *gyrA* and *rpoB* sequences proved to be effective for *Bacillus* taxonomy (Roberts, Nakamura and Cohan, 1994; Reva *et al.*, 2004; Fan *et al.*, 2017). The previous uses of the *gyrA* sequence (Reva *et al.*, 2004; Borriss *et al.*, 2011) and *rpoB* sequence (Fan *et al.*, 2017; Grady *et al.*, 2019) as phylogenetic markers had drawn clear distinction among closely related taxa of the *Bacillus* groups. In the present study, *gyrA* and *rpoB* sequences were amplified and aligned to determine *Bacillus* strains to the species level. The BLASTN comparison showed high similarities between the examined strains and corresponding records in the GenBank database. The identification revealed an isolated strain as *B. endophyticus* with approximately 100% similarity with numerous *B. endophyticus* in GenBank. Besides, the *gyrA* and *rpoB* sequences of the other twenty isolated strains displayed approximately 100% similarity with both *B. velezensis* and *B. amyloliquefaciens* records in

GenBank. Thus, the classification using both *gyrA* and *rpoB* genes revealed high relatedness values between *B. velezensis* and *B. amyloliquefaciens* as also reported in the literature, and the BLAST results also showed the presence of sequences from possibly misidentified strains deposited in the GenBank. To investigate the relatedness of strains, a phylogenetic tree was also built using the Neighbor-Joining method with 1000 bootstrap replicates. The *B. subtilis* ATCC 6633 strain was considered as the outgroup. Analyses with the *gyr*A sequences (Figure S1), *rpo*B sequences (Figure S2), and their concatenation (Figure 9) generated similar phylogenetic trees without notable differences. The analysis separated *B. velezensis* and *B. amyloliquefaciens* strains into two corresponding clades of the phylogenetic tree in the case of the type strains; other databases collected strains and the field isolates (Table S11) with the bootstrap values of 83 and 98%, respectively (Figure 9). The phylogenetic tree, based on *gyr*A and *rpo*B sequences, shows the existence of two tightly related monophyletic groups: (1) *B. velezensis*, containing our field *Bacillus* isolates, type strain DSM 23117T together with the other reference strains At1, AS43.3, BIM B-439D, AP183, KKLW, SQR9, S141, QST713, BvL03, LF01, WRN014, and SGAir0473; (2) *B. amyloliquefaciens*, containing type strain DSM 7T and DSM 1061T together with the other reference strains LL3, TA208, and XH7.

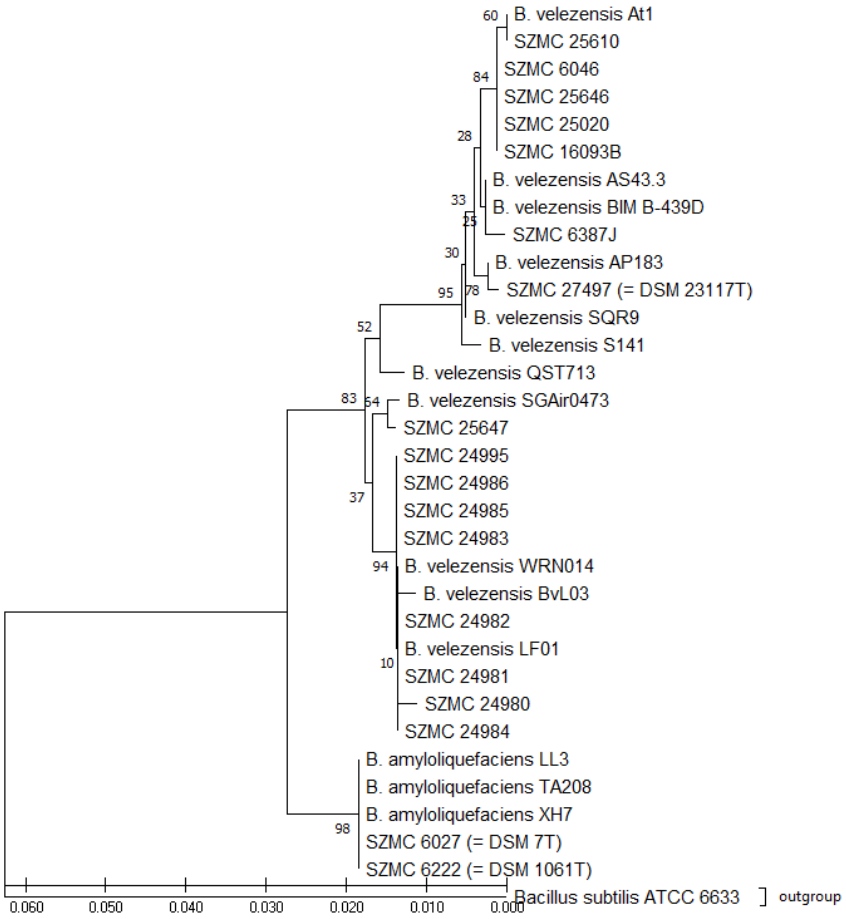

Figure 9. The Neighbour-Joining phylogenetic tree based on the concatenation of *gyrA* and *rpoB* gene sequences. Evolutionary distances were computed by the Tamura-Nei method. Bars, 0.010 substitutions per nucleotide position.

Subsequently, the FAME profiles of identified strains were considered as samples (n = 3) for developing the new library RTSBA7. Consequently, the FAME profiles of a *B. endophyticus* strain and twenty *B. velezensis* strains (n = 3) were introduced as new entries in library RTSBA7. The dendrogram analysis drawn from diverse FA profiles of *Bacillus* species revealed a relationship among FA profiles of *Bacillus* species included in the library RTSBA6 and RTSBA7 (Figure 10) via the ED index. All identified samples exhibited high matches with SI > 0.5 and well-SI-separations (> 0.1) confirming that the method is reliable with high confidence. As a result, the *Bacillus* strains were classified as *B. amyloliquefaciens*, *B. atrophaeus*, *B. cereus*, *B. endophyticus*, *B. licheniformis*, *B. megaterium*, *B. pumilus*, *B. simplex*, *B. subtilis* and *B. velezensis* without misreading (Table S2). Remarkably, the

classification using whole-cell FAs can distinguish between *B. velezensis* and *B. amyloliquefaciens*, which were taxonomic trouble.

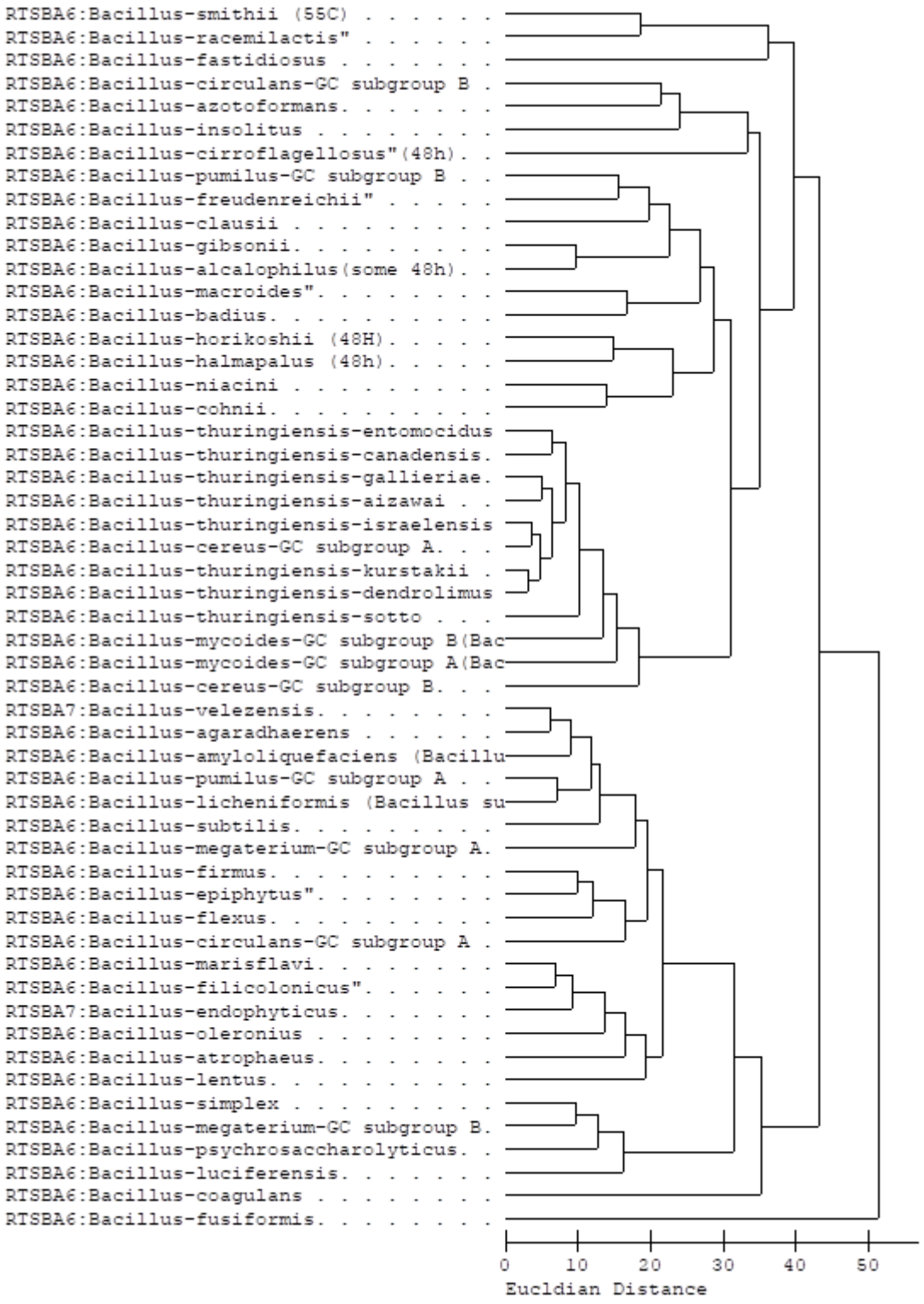

Figure 10. The relationship between FA profiles of *Bacillus* species included in the library RTSBA6 and RTSBA7.

7.1.3. FAME profiles in *Bacillus*

The information observed in Table 3 has illustrated remarkable features of *Bacillus* FAs. In the current work, FAs were identified based on their estimated carbon lengths determined relative to the calibration standard and by comparing them with the peak table. These FA features built from many analyzed FA profiles by both MIDI and the present study are evidence of the accurate composition of whole-cell FAs. Accordingly, FA composition has been varied drawing distinctions among *Bacillus* species as remarkable biomarkers. Furthermore, FA compositions in some species such as *B. cereus*, *B. megaterium*, and *B. pumilus* have been divided into two distinguishable groups named GC subgroup A and B in the library.

Table 3. Average cellular FA compositions (%) in the examined *Bacillus* species

Features	13:0 iso	14:0 iso	14:0	15:0 iso	15:0 anteiso	16:1 ω7c	16:0 iso	16:1 ω11c	16:0	17:1 iso ω10c	17:0 iso	17:1 iso ω5c	17:0 anteiso	Summed Feature 4[1]
B. amyloliquefaiens	-	1.48	0.7	28.63	33.1	-	3.12	2.73	5.4	2.05	13.2	-	8.65	-
B. atrophaeus	-	1.37	-	13.53	46.28	-	4.11	1.82	2.97	1.81	6.29	-	17.92	-
B. cereus (GC subgroup A)	9.69	3.61	2.91	34.78	3.93	-	5.56	-	4.97	4.69	9	4.5	0.96	-
B. endophyticus	-	7.46	3.36	15.89	42.64	-	7.45	2.21	7.07	-	1.24	-	8.28	-
B. licheniformis	-	0.87	0.49	32.89	33.66	0.73	3.8	1.46	3.64	1.49	8.44	-	11.38	1.1
B. megaterium (GC subgroup A)	-	4.31	1.72	38.02	41.56	-	0.62	3.85	2.7	0.57	1.86	-	3.25	-
B. megaterium (GC subgroup B)	-	4.7	1.27	16.33	60.84	-	1.63	2.65	3.81	-	1.21	-	6.17	-
B. pumilus (GC subgroup B)	0.5	0.79	1.23	50.83	23.48	-	1.44	1.88	4.15	2.26	8.12	-	4.56	-
B. simplex	-	4.01	3.2	10.42	59.65	1.84	2.89	6.57	7.05	-	1.15	-	2.62	0.54
B. subtilis	-	0.85		24.24	39.18	-	2.37	1.74	3.39	2.44	10.9	-	12.34	-
B. velezensis	0.93	1.05	3.04	30.25	32.54	-	1.56	1.71	13	0.82	8.18	-	5.43	-

[1]Summed Feature 4 includes 17:1 iso I/anteiso B and 17:1 anteiso B/iso I

As given, the *Bacillus* species possess higher content of branched-odd FAs including 13:0 iso, 15:0 iso, 15:0 anteiso, 17:0 iso, and 17:0 anteiso as common features of *Bacillus*'s taxonomy (Diomandé et al., 2015; De Carvalho & Caramujo, 2018; O'Leary, 1962). The presence of branched-chain FAs is expected to increase the membrane's fluidity because of their low melting point temperatures, and are already remarkable biomarkers used in *Bacillus* taxonomy (Diomandé *et al.*, 2015). Furthermore, the prominent proportion in 15:0 iso and 15:0 anteiso FAs as well as their high ratio has been indicated as a common feature in *Bacillus*

species (Diomandé *et al.*, 2015). The FA compositions, as well as their proportion, are diverse among *Bacillus* species (De Carvalho and Caramujo, 2018), even within a tightly related "*B. subtilis* species complex" (Ruiz-García *et al.*, 2005).

In the present study, the content of 13:0 iso, 17:1 iso ω5c, and 17:1 iso ω10c were detected in high amounts in *B. cereus* (GC subgroup A), but low in other species. Besides, the 15:0 iso (ranging from 10.42 to 50.83%) and 15:0 anteiso (ranging from 3.93 to 46.28%) are revealed as predominant features. The 15:0 iso/15:0 anteiso ratios are 28.63/33.10 in *B. amyloliquefaciens*, 13.53/46.28 in *B. atrophaeus*, 34.78/3.93 in *B. cereus* (GC subgroup A), 15.89/42.64 in *B. endophyticus*, 32.89/33.66 in *B. licheniformis*, 38.02/41.56 in *B. megaterium* (GC subgroup A), 16.33/60.84 in *B. megaterium* (GC subgroup B), 50.83/23.48 in *B. pumilus* (GC subgroup B), 10.42/59.65 in *B. simplex*, 24.24/39.18 in *B. subtilis*, and 30.25/32.54 in *B. velezensis*, respectively. The distinguishable ratios between 15:0 iso and 15:0 anteiso are indicated as principal biomarkers. In addition, *Bacillus* contains a high amount of 17:0 iso (ranging from 1.15 to 13.18%) and 17:0 anteiso (ranging from 0.96 to 17.92%) as biomarkers as well. The 17:0 iso/17:0 anteiso ratios were detected including 13.18/8.65 in *B. amyloliquefaciens*, 6.29/17.92 in *B. atrophaeus*, 9.00/0.96 in *B. cereus* (GC subgroup A), 1.24/8.28 in *B. endophyticus*, 8.44/11.38 in *B. licheniformis*, 1.86/3.25 in *B. megaterium* (GC subgroup A), 1.21/6.17 in *B. megaterium* (GC subgroup B), 8.12/4.56 in *B. pumilus* (GC subgroup B), 1.15/2.62 in *B. simplex*, 10.94/12.34 in *B. subtilis*, and 8.18/5.43 in *B. velezensis*, respectively. Furthermore, the large contribution of even-chain FAs including 16:0 (ranging from 2.70 to 13.00%), 16:0 iso (ranging from 0.62 to 7.45%), 14:0 iso (ranging from 0.79 to 7.46%) and 14:0 (ranging from 0.49 to 3.36%) have been investigated as *Bacillus* biomarkers.

B. velezensis and *B. amyloliquefaciens*, together with the *B. siamensis* and a black pigment-producing strain, *B. nakamurai*, are members of the operational group *B. amyloliquefaciens*. This operational group belongs to the *B. subtilis* species complex with an eventful taxonomic history (Fan *et al.*, 2017). *B. amyloliquefaciens* was first described by Fukumoto (Fukumoto, 1943; Priest et al., 1987) and later revised by Priest et al. (Fukumoto, 1943; Priest et al., 1987) as an industrial producer of amylase, while *B. velezensis*, first isolated from the river Vélez in Málaga (southern Spain), was initially described as a distinct ecotype of *B. amyloliquefaciens* by Ruiz-García et al. (Ruiz-García *et al.*, 2005). Morphological, physiological, chemotaxonomic, and phylogenetic interrelations have indicated that the two taxa are highly similar (Ruiz-García *et al.*, 2005; Wang *et al.*, 2008; Borriss *et al.*, 2011; Dunlap *et al.*, 2016). Furthermore, detailed examinations of the members of these two species, including phenotype analysis, phylogenetics, FAME analysis, DNA–DNA hybridization, microarray-

based comparative genomic hybridization, genomic analysis, HPLC-electrospray ionization MS, and MALDI-TOF MS have revealed *B. velezensis* as plant-associated *B. amyloliquefaciens* subsp. *plantarum* subsp. nov., and *B. amyloliquefaciens* as non-plant-associated *B. amyloliquefaciens* subsp. *amyloliquefaciens* subsp. nov., respectively (Borriss *et al.*, 2011). Subsequently, *B. methylotrophicus*, *B. amyloliquefaciens* subsp. *plantarum*, and *B. oryzicola* were reclassified later as heterotypic synonyms of *B. velezensis*, while *B. amyloliquefaciens* subsp. *amyloliquefaciens* was considered as *B. amyloliquefaciens* (Dunlap *et al.*, 2016). The earliest description differentiated *B. velezensis* and *B. amyloliquefaciens*, as well as other closely related taxa based on phenotypic and genetic differences (Ruiz-García *et al.*, 2005), but in many cases, these taxonomical descriptions were later revised according to the current state of *Bacillus* taxonomy. Thus, the classification of *B. velezensis* and *B. amyloliquefaciens* has usually been a particularly confounding taxonomic problem. Over the last 15 years, interest in understanding the genetic relationship of the two taxa has led to many studies being published (Borriss et al., 2018; Choi et al., 2021; Dunlap et al., 2015, 2016; Emam & Dunlap, 2020; Fan et al., 2018; Grady et al., 2019; Rabbee et al., 2019; Reva et al., 2019; Ruiz-García et al., 2005; J. Wang et al., 2019; L. T. Wang et al., 2008). Moreover, it was also concluded in previous reports that the whole-cell FAME profiles had not yielded satisfying results for discriminating between these two species (Fan et al., 2018; Grady et al., 2019, De Carvalho & Caramujo, 2018). However, our research efforts, aimed at developing a whole-cell FAME profile-based method for distinguishing both taxa, led to other conclusions (Huynh *et al.*, 2022). Accordingly, the FAs 16:0, 17:0 iso, and 17:0 have drawn a distinction between *B. velezensis* and *B. amyloliquefaciens*. In the case of *B. velezensis*, the proportions of 16:0, 17:0 iso, and 17:0 anteiso were 12.53 ± 1.82, 8.52 ± 0.96, and 5.50 ± 0.85 (%), respectively, which were compared with those for the *B. amyloliquefaciens* strains, which were 4.55 ± 0.54, 15.98 ± 1.95, and 8.97 ± 0.73 (%), respectively. Besides, the FA profiles of *B. velezensis* could be characterized by higher 14:0 and 16:0 contents and lower 16:0 iso, 17:0 iso and 17:0 anteiso contents in comparison to *B. amyloliquefaciens* (Figure 11). As regards, discriminating biomarkers useful for distinguishing between the two taxa were 14:0, 16:0, 16:0 iso, 17:0 iso, and 17:0 anteiso.

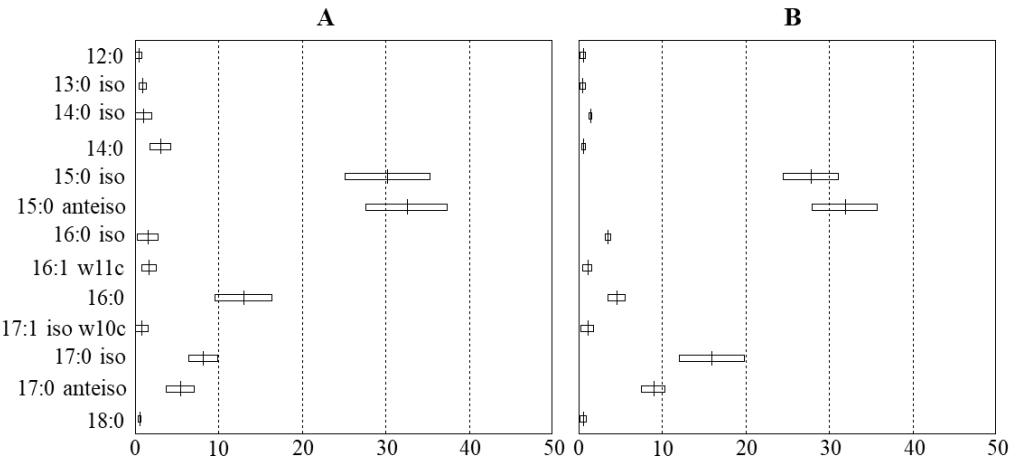

Figure 11. Comparison charts of *B. velezensis* and *B. amyloliqefaciens* based on FA profiles created in the MIS library.

Besides, principal component (PC) analysis enabled us to look at data with high dimensionality and observe the most critical aspects of the data in two or three dimensions. The 2D plot built from PC 1 and PC 2 (Figure 12) showed a separation of the two taxa in n-dimensional space. Group A represents FA components of *B. amyloliquefaciens* with ED^2 (Euclidean distance squared) ~ 36, and group B represented FAs of *B. velezensis* with ED^2 ~ 100. A group with calculated $ED^2 \leq 100$ was considered as the same species. The FA profiles of the two taxa could be distinguished into two separate groups of strains.

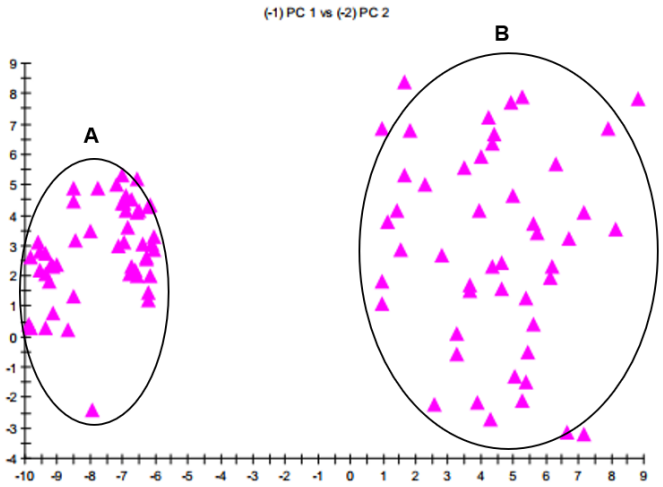

Figure 12. The 2-D Plot between FA components of *B. velezensis* and *B. amyloliquefaciens*. (A) FA components group of *B. amyloliquefaciens*, (B) FA components group of *B. velezensis*.

Our comprehensive study proved that FA features are valuable taxonomical biomarkers with high discriminatory power in the discrimination of the *Bacillus* taxonomy. By taking advantage of the current knowledge regarding biomarkers, the FA-based identification proved to be applicable for the differentiation among closely related *Bacillus* species. To the best of our knowledge, this is the first time that the method based on whole-cell FA profiles operated by MIS has been applied to distinguish between *B. velezensis* and *B. amyloliquefaciens* with comprehensive evidence.

7.2. Analysis of FA profiles of *C. auris* strains

7.2.1. FA compositions in *C. auris* strains

The main feature of FAs constructed from the MIS analysis of twelve strains (n = 10) was revealed in table 4. As recommended, a high-quality library plays an important role in the classification. As the samples were analyzed, a total of FAs was detected including ghost and irregular peaks. However, MIS analysis with many replicates of samples (n = 10) can detect and remove these variations generating precise whole-cell FA features (Table 4-6). Accordingly, the FA 16:0 (palmitic), 18:0 (stearic), 18:1 (oleic), 18:2 (linoleic), and some peaks of summed feature were primarily detected. The FA 16:0, 18:2 is 9,12/18:0a and Summed Feature 8 (sum area of 18:1 Cis 9 (ω9) and 18:1 (ω8)) have predominated.

Table 4. Main cellular FA compositions among *C. auris* strains (Mean (%) ± SD)

Strain number	Clades	16:1 Cis 9 (ω7)	16:0	17:1 Cis 9 (ω8)	17:0	18:2 Cis 9,12/18:0a	18:0	Summed Feature 8[1]	Summed Feature 10[2]
B11109	I	5.45 ± 0.64	19.20 ± 0.32	2.88 ± 0.34	1.55 ± 0.27	28.57 ± 0.68	3.00 ± 0.39	35.80 ± 0.79	1.29 ± 0.14
B8441	I	5.21 ± 0.58	20.79 ± 0.28	3.79 ± 0.72	2.56 ± 0.53	27.86 ± 0.68	3.32 ± 0.31	35.67 ± 0.96	-
B11098	I	5.49 ± 0.78	20.39 ± 0.40	2.41 ± 0.74	0.53 ± 0.52	35.96 ± 0.61	3.51 ± 0.51	30.94 ± 1.67	-
B11203	I	4.70 ± 0.36	18.95 ± 0.52	3.21 ± 0.73	-	39.39 ± 1.04	2.56 ± 0.36	30.64 ± 1.17	-
AR0390	I	3.82 ± 0.72	17.32 ± 0.86	3.28 ± 0.75	2.00 ± 0.44	36.04 ± 0.92	4.03 ± 0.42	33.17 ± 1.24	-
MMC-1	I	4.69 ± 0.30	18.77 ± 0.60	3.57 ± 1.11	1.17 ± 1.06	36.95 ± 0.52	3.35 ± 029	30.83 ± 1.27	-
B11220	II	3.10 ± 0.23	13.54 ± 0.44	4.80 ± 0.40	2.42 ± 0.10	27.54 ± 0.63	4.53 ± 0.35	41.04 ± 0.45	0.69 ± 0.10
B11221	III	3.64 ± 0.13	18.15 ± 0.27	2.00 ± 0.25	1.44 ± 0.19	29.56 ± 0.29	4.07 ± 0.30	37.48 ± 0.50	1.41 ± 0.25
B11222	III	3.70 ± 0.05	17.86 ± 0.29	1.94 ± 0.21	1.46 ± 0.13	30.08 ± 0.55	3.52 ± 0.15	38.04 ± 0.38	1.47 ± 0.07
B11244	IV	2.84 ± 0.21	15.82 ± 0.32	2.17 ± 0.34	1.62 ± 0.22	27.25 ± 0.56	4.55 ± 0.24	43.08 ± 1.07	0.76 ± 0.07
B11245	IV	3.50 ± 0.23	16.77 ± 0.34	2.29 ± 0.28	1.47 ± 0.23	28.41 ± 0.39	3.92 ± 0.21	40.87 ± 0.73	0.81 ± 0.09
MMC-2	nd	6.68 ± 0.55	18.96 ± 0.28	10.51 ± 0.56	3.81 ± 0.27	30.20 ± 0.62	3.20 ± 0.31	26.43 ± 0.51	-

[1]Summed Feature 8: including 18:1 Cis 9 (ω9) and 18:1 (ω8)
[2]Summed Feature 10: including 18:1 Cis 9 DMA and a sub-peak with ECL 18.218

As shown in table 4, the FA profiles varied among strains. The content of 16:1 Cis 9 (ω7) in strains of clade I (3.82 -5.49%) and MMC-2 (6.68%) is higher than those of clade II, III, IV (2.84 - 3.70%). The content of 16:0 of strain B11220 (clade II) is 13.54% lower than others (15.82 – 20.79%). The strain MMC-2 contains 10.51% of 17:1 Cis 9 (ω8), which is only 1.94 – 4.80% in others. Remarkably, the main FA 18:2 Cis 9,12/18:0a and Summed Feature 8 have distinguished 12 strains. Accordingly, the strains B11220 (clade II) and B11244, B11245 (clade IV) share a similar ratio with the lowest 18:2 Cis 9,12/18:0a (27.25 – 28.41%) and the highest Summed Feature 8 (40.87 – 43.08%). Compared to strains of clade II and IV, the strain B11221 and B11222 (clade III) contain higher 18:2 Cis 9,12/18:0a (29.56 – 30.08%) but lower Summed Feature 8 (37.48 – 38.04%). The strain B11109 and B8441 of clade I share a similar ratio of 18:2 Cis 9,12/18:0a (27.86 -28.57%) but lower Summed Feature 8 (35.67 – 35.80%) with strains of clade II and IV. Contrarily, the content of 18:2 Cis 9,12/18:0a (35.96 – 39.39%) in the other strains of clade I such as B11098, B11203, AR0390, and MMC-1 share higher content of Summed Feature 8 (30.64 – 33.1%). Besides, the strain MMC-2 is distinguishable with 30.20% of 18:2 Cis 9,12/18:0a and 26.43% of Summed Feature 8.

7.2.3. Identification of FAME subgroups within the *C. auris* species

Cluster and PC analysis of the resulting FAME profiles (Tables 4 and 5) drew a distinction dividing 12 strains of *C. auris* into three GC subgroups (Figures 13 and 14). The GC subgroup A includes strains of B11220, B11109, B11221, B11222, B11244, B11245, and B8441. The GC subgroup B includes strains of B11098, B11203, AR0390, and MMC-1 while the GC subgroup C includes strain MMC-2.

The FA profiles were consistently typical and distinguishable between the three subgroups. PC analysis allowed us to look at data that has high dimensionality and see the most critical aspects of the data in two or three dimensions. The 2-D plot built from PC 1 and PC 2 (Figure 13) showed a separation of taxa in n-dimensional space. The group A represented for FA components of subgroup A with $ED^2 \sim 100$, the group B represented for FAs of subgroup B with $ED^2 \sim 72$, and the group C represented for FAs of subgroup C with $ED^2 \sim 13.5$ confirming that the FA profiles of the three groups can be distinguished.

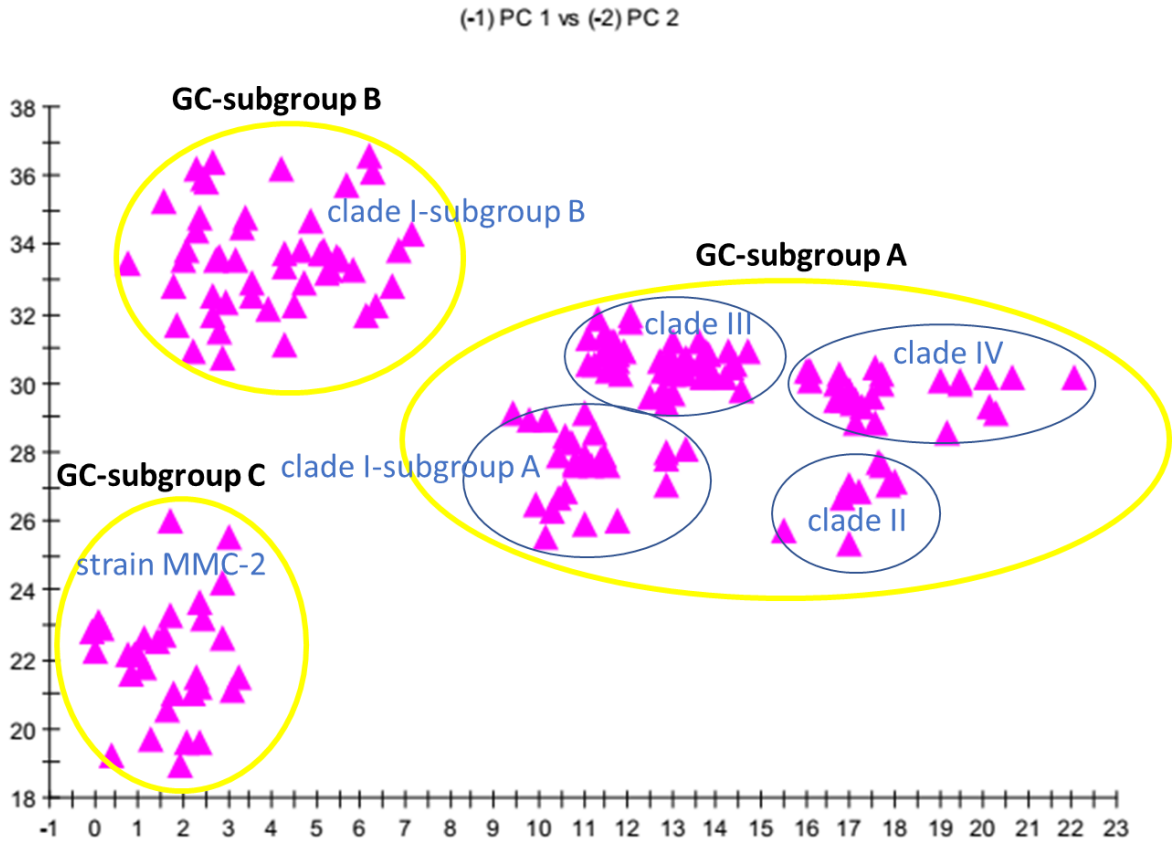

Figure 13. The 2-D plot of PCA based on FA components of *C. auris* strains. (A) FA components group of GC subgroup A, (B) FA components group of GC subgroup B and (C) FA components group of GC subgroup C.

The FA 17:1 Cis 9 (ω8), 17:0, 18:2 Cis 9,12/18:0a, and Summed Feature 8 have been considered as biomarkers between three GC subgroups of *C. auris* (Table 5). The lower content of 17:1 Cis 9 (ω8) and 17:0 in subgroup A (2.84 and 1.79%) and subgroup B (3.12 and 1.01%) can be distinguished from subgroup C (10.51 and 3.81%), respectively. Besides, subgroup A contains a lower proportion of 18:2 Cis 9,12/18:0a (28.47%) and a higher proportion of Summed Feature 8 (38.85%) than two other subgroups. Whereas the subgroup B and C contains a higher proportion of 18:2 Cis 9,12/18:0a (37.08 and 30.20%) and a lower proportion of Summed Feature 8 (31.39 and 26.43%) than subgroup A, respectively. The different amounts between 18:2 Cis 9,12/18:0a and Summed Feature 8 have drawn discrimination between groups as well.

Table 5. Cellular FA compositions in three GC subgroups of *C. auris* (Mean (%) ± SD)

Subgroups	16:1 Cis 9 (ω7)	16:0	17:1 Cis 9 (ω8)	17:0	18:2 Cis 9,12/18:0a	18:0	Summed Feature 8[1]
GC subgroup A	3.92 ± 1.00	17.45 ± 2.22	2.84 ± 1.08	1.79 ± 0.52	28.47 ± 1.11	3.84 ± 0.62	38.85 ± 2.75
GC subgroup B	4.68 ± 0.82	18.85 ± 1.25	3.12 ± 0.92	1.01 ± 0.96	37.08 ± 1.60	3.36 ± 0.66	31.39 ± 1.67
GC subgroup C	6.68 ± 0.55	18.96 ± 0.28	10.51 ± 0.56	3.81 ± 0.27	30.20 ± 0.62	3.20 ± 0.31	26.43 ± 0.51

[1]Summed Feature 8: including 18:1 Cis 9 (ω9) and 18:1 (ω8)

7.2.2. FA compositions in *C. auris* clades

Our results (Table 6, Figure 13) revealed that the different *C. auris* clades have also distinct FA compositions.

Table 6. Main cellular FA compositions among *C. auris* clades (Mean (%) ± SD)

Clades and strains[1]	GC subgroup	16:1 Cis 9 (ω7)	16:0	17:1 Cis 9 (ω8)	17:0	18:2 Cis 9,12/18:0a	18:0	Summed Feature 8[2]	Summed Feature 10[3]
Clade I	A	5.33	19.99	3.33	2.06	28.22	3.16	35.73	0.7
	B	4.68	18.85	3.12	1.01	37.08	3.36	31.39	-
Clade II	A	3.1	13.54	4.8	2.42	27.54	4.53	41.04	0.69
Clade III	A	3.67	18.01	1.97	1.45	29.82	3.79	37.76	1.44
Clade IV	A	3.17	16.29	2.23	1.55	27.83	4.24	41.97	0.79
MMC-2	C	6.68	18.96	10.51	3.81	30.20	3.20	26.43	-

[1]The clade of MMC-2 is not known.
[2]Summed Feature 8: including 18:1 Cis 9 (ω9) and 18:1 (ω8)
[3]Summed Feature 10: including 18:1 Cis 9 DMA and a sub-peak with ECL 18.218

FAs in *C. auris* has involved with structural sphingolipids, glycerophospholipids, and glycerolipids (Zamith-Miranda *et al.*, 2019). Regarding the close interaction between membrane lipids and drug sensitivities (Mukhopadhyay, Kohli and Prasad, 2002; Mukhopadhyay *et al.*, 2004; Pan, Hu and Yu, 2018; Zamith-Miranda *et al.*, 2019), the traits of phylogeny and antifungal susceptibility have explained the clustering of FA profiles in *C. auris*. As revealed, *C. auris* clades shared similar FA components, but they are in discriminative proportions. The differences in proportions of 16:1 Cis 9 (ω7), 16:0, 17:1 Cis 9 (ω8), 17:0, 18:2 Cis 9,12/18:0a, 18:0 and Summed Feature 8 have been considered as taxonomic markers distinguishing among *C. auris* clades.

Additionally, Figure 14 exhibits the relationship between FA profiles among *C. auris* strains, clades and subgroups. As given, strains within each clade have shared similar FA profiles such as clade II including strain B11220, clade III including strain B11221 and B11222

and clade IV including strain B11244 and B11245. Besides, FA profiles of strains belonging to clade I have been discriminated into two distinct clusters of clade I-subgroup A (strain B11109 and B8441) and clade I-subgroup B (strain B11098, B11203, AR0309, and MMC-1). The FA composition of strain MMC-2 (clade unknown) is significantly divergent to others forming a distinct cluster named subgroup C. Our significant evidence revealed FA compositions as remarkable biomarkers for the classification of *C. auris* isolates at clade level.

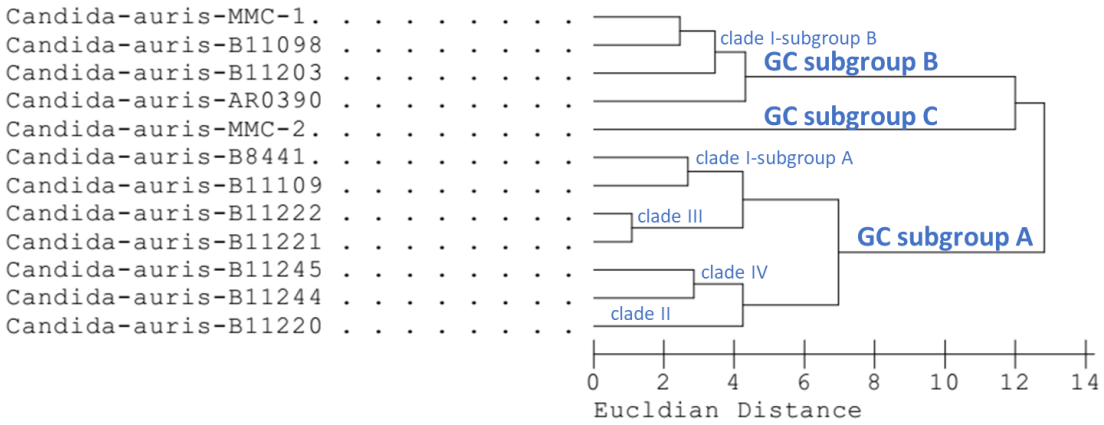

Figure 14. The relationship of FA profiles in *C. auris* clades and GC subgroups.

7.2.4. Application of FAME profiles as a taxonomic biomarker in *C. auris*

Analysis of whole-cell FAs using MIS for the identification in yeasts has been used as an alternative for taxonomic purposes (Peltroche-llacsahuanga *et al.*, 2000; Peltroche-Llacsahuanga *et al.*, 2000; Patel, Tipre and Dave, 2009). This study aimed to draw a comprehensive illustration of whole-cell FA profiles and develop a supplementary method for identifying *C. auris*. In this study, the library CAN1 was carefully generated including FA components of clades and GC subgroups and the library CAN2 including FA components of 12 strains from *C. auris*. The amount and frequency of FAs using library training files were n = 10 for each strain. Besides, the standard libraries YST28 and YSTCLN containing other yeast and *Candida* species constructed by MIDI were referenced.

For testing the performance of the new libraries, various strains genetically assigned to the respective species were chromatographically analyzed with SI indicating a hierarchy of possible strain fits. In our case, all identified samples exhibited good matches to *C. auris* (SI > 0.7) without misreading (Table S5 and S6). In addition, well-SI-separations (> 0.1) between *C. auris* and other generated species in libraries YST28 and YSTCLN confirmed that the method is reliable with high confidence (Figure 15). Furthermore, FA profiles were distinguishable among clades of *C. auris* (Table 5 and Figure 14). Between clades, the significant library matches (SI > 0.7) and well separation to a second hierarchical strain fit (> 0.1) were observed.

There was no misidentification between divergent clades. Within clades, FA profiles revealed poor library comparisons with SI > 0.7 and narrow-SI-separation (< 0.1) confirming that clades share similar FA profiles.

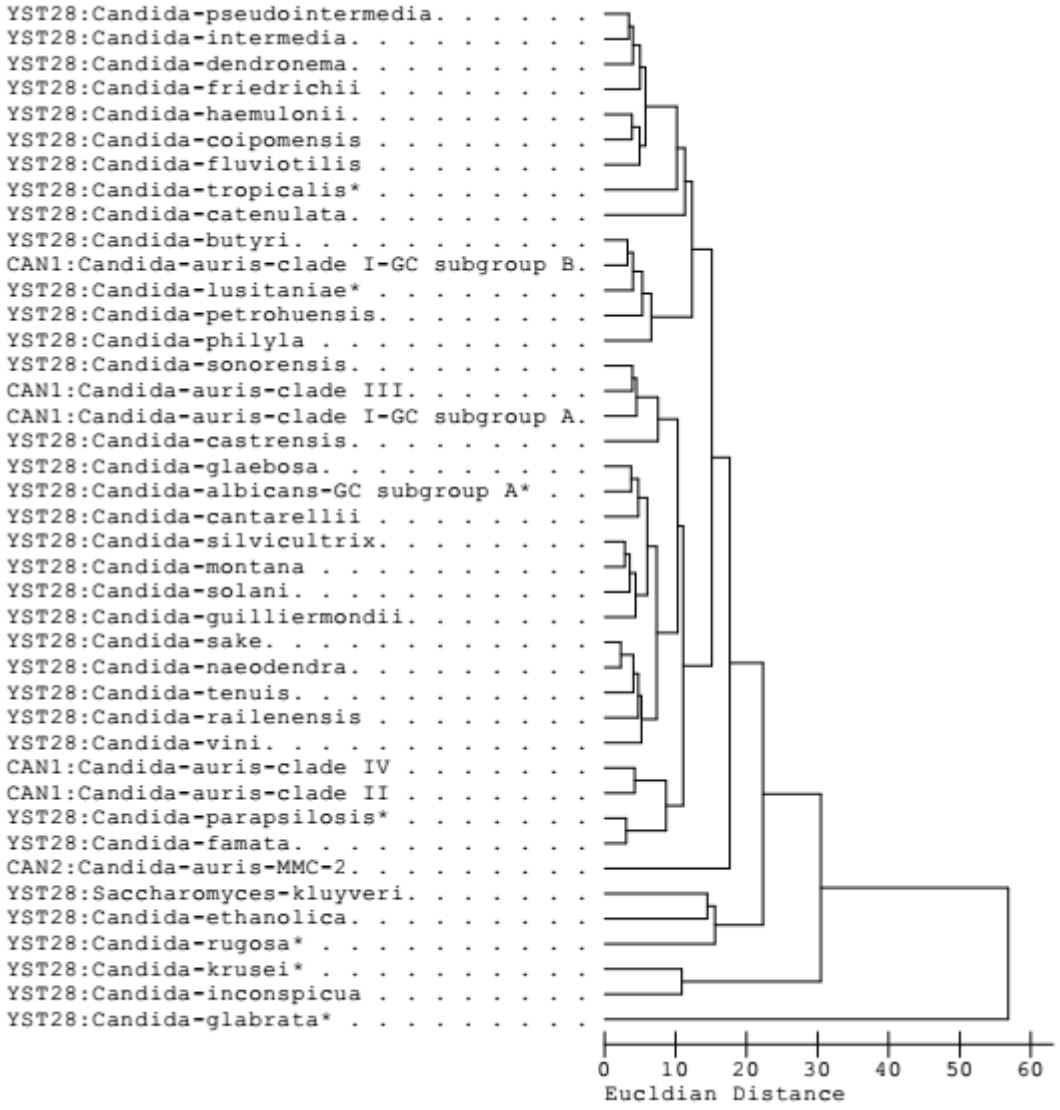

Figure 15. The relationship of FA profiles from *yeast* species, the clinical species are marked with asterisk.

The dendrogram analysis drawn from diverse FAME profiles of *C. auris* and relative species showed a relationship between them (Figure 15) using ED index. These profiles were obtained from the Sherlock library YST28 that had been built from diverse strains (more than 20 strains) within each species. The samples were collected from over the world to avoid potential geographic bias and carefully analyzed with many replications to make entries of the library (MIDI Inc., 2018). The FA profiles of clade I - GC subgroup A together with its relative species formed a tight cluster closed to *C. sonorensis*. The FA profiles of GC subgroup B

together with its relative species formed another cluster closed to *C. butyri, C. lusitaniae, C. petrohuensis, C. philyla* and *C. castrensis*. Besides, the FA profiles of GC subgroup C formed a separated cluster, which could be distinguished from other clusters.

Currently, *C. auris* was diverged into four major clades, which are specific to each geographic region displaying distinct biological and drug resistance properties: clade I (South Asian), clade II (East Asian), clade III (South African), and clade IV (South American) (Muñoz *et al.*, 2018; Keighley *et al.*, 2021). Average pairwise nucleotide identity of 98.7% between genomic assemblies of clades was observed (Muñoz *et al.*, 2018). In addition, the high genetic diversity between clades was discriminated by 10,000 single-nucleotide polymorphisms (SNP) (Lockhart *et al.*, 2017). The distinct clade V (diverged from the other clades by > 200,000 SNP) from Iran has been described to date recently (Chow *et al.*, 2019; Keighley *et al.*, 2021; Muñoz *et al.*, 2021). While sequencing of genetic loci has been applied in the discrimination of *C. auris* from related species, whole-genome sequencing (WGS) and amplified fragment length polymorphism (AFLP) analysis have been preferred to diverge between geographic-specific clades (Lockhart *et al.*, 2017; Jeffery-Smith *et al.*, 2018; Spivak and Hanson, 2018). Given that the classification of *C. auris* at clade level by genetic platforms requires in-depth genetic knowledge and significant bioinformatics expertise. Efforts to investigate the application of FAME profiles as taxonomic markers showed sufficiently discriminatory power not only between *C. auris* and related species but also between *C. auris* clades with high confidence (Figure 15). The result shows that *C. auris* can be classified at both species and clade levels using FAME profiles.

7.2.5. Discussion on *C. auris* FAME profiles

The MIS system analyzes by identifying and quantifying long-chain FAs from 9 to 20 carbon atoms of samples compared to those of well-characterized strains in database library for identifying (MIDI Inc., 2018). In general, the three subgroups of FAs in *C. auris* have some differences compared to other *Candida* species in previous reports (Table 7). *C. auris* contains FA 17:0 which was a lack in other reported profiles (Table 7). Besides, the proportion of 18:2 Cis 9,12/18:0a in *C. auris* is higher while those of 18:0 and Summed Feature 8 were lower than other species.

To make a comparison between *C. auris* and relative species, FA profiles of species in the commercial library YST28 created by MIDI (MIDI Inc., 2018) were referenced (Table 8).

Table 7. Cellular FA components in *C. auris* and other species

	12:0	**14:0**	**15:0**	**16:1 Cis 9 (ω7)**	**16:0**	**C16:0 2OH**	**17:1 Cis 9 (ω8)**	**17:0**	**18:2 Cis 9,12/18:0a**	**18:0**	**Summed Feature 8**
C. auris GC subgroup A	-	0.32	-	3.92	17.45	-	2.84	1.79	28.47	3.84	38.85
C. auris GC subgroup B	-	-	-	4.68	18.85	-	3.12	1.01	37.08	3.36	31.39
C. auris GC subgroup C	-	-	-	6.68	18.96	-	10.51	3.81	30.2	3.2	26.43
C. albicans (Peltroche-llacsahuanga *et al.*, 2000)	-	0.91	-	8.41	14.96	-	1.66	-	27.85	4.2	41.43
C. dubliniensis (Peltroche-llacsahuanga *et al.*, 2000)	-	0.5	-	8.91	15.01	-	2.22	-	18.65	5.7	47.31
C. digboiensis (Patel, Tipre and Dave, 2009)	0.48	1.48	0.48	5.37	25.23	0.83	0.72	-	19.5	5.22	40.68

Accordingly, FA compositions detected in *C. auris* were qualitatively similar but quantitatively different to other *Candida* species as revealed. The FA profiles of GC subgroup A and neighboring *C. sonorensis* have shared a cluster. However, *C. auris* GC subgroup A contains a lower proportion of 16:0 and 18:2 Cis 9,12/18:0a and a higher proportion of 17:0 and Summed Feature 8 than relative species. Compared to closely related *C. butyri, C. lusitaniae, C. petrohuensis, C. philyla and C. castrensis*, GC subgroup B contains a higher proportion of 17:1 Cis 9 (ω8) and different proportion of 16:1 Cis 9 (ω7), 16:0, 18:2 Cis 9,12/18:0a, 18:0 and Summed Feature 8. Furthermore, frequent misidentification cases of *C. auris* such as *C. famata*, *C. guilliermondii, C. lusitaniae, C. parapsilosis*, *C. intermedia, C. catenulata*, *C. haemulonii*, *C. sake*, and *S. kluyveri* (Caceres *et al.*, 2019; Kordalewska and Perlin, 2019; Centers for Disease Control and Prevention, 2020b) were discriminated into distinct clusters by FAMEs (Figure 15).

Besides, *Candida* species phylogenetically relating to *C. auris* such as *C. catenulate*, *C. ethanolica*, *C. glabrata*, *C. guilliermondii, C. haemulonii*, *C. inconspicua*, *C. intermedia, C. krusei*, *C. lusitaniae, C. parapsilosis*, *C. rugosa* and *C. tropicalis* (Satoh *et al.*, 2009; Lockhart *et al.*, 2017; Muñoz *et al.*, 2018) were distinguished into distinct clusters by FAMEs as well (Figure 16). The present investigation revealed FA compositions as taxonomic biomarkers of *C. auris* at the species level (Table 8).

As observed in Table 6, the clade I – GC subgroup B is distantly related to from clades of GC subgroup A by a higher proportion of 18:2 Cis 9,12/18:0a and a lower proportion of Summed Feature 8 (including 18:1 Cis 9 (ω9) and 18:1 (ω8)). According to phylogenetic analysis, there have been two smaller clusters within clade I. The WGS analysis regarding to strain B8441 and strain B11098 aimed that the strain B8441 of clade I – GC subgroup A and strain B11098 of clade I – GC subgroup B were divergent into two sub-branches of clade I (Lockhart *et al.*, 2017). In addition, the interaction between ergosterols and sphingolipids intercorrelated yeast's drug susceptibilities has altered membrane lipids (Mukhopadhyay, Kohli and Prasad, 2002; Mukhopadhyay *et al.*, 2004; Zamith-Miranda *et al.*, 2021).

Table 8. Cellular FA components in *C. auris* and relative species based on the library YST28

	12:0	**14:0**	**15:0**	**16:1 Cis 9 (ω7)**	**16:0**	**17:1 Cis 9 (ω8)**	**17:0**	**18:2 Cis 9,12/18:0a**	**18:0**	**Summed Feature 8**	**Summed Feature 9[1]**	**Summed Feature 10**
GC subgroup A	-	0.32	0.28	3.92	17.45	2.84	1.79	28.47	3.84	38.85	-	0.94
GC subgroup B	-	-	-	4.68	18.85	3.12	1.01	37.08	3.36	31.39	-	-
GC subgroup C	-	-	-	6.68	18.96	10.51	3.81	30.20	3.20	26.43	-	-
C. albicans	-	0.90	-	9.94	16.09	1.47	0.51	26.26	4.60	39.52	-	0.50
C. butyri	-	0.51	0.57	3.93	18.46	1.61	0.96	38.12	2.30	31.13	-	1.81
C. castrensis	-	-	0.45	1.47	23.17	0.78	0.6	31.96	4.37	36.09	-	-
C. catenulata	-	3.49	3.33	16.33	11.25	3.79	-	30.03	0.48	28.42	-	1.22
C. ethanolica	-	-	-	18.95	10.64	-	-	23.98	0.87	43.47	-	1.43
C. famata	-	-	-	2.83	13.57	0.75	-	27.89	2.65	49.23	-	1.04
C. glabrata	-	-	-	49.59	4.91	-	-	-	5.02	36.18	2.94	-
C. guilliermondii	-	0.44	-	8.03	14.75	0.82	-	28.61	2.67	42.62	-	1.63
C. haemulonii	-	0.73	-	9.98	13.61	2.02	-	37.28	1.25	33.66	-	1.08
C. inconspicua	-	-	-	2.83	11.72	1.08	-	15.50	1.45	64.24	-	1.93
C. intermedia	-	1.73	0.85	11.04	17.9	1.05	-	33.65	1.53	30.25	-	1.29
C. krusei	-	-	-	5.14	13.30	0.54	-	20.63	1.13	55.98	-	1.68
C. lusitaniae	-	0.92	-	3.97	19.53	-	-	37.69	3.62	33.11	-	0.94
C. parapsilosis	-	-	-	2.92	14.61	2.36	0.82	26.47	3.32	48.21	-	0.83
C. petrohuensis	-	-	1.28	5.16	22.29	1.71	-	37.82	1.81	29.72	-	-
C. philyla	-	1.22	-	0.69	20.80	-	-	37.88	4.35	34.63	-	-
C. rugosa	-	1.57	1.57	17.19	11.18	9.14	0.49	22.26	1.06	34.00	-	1.02
C. sake	-	0.82	-	10.47	15.17	0.75	-	31.24	1.59	37.84	-	1.49
C. sonorensis	-	-	1.08	5.71	18.30	2.08	-	30.35	1.97	36.65	-	1.84
C. tropicalis	1.28	2.56	-	12.14	17.92	1.63	-	27.68	2.22	33.04	-	0.81
S. kluyveri	-	0.67	-	27.53	13.65	-	-	16.54	2.42	36.92	-	0.56

[1]Summed Feature 9: including 18:1 Cis 11/t 9/t 6, 18:1 Trans 9/t6/c11, 18:1 Trans 6/t9/c11 and 18:1 at 10 (ω8)

As the ergosterol biosynthesis-related gene *erg11* encoding the azole target, discriminative amino acid substitutions in the gene were significantly associated with

geographic clades of *C. auris* (Lockhart *et al.*, 2017). The clade I – GC subgroup A had been considered as subclade Ia, while the clade I – GC subgroup B had been observed as subclades Ib and Ic containing a specific drug-resistant mutation in lanosterol 14-α-demethylase ($ERG11^{Y132F}$ and $ERG11^{K143R}$) (Muñoz *et al.*, 2021). Given that strains of clade I – GC subgroup A showed no fluconazole harbored amino acid substitution in the *erg11* gene including, while strains of clade I – GC subgroup B contained amino acid substitution Y132F in B11203 or K143R in B11098 and AR0390 (Kwon *et al.*, 2019). Furthermore, the two clade I - subgroups have represented the dissimilarity of antifungal susceptibility (Table 9) regarding lipids as major targets of antifungal drugs and part of resistance mechanisms (Zamith-Miranda *et al.*, 2019). As fluconazole is revealed as a common resistance feature (Muñoz *et al.*, 2018), the strain B11109 and B8441 of clade I – GC subgroup A have a low susceptibility with MIC = 16 μg/ml and 8 μg/ml, respectively. In contrast, the clade I – GC subgroup B has been resistant to fluconazole with MIC ≥ 256 μg/ml. In the case of amphotericin B and voriconazole, the strains of clade I – GC subgroup A have been considered more susceptible than the other group.

The FA composition of strain MMC-2 (clade unknown) is significantly divergent from others forming a distinct cluster named subgroup C. The subgroup C contains a significantly higher content of 17:1 Cis 9 (ω8) and lower content of Summed Feature 8. Notably, the discriminated traits between strain MMC-2 and MMC-1 were investigated such as fluconazole resistance and lipid biosynthesis (Zamith-Miranda *et al.*, 2019, 2021). The strain MMC-1 of subgroup B was reported to contain a higher abundance of sphingolipids and ergosterols, which relate to antifungal resistance and drug efflux pumps (Zamith-Miranda *et al.*, 2019, 2021). The strain MMC-2 was susceptible to amphotericin B, caspofungin, and fluconazole, however, strain MMC-1 was significantly resistant to fluconazole (Table 9). As an indication of higher phospholipase activity, lysophospholipids were enhanced in strain MMC-1 and to a lesser extent in strain MMC-2 (Zamith-Miranda *et al.*, 2019). However, higher abundances of lysophosphatidylcholine and lysophosphatidylethanolamine in extracellular vesicles were detected in strain MMC-2 suggesting an intense activity of lipid catabolic enzymes such as phospholipases (Zamith-Miranda *et al.*, 2021). Besides, more abundant phosphatidylcholines, sphingolipids, and lipids containing odd-chain FAs were detected in strain MMC-2 (Zamith-Miranda *et al.*, 2019). As similar to our data, FA 17:0 and 17:1, which were more abundant in strain MMC-2 were determined in the previous study (Zamith-Miranda *et al.*, 2019). The discriminated FA features are specific, so the further investigation about genetic features of strain MMC-2 is recommended.

Table 9. Antifungal susceptibility of studying strains (MIC (µg/ml)) (Zamith-Miranda *et al.*, 2019; Centers for Disease Control and Prevention, 2021)

Strain	**B11220**	**B11109**	**B11221**	**B11222**	**B11244**	**B11245**	**B8441**	**B11098**	**B11203**	**AR0390**	**MMC-1**	**MMC-2**
# AR Bank/CDC	**0381**	**0382**	**0383**	**0384**	**0385**	**0386**	**0387**	**0388**	**0389**	**0390**	**nd**	**nd**
Clade	**II**	**I**	**III**	**III**	**IV**	**IV**	**I**	**I**	**I**	**I**	**I**	**nd**
Clade name	**East Asia**	**South Asia**	**Africa**	**Africa**	**South America**	**South America**	**South Asia**	**South Asia**	**South Asia**	**South Asia**	**South Asia**	**nd**
Drug	**MIC (µg/ml)**											
Amphotericin B	0.38	0.38	0.38	0.5	0.5	0.5	0.75	1.5	4	4	1.6	0.8
Anidulafungin	0.25	0.25	1	2	1	1	0.5	0.5	1	1	nd	nd
Caspofungin	0.125	0.5	0.25	16	0.5	0.5	0.25	1	0.5	0.5	2	1.6
Fluconazole	4	16	128	128	>256	>256	8	>256	256	>256	>256	8
Flucytosine	2	0.125	0.5	0.5	0.5	0.5	8	0.125	128	128	nd	nd
Itraconazole	0.125	1	0.5	1	1	0.5	0.5	0.5	0.25	1	nd	nd
Micafungin	0.125	0.25	1	2	0.5	0.25	0.5	0.125	0.25	0.25	nd	nd
Posaconazole	0.06	0.5	0.5	0.5	1	0.5	0.25	0.25	0.25	0.5	nd	nd
Voriconazole	0.03	0.5	4	1	16	16	0.06	2	4	8	nd	nd

In our examinations, an identification method was successfully developed based on FAME profiles for this emerging threat. As with all methods, factors such as costs, technical skills, and time involved play important roles. Therefore, the MIS with cost-effective, sensitive, reliable, and rapid analysis has been considered as an applicable method. Concerning routine use, a technician averages about 10 minutes per sample for extracting a batch of 20 samples and 21 minutes per sample for operating the GC system. The FA profiles are accurately delivered without a long-waiting time. As the method was developed, the classification of *C. auris* at both species and clade levels has had an additional solution.

7.3. Analysis of FA profiles in *Armillaria*

7.3.1. Optimization of *Armillaria* cultivation

This study developed the MIS method for *Armillaria* species using nine isolates of *A. cepistipes*, 13 isolates of *A. gallica*, 11 isolates of *A. mellea*, and ten isolates of *A. ostoyae* (Table S4). Regarding the *Armillaria* cultivation (n = 3) on PDA, MEA, and RS agar plates, all strains grew well on all three types of agar medium (Figure 16). In addition, the cultivation in PDB, MEB, and RSB (liquid cultures) also showed well-supported growth. There was no FA detected from the free-cultivation medium.

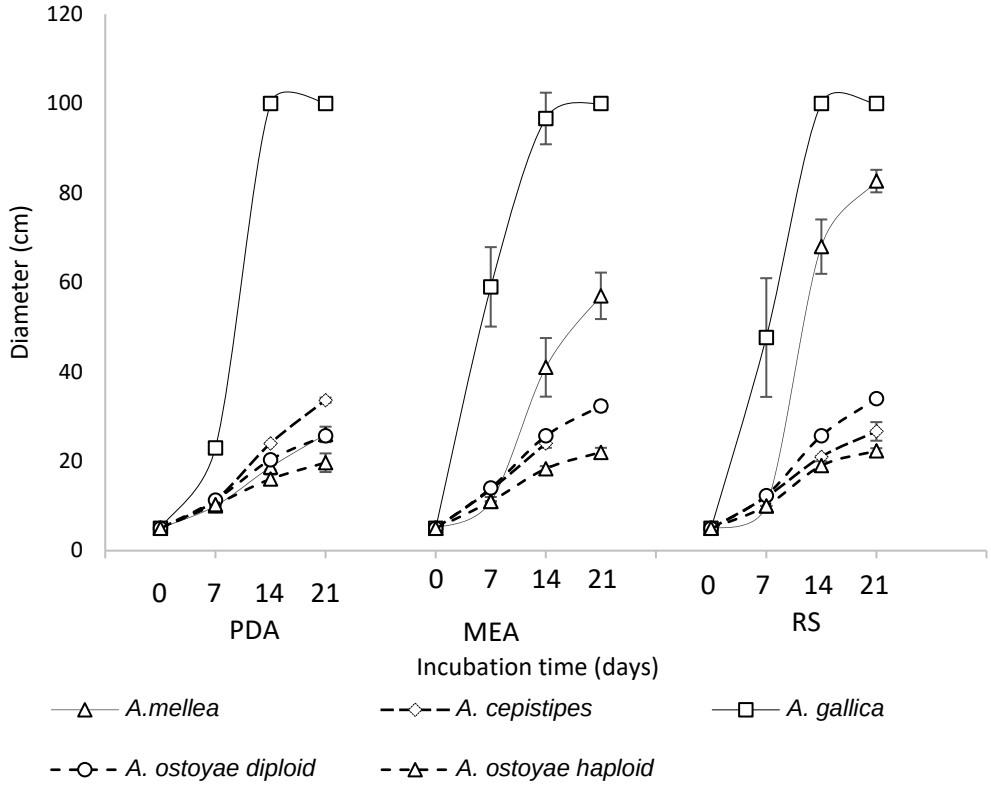

Figure 16. Growth of *Armillaria* strains on different media.

PDA was chosen based on the Sherlock criteria that the acceptable medium must support the growth of all species, must not contain a detectable amount of FA, and must be commercially available (MIDI Inc., 2018). When three *Armillaria* strains were cultured in PDB at 25 ℃ in the dark without shaking, the mycelial mass in the media started to expand from day 15 and then increased significantly from day 20 (Figure 17). After 30 days, the final yields varied depending on the backgrounds of the different strains and species. Accordingly, for FA profiling, PDB media was used to cultivate the *Armillaria* cultures at 25 ℃ in the dark without shaking for 30 days.

Day 5 Day 10 Day 15 Day 20 Day 25 Day 30

Figure 17. The mycelial mass production of *Armillaria* in PDB after 5 - 30 days.

7.3.2. Sample preparation from *Armillaria* isolates

7.3.2.1. Mycelial biomass

The amount of mycelial cell mass used for the FA extraction significantly impacted the FAME profiles. A certain minimum amount of mycelial mass did not yield a sufficient level of FAs for a reliable comparison to the library. On the other hand, a higher amount of mycelia resulted in excessively high area counts and column overloads, resulting in the shifting of peak RTs. The FA ratios changed, and the area counts decreased with an increased mycelial cell mass.

When applying the extract from 20 mg of mycelia, the GC column already became overloaded resulting in a > 2 x 10^6 complete calibration response. For a 10 mg sample, the total response was ~ 300 x 10^3 – 1.000 x 10^3, which then offered a reliable signal for the comparative tests (Table 10).

Table 10. The total response of FAME profiles to varying amount *Armillaria* mycelia

Mycelial mass (mg)	10	20	30	40	50
The total response	~ 300x10^3 – 1.000x10^3	> 2x10^6	> 2x10^6	> 2x10^6	> 2x10^6

7.3.2.2. Saponification time

Treating cells with a saponification procedure promotes cell lysis and liberates FAs from the cellular lipid pools. The time cells are exposed to the treatment may significantly affect the efficiency of extracting FAs and the reproducibility of the recovered FA profiles.

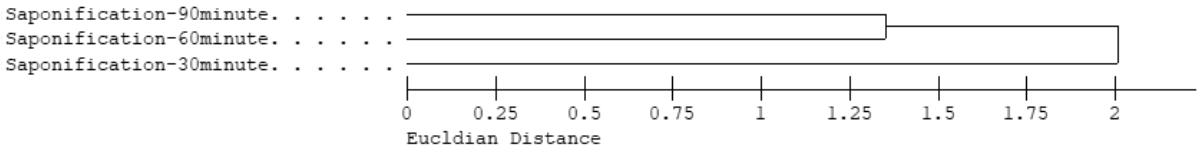

Figure 18. Euclidean distances between the profiles originated from different saponification times by *Armillaria*

In an experiment to optimize conditions, 10 mg of lyophilized fungal mycelium was used and aliquots were treated for 30, 60, and 90 minutes. The data were collected from 480 runs (with the replicates) of four *Armillaria* species.

The correlation between FA profiles originated from different saponification procedures is shown in figure 20. The ED = 2 value indicates that the compositions of the FAME profiles were very comparable for all saponification times used. Therefore, a minimum incubation time of 30 minutes could be set for the saponification treatments.

7.3.3. The FA profiles of *Armillaria* strains

The lists of the main FA profiles identified from various *Armillaria* strains are shown in Table 11 and Table S4 (n = 70 for each species including repetitions).

Table 11. The cellular FA compositions (Mean (%) ± SD) of four *Armillaria species*

Feature	***A. cepistipes***	***A. gallica***	***A. mellea***	***A. ostoyae***
12:0	7.89 ± 4.54	11.99 ± 8.35	4.09 ± 2.00	3.96 ± 1.84
15:0	1.38 ± 0.59	1.67 ± 0.53	2.47 ± 0.78	1.30 ± 0.72
16:0	18.59 ± 2.48	16.70 ± 1.43	20.41 ± 2.71	18.19 ± 2.17
16:0 2OH	0.89 ± 0.20	0.98 ± 0.31	1.63 ± 0.47	1.05 ± 0.34
18:2 ω6c	59.51 ± 6.46	56.43 ± 6.56	53.65 ± 5.41	59.76 ± 6.25
18:0	1.82 ± 0.69	1.62 ± 0.37	1.91 ± 0.49	1.84 ± 0.60
Arm 21.035	-	-	1.10 ± 0.80	-
23:0	-	-	1.26 ± 0.56	-
Arm 24.337	-	-	1.04 ± 0.53	-
Arm 23.440	-	-	-	1.57 ± 0.89
24:1 ω3c	-	-	-	1.83 ± 1.32
ΣSFA	32.11	34.59	34.65	27.19
ΣUFA	61.98	59.44	56.85	64.07
ΣMUFA	1.72	1.95	2.32	3.41
ΣPUFA	60.26	57.49	54.53	60.66

Based on the data, even-chain FAs such as 12:0, 16:0 and 18:2 ω6c could be considered as the prevalent FA components. Amongst them, the most significant FA was linoleic acid (18:2 ω6c), 59.51% in *A. cepistipes*, 56.43% in *A. gallica*, 53.43% in *A. mellea* and 59.76% in *A. ostoyae*. The levels of palmitic acid (16:0) and lauric acid (12:0) were 16.70 to 20.41% and 3.96 to 11.99%, respectively, depending on the species background. It is noteworthy that *Armillaria* species contained a number of unidentified FAs, termed “Arm” and “ELC” (Table 11). Other FAs were also identified at detectable levels (< 3%). In particular, Arm 21.035, FA 23:0, and

Arm 24.337 were detectable at about 1% in *A. mellea* alone. While Arm 23.440 and 24:1 ω3c were present only in *A. ostoyae* in amounts of 1.57% and 1.83%, respectively.

7.3.4. Applying *Armillaria* FAs as potential biomarkers

The system designed for taxonomic identification of *Armillaria* isolates relied on the MIS method by building on data from four species, namely *A. cepistipes*, *A. gallica*, *A. mellea* and *A. ostoyae.* Using the collected profiles an *Armillaria* library was constructed. Strains genetically well-representing our species of interest were analyzed by SI chromatography analysis to identify the hierarchy of possible strain matches and to test the validity of the newly created *Armillaria* genus-related libraries. As a result, 90.00% of *A. cepistipes*, 88.70% of *A. gallica*, 100.00% of *A. mellea*, and 100.00% of *A. ostoyae* could be accurately identified by the new method (Table S7-S10).

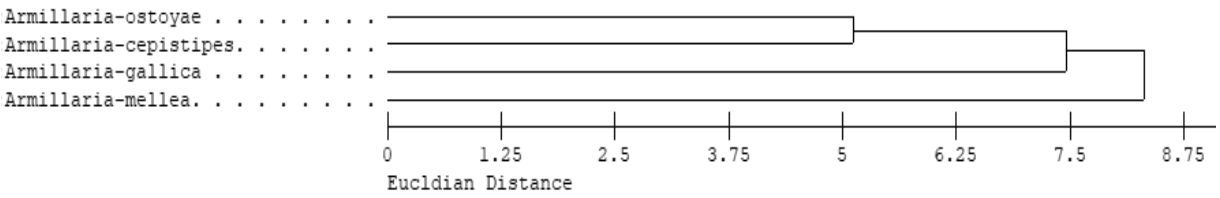

Figure 19. Correlations between *Armillaria* species regarding FA profiles.

According to our data, the FA profiles of the four species were found on four well-separable branches of the dendrogram (Figure 19). In terms of species-specific features the FA profiles of *A. cepistipes* and *A. ostoyae* showed similar characteristics and neither of them showed any overlapping details with *A. gallica* and *A. mellea*.

Approached from the other side, the FA profile of *A. gallica* showed a clear difference compared to the FA profiles of *A. cepistipes* and *A. ostoyae*. Finally, the FA profile of *A. mellea* was remarkably different from that of the other three species. Therefore, the FA profiles of *Armillaria* species can be considered biomarkers to differentiate between them.

7.3.5. Discussion – FA profiles of the *Armillaria* species

In the case of the *Armillaria* genus, before our experiments, no appropriate parameters were available for the cultivation, extraction, and FA profiling in the MIS system; thus, a suitable methodology was necessary to develop a reproducible FA profiling system.

In our study, the detected FAs were SFA or UFA, including MUFA and PUFA, with chains containing 10 – 24 carbon atoms. These gathered FA features built from several FAME profiles were evidence of the accurate composition of whole-cell FAME. The percentage of ΣPUFA (54.53 – 60.66%) was the highest in *Armillaria*, followed by ΣSFA (27.19 – 34.65%) and ΣMUFA (1.72 – 3.41%). The UFA levels were predominant over SFA in all the studied species due to the high contribution of linoleic acid. The UFA/SFA ratio was approximately 1.93 in *A. cepistipes*, 1.72 in *A. gallica*, 1.64 in *A. mellea*, and 2.36 in *A. ostoyae*. The amount of UFA in these *Armillaria* resembled the patterns of FA components in various other fungi (Brondz, Høiland and Ekeberg, 2004; Kavishree *et al.*, 2008; Heleno *et al.*, 2009; Sinanoglou *et al.*, 2015; Çayan *et al.*, 2017). Our result was also consistent with other published research on FAs in the *Armillaria* species (Brondz, Høiland and Ekeberg, 2004; Cox, Scherm and Riley, 2006; Jing *et al.*, 2012; Çayan *et al.*, 2017).

We observed that the relative percentages of FA varied from < 0.30 to 59.76%. The main SFAs were lauric acid (3.96 to 11.99%) and palmitic acid (16.70 to 20.41%), while linoleic acid (53.65 to 59.76%) was the main UFA. We identified the most abundant FA to be linoleic acid, which is the precursor of 1-octen-3-ol responsible for contributing flavours to mushrooms (Heleno *et al.*, 2009). Many previous reports indicated that fungi have significant palmitic and linoleic acid FA profiles and therefore the results obtained for *Armillaria* confirm previous findings for some other fungal species such as *Laetiporus sulphurous* (16:0 ~ 11% and 18:2 ω6c ~ 57%) (Sinanoglou *et al.*, 2015), *Leucopaxillus gentianeus* (16:0 ~ 7.95% and 18:2ω6 ~ 40.92%), *Pleurotus eryngii* (16:0 ~ 14.04% and 18:2 ω6c ~ 68.24%) and *Suillus granulatus* (16:0 ~ 14.43% and 18:2 ω6c ~ 47.64%) (Çayan *et al.*, 2017), *Cortinarius glaucopus* (16:0 ~ 12.05% and 18:2 ω6c ~ 54.99%), *Fistulina hepatica* (16:0 ~ 10.42% and 18:2 ω6c ~ 52.37%), *Hygrophoropsis aurantiaca* (16:0 ~ 9.97% and 18:2 ω6c ~ 55.54%), *Hypholoma capnoides* (16:0 ~ 16.43% and 18:2 ω6c ~ 35.67%), *Laccaria laccata* (16:0 ~ 11.64% and 18:2 ω6c ~ 20.45%), *Lactarius salmonicolor* (16:0 ~ 7.35% and 18:2 ω6c ~ 26.44%), *Lepista inversa* (16:0 ~ 16.36% and 18:2 ω6c ~ 44.58%), *Russula delica* (16:0 ~ 12.02% and 18:2 ω6c ~ 27.15%), *Suillus mediterraneensis* (16:0 ~ 11.93% and 18:2 ω6c ~ 43.72%), *Tricholoma imbricatum* (16:0 ~ 7.44% and 18:2 ω6c ~ 33.0 %) (Heleno *et al.*, 2009). The contents of palmitic and linoleic acid in *Armillaria* were as *A. mellea* (16:0 ~ 21.1% and 18:2 ω6c ~ 39.6%), *A. tabescens*

(16:0 ~ 21.7% and 18:2 ω6c ~ 44.6%), *A. gallica* (16:0 ~ 23.3% and 18:2 ω6c ~ 45.2%) (Cox, Scherm and Riley, 2006), *A. luteo-virens* (16:0 ~ 8.29% and 18:2 ω6c ~ 47.14%) (Jing *et al.*, 2012), *A. borealis* (16:0 ~ 13.3% and 18:2 ω6c ~ 27.4%) (Brondz, Høiland and Ekeberg, 2004), *A. mellea* (Vahl: Fr.) Kummer (16:0 ~ 12.63% and 18:2 ω6c ~ 63.80%) (Kostić *et al.*, 2017). In our study, we considered FAs 12:0, 16:0 and 18:2 ω6c as biomarkers to discriminate *Armillaria* species as opposed to FAs 18:1 ω6c, 18:1 ω9c, and 16:0 2OH which were used in previous studies (Cox, Scherm and Riley, 2006). The 18:2 ω6c/C18:1 ω9c ratio is a chemotaxonomic marker for the taxonomic discrimination between fungal species (Brondz, Høiland and Ekeberg, 2004; Kavishree *et al.*, 2008; Heleno *et al.*, 2009). Interestingly, 18:1 ω9c, which is a major fungal MUFA, was not detected in *Armillaria*. The 18:2 ω6c percentage varied greatly among different *Armillaria* species: 59.51% in *A. cepistipes*, 56.43% in *A. gallica*, 53.43% in *A. mellea* and 59.76% in *A. ostoyae*. Remarkably, *D. tabescens*, showed a distinct percentage of C18:1 ω9c (35.92%, 5.60%), 18:2 ω6c (27.64%, 44.30%), 16:0 (19.40, 21.70%) in the independent studies performed by Çayan et al. (2017) and Cox et al. (2006), respectively. In a recent study, Kostic et al. (2017) identified 63.8% for 18:2 ω6c.

FA 12:0, which was considered as a main SFA of *Armillaria*, had been found in trace amounts in other mushrooms (Brondz, Høiland and Ekeberg, 2004; Heleno *et al.*, 2009; Sinanoglou *et al.*, 2015; Çayan *et al.*, 2017) as well as in *Armillaria* (Brondz, Høiland and Ekeberg, 2004; Cox, Scherm and Riley, 2006; Çayan *et al.*, 2017). Insignificant FAs, which were detected at lower 3% were not present in the same proportions in all *Armillaria* species due to the selectivity in neutral and polar lipid molecules during extractions, and growth conditions. However, the content of 18:2 ω6c was detected without significant variations regardless of the extraction methods (Sinanoglou *et al.*, 2015). Since methods of cultivation and extraction contributed greatly to the proportions of FAs, we considered those confounding factors in our comparison while thallus morphologies and host physiology were rejected as they had no significant effect on *Armillaria* FA profiles. The classification by FA profiles using mycelia from both naturally infected host tissue and cultures had similar results (Bentivenga and Morton, 1994; Cox, Scherm and Riley, 2006). Therefore, it is applicable to use FA profiles as a taxonomic tool that could complement existing molecular methods for the classification of *Armillaria*.

When using the newly created library ARMI, the SI for *A. cepistipes, A. gallica, A. mellea* and *A. ostoyae* ranged from 0.284 to 0.935, 0.594 to 0.941, 0.431 to 0.859 and 0.301 to 0.905, respectively (Table S7-S10). The differentiation accuracy was 90.00% for *A. cepistipes*, 88.70% for *A. gallica*, 100.00% for *A. mellea*, and 100.00% for *A.* ostoyae,

respectively. Remarkably, 100% of samples were identified correctly without misidentification in secondary choice, and *A. cepistipes, A. gallica, A. mellea*, and *A. ostoyae* were grouped together. *A. cepistipes*, and *A. gallica* shared a relatively tight cluster that was in distance to *A. mellea*, and *A. ostoyae*. This showed that the FA profiles at the genus level were convergent. We built the dendrogram using the pairwise comparison of entries ranging from the most similar to the least similar. The method used was unweighted clustering algorithms to estimate overall similarity rather than common ancestry do not confound phylogenetic relationships. The MIDI's manual instructs this analysis with high accuracy and confidence for relationships at the family level and below (Bentivenga and Morton, 1994).

In summary, *Armillaria* species have distinct FA compositions, and among them, 12:0, 16:0, and 18:2 ω6c FAs are most crucial for species separation as remarkable biomarkers. Furthermore, based on the library data, FA profiles of *Armillaria* species were distinguishable from other mushrooms. The knowledge of the quantitative and qualitative composition of FAs opened the potential for developing a supplementary classification method for *Armillaria* species. As we developed the technique, the reliable classification of our *Armillaria* isolates offered an additional alternative. However, the routine application of the Sherlock CAS for the identification of *Armillaria* species appears to be quite difficult due to the slow growth of this fungus in the laboratory environment. Therefore, other methods which do not need pre-cultivation steps are preferred.

8. CONCLUSION

In our current studies, we analyzed whole-cell FA profiles to develop a new taxonomic classification system for three groups of fungi and bacteria. The method applies automated GC analysis of 9-24 carbon FAs and performs qualitative and quantitative whole-cell FA profiling as a taxonomic tool driven by the Sherlock CAS software. Our research interests included various *Bacillus* species, the *C. auris* clade and the prevalent European species of the *Armillaria* genus. Based on our data and results, we were able to identify the critical components of the FA profiles that could be used as reliable, authentic taxonomic tools for all three study groups.

The major findings of our work were the followings:

- The Sherlock CAS had been considered as an additional method to discriminate among *Bacillus* at species level, even within closely related groups. The FAME-based identification has confirmed our isolates as *B. amyloliquefaciens*, *B. atrophaeus*, *B. cereus*, *B. endophyticus*, *B. licheniformis*, *B. megaterium*, *B. pumilus*, *B. simplex*, *B. subtilis*, and *B. velezensis*. Besides, the classification based on whole-cell FAs could also distinguish between *B. velezensis* and *B. amyloliquefaciens*, which were taxonomically real troublesome cases within a tightly related "*B. subtilis* species complex".
- The Sherlock CAS can distinguish not only between *C. auris* and relative species, but also among *C. auris* clades. The result of testing the performance of the method and library showed the sufficiently discriminatory power between *C. auris* clades as well as between *C. auris* and other species with high confidence. As FA-based classification, *C. auris* can be distinguished to either frequently misidentification cases including *C. famata*, *C. guilliermondii*, *C. lusitaniae*, *C. parapsilosis*, *C. intermedia*, *C. catenulata*, *C. haemulonii*, *C. sake*, and *S. kluyveri* or phylogenetically relating species including *C. catenulate*, *C. ethanolica*, *C. glabrata*, *C. guilliermondii*, *C. haemulonii*, *C. inconspicua*, *C. intermedia*, *C. krusei*, *C. lusitaniae*, *C. parapsilosis*, *C. rugosa* and *C. tropicalis*.
- The Sherlock CAS can distinguish among *Armillaria* at species level. The differentiation accuracy was 90.00% for *A. cepistipes*, 88.70% for *A. gallica*, 100.00% for *A. mellea* and 100.00% for *A.* ostoyae, respectively.

In assessing the usability of a new technique, the technical needs and conditions, the time required for implementing and running the tests, and the costs are crucial. In routine use, the technician spends about 10 minutes per sample to extract a batch of 12 pieces, then 7 minutes per *Bacillus* sample, 21 minutes per *C. auris* sample and 12 minutes per *Armillaria*

sample to operate the GC system. The actual FA profiles are always available without long waiting times. Therefore, our studies offer an easy-to-apply, cost-effective, sensitive and fast-automated technology that allows the reliable taxonomic identification of otherwise complex fungal and bacterial taxa.

9. SUMMARY

Organisms synthesize a variety of structural, storage, and signaling FAs for essential functions such as building blocks of complex lipids, energy stores, and signaling molecules. The FAS pathway is conserved, but different substrate specificities of the enzymes can lead to altering sets of FAs in different genera. For these reasons, cellular FA profiles are diverse and species-specific and may reflect differences in the biological mechanisms. The varied FAs among organisms, especially in prokaryotes, have already been considered as potential taxonomic biomarkers. The aim of our current study was to demonstrate the power of using the cellular FAs as a taxonomic and diagnostic tool with help of applying Sherlock CAS.

The genus *Bacillus* belongs to the phylum Firmicutes, class Bacilli, order Bacillales and family Bacillaceae. The *Bacillus* genera is a phylogenetically incoherent taxon and appears to be heterogeneous. From a taxonomic point of view, significant phenotypic and genotype similarities between different *Bacillus* species suggested close taxonomic relationships, so classification between *Bacillus* species posed a significant challenge. Based on our analysis, *Bacillus* species have higher branched-odd FA content, including 13:0 iso, 15:0 iso, 15:0 anteiso, 17:0 iso and 17:0 anteiso, which thus can provide a common ground for establishing the taxonomy for *Bacillus* species. The diverse FA composition gives an opportunity to differentiate *Bacillus* species and use the FAs as biomarkers. The FAME-based identification has confirmed our isolates as *B. amyloliquefaciens, B. atrophaeus, B. cereus, B. licheniformis, B. megaterium, B. pumilus, B. simplex,* and *B. subtilis*. Additionally, the available library in the MIS have contained altogether 40 *Bacillus* species, but numerous species were not included in it. During our work, based on the FA profiles of the molecularly identified isolates we constructed a new extended library, which contains the new *Bacillus* entries. For the molecular taxonomical basis, the partial sequences of *gyrA* and *rpoB* were applied. Consequently, new entries of *B. endophyticus* and *B. velezensis* were added to the original Sherlock library. The *Bacillus* species were identified with high SI (SI > 0.5) and well-SI-separations (> 0.1), confirming that these strains belong to the *Bacillus* genus with high confidence. Based on the results so far, the FA-based identification used as a biomarker can be considered as a credible differentiating factor for *Bacillus* species that works even within closely related groups. As an ultimate test, the classification based on whole-cell FAs could also distinguish between *B. velezensis* and *B. amyloliquefaciens* which were taxonomically real troublesome cases within a tightly related "*B. subtilis* species complex".

Candida auris is an emerging multidrug-resistant pathogen which has been recognized as a cause of invasive candidiasis and healthcare outbreaks worldwide, causing bloodstream

infections and other invasive and superficial infections with a high mortality rate. Currently, accurate identification of *C. auris* is critical due to problems with the conventional methods. The challenges in identifying *C. auris* underscore the importance of developing more precise and routine procedures to facilitate disease management, improve infection control, and reduce potential transmission. Then, applying the Sherlock CAS system in FA profile-based analysis and developing a reliable taxonomic identification of *C. auris* isolates became an obvious option to fulfil the expectations. According to the *C. auris* data, the FA profiles contained 16:0, 18:0, 18:1, 18:2 and some peaks of summed feature which varied among *C. auris* strains. The FA 16:0, 18:2 Cis 9,12/18:0a and Summed Feature 8 have been predominant. Cluster analysis and PC analysis of the resulting FAME profiles drew a distinction dividing 12 strains of *C. auris* into three GC subgroups. The GC subgroup A includes strains of clade I – GC subgroup A (B11109 and B8441), clade II (B11220), clade III (B11221 and B11222), and clade III (B11244 and B11245). The GC subgroup B includes strains of clade I – GC subgroup B (B11098, B11203, AR0390 and MMC-1). Besides, the GC subgroup C includes strain MMC-2. Interestingly, strains belonging to the clade could be differentiated into two distinct clusters of subgroup A (strain B11109, and B8441) and subgroup B (strain B11098, B 11203, AR0309 and MMC-1). The two clusters have represented for dissimilarity of antifungal susceptibility in the clade I. This study carefully constructed a library (CAN1) including FA components of 3 subgroups and a library (CAN2) including FA components of 12 strains from *C. auris*. The FA profiles were consistently typical and distinguishable between subgroups and clades. When using the newly created libraries, subgroups and clades of *C. auris* were distinguishable. As testing the performance of the new libraries, all identified samples exhibited good matches to *C. auris* (SI > 0.7) without misreading. As FA-based classification, *C. auris* can be distinguished to either frequently misidentification cases including *C. famata*, *C. guilliermondii*, *C. lusitaniae*, *C. parapsilosis, C. intermedia*, *C. catenulata*, *C. haemulonii*, *C. sake*, and *S. kluyveri* or phylogenetically relating species including *C. catenulate*, *C. ethanolica*, *C. glabrata*, *C. guilliermondii*, *C. haemulonii*, *C. inconspicua*, *C. intermedia*, *C. krusei*, *C. lusitaniae*, *C. parapsilosis*, *C. rugosa*, and *C. tropicalis*. The result of testing the performance of the method and library showed the sufficiently discriminatory power between *C. auris* clades as well as between *C. auris* and other species with high confidence. Our significant evidence revealed FA compositions as remarkable biomarkers, which can be applied as a classification feature of *C. auris* at both species and clade levels.

Armillaria (Basidiomycota, Agaricales, Physalacriaceae) represent a widespread pathogen of woody plants worldwide, primarily known as a pathogen of *Armillaria* root rot in

a variety of woody dicotyledonous hosts causing devastating forest damage and substantial economic losses.

In addition to acting as primary necrotrophs on woody hosts, some *Armillaria* species have also been identified as symbionts of specific orchids (*Galeola* and *Gastrodia*). Importantly, most *Armillaria* species are edible with careful preparation, and they may offer beneficial secondary metabolites and polysaccharides for biomedical applications. For example, the honey mushroom *A. mellea* is a rich source of carbohydrates, ash, fat, proteins and organic acids. Due to its exciting characteristics, a comprehensive understanding of the *Armillaria*-specific secondary metabolite and FA-related pathways is a very attractive topic to investigate. Therefore, the cultivation conditions, the FA extraction protocol, and the saponification procedure were optimized for working with *Armillaria* mycelia. Furthermore, the new method (ARMI) and a new library (ARMI) were also constructed. As FAME analyzing, FA profiles varied depending on *Armillaria* species. Accordingly, even-chain FAs have been regarded as predominant content. The linoleic acid (18:2 ω6c) was 59.51% in *A. cepistipes*, 56.43% in *A. gallica*, 53.43% in *A. mellea* and 59.76% in *A. ostoyae* regarding as the most prominent FA. As follows, the palmitic acid (16:0) was from 16.70 to 20.41% and lauric acid (12:0) was from 3.96 to 11.99%, respectively. Other FAs were identified in detectable levels (< 3%). Remarkably, the ΣPUFA presented in the highest percentage followed by ΣSFA and ΣMUFA. UFA amounts predominated over SFA in all the studied species due to the high contribution of linoleic acid. The UFA/SFA ratio presented at approximately 1.93 in *A. cepistipes*, 1.72 in *A. gallica*, 1.64 in *A. mellea* and 2.36 in *A. ostoyae*. As regards, FA composition has been diverse drawing a distinction between *Armillaria* species with FAs 12:0, 16:0, and 18:2 ω6c being most important for species separation as remarkable biomarkers. When using the new created library, FA profiles of four *Armillaria* species were clearly distinguishable with minor misidentifications. The SI for *A. cepistipes, A. gallica*, *A. mellea*, and *A. ostoyae* ranged from 0.284 to 0.935, 0.594 to 0.941, 0.431 to 0.859 and 0.301 to 0.905, respectively. Accordingly, the differentiation accuracy was 90.00% for *A. cepistipes*, 88.70% for *A. gallica*, 100.00% for *A. mellea* and 100.00% for *A. ostoyae*, respectively. Remarkably, 100.00% of samples were identified correctly without misidentification in secondary choice. As drawing a distinction between these *Armillaria* species, FA compositions can be considered as biomarkers for *Armillaria* species.

As with all routine methods, factors such as costs, technical skills, and the time involved play important roles. For the routine use, a technician averages about 10 minutes per sample for the preparation a batch of 12 samples together with 7 minutes per *Bacillus* sample, 21

minutes per *C. auris* sample, and 12 minutes per *Armillaria* sample for operating the GC system. The FA profiles are accurately delivered without a long-waiting time. Therefore, this study contributed here an applicable, cost-effective, sensitive, reliable, and fast-automated method of taxonomic identification.

10. ÖSSZEFOGLALÁS

Az élőlényekben a zsírsavak (FA) energiatároló és jelátviteli feladatokat láthatnak el, valamint különféle szerkezeti funkcióik is lehetnek, mint az összetett lipidek építőkövei. Az FA-k bioszintetikus útvonala konzervált, de az abban résztvevő enzimek eltérő szubsztrát-specificitása különböző nemzetségekben eltérő FA-kat hoz létre. Ennek a változatosságnak köszönhetően az egyes fajok között eltérőek és meglehetősen specifikusak az FA profilok, jól tükrözve a háttérben zajló biokémiai mechanizmusok különbségeit. A mikroorganizmusok – különösen a prokarióták – változatos FA-profiljai így taxonómiai biomarkerekként alkalmazhatók. A munkánk során, három kiválasztott mikroorganizmus-csoport esetében megvizsgáltuk az FA profilok taxonómiai és diagnosztikai eszközként való alkalmazásának lehetőségét a Sherlock Mikrobiológiai Identifikáló Rendszer alkalmazásával.

A *Bacillus* nemzetség a Firmicutes törzs, Bacilli osztályának, Bacillales rendjébe és Bacillaceae családjába tartozik. A *Bacillus* nemzetség filogenetikailag inkoherens és heterogén rendszertani egység. Taxonómiai szempontból azonban a különböző *Bacillus* fajok fenotípusa és genotípusa nagy fokú hasonlóságot mutat, így mindenképpen közeli rokonoknak tekinthetők. A *Bacillus* fajok rendszerezése azonban számos esetben nehezen megválaszolható kérdéseket vet fel. A Sherlock Mikrobiológiai Identifikáló Rendszerben rendelkezésre állt az RTSBA6 meghatározási módszer és a hozzátartozó RTSBA6 könyvtár a *Bacillus* izolátumok meghatározására. Az elemzéseink alapján kijelenthető, hogy a *Bacillus* fajok főként elágazó szénláncú, páratlan szénatomszámú FA-kat tartalmaztak, mint a 13:0 izo, 15:0 izo, 15:0 anteizo, 17:0 izo és a 17:0 anteizo, melyek általános bélyegek a *Bacillus* nemzetség taxonómiájában. Ezen biomarkerek mennyiségi különbségei azonban megfelelő variabilitást mutattak az egyes *Bacillus* fajok elkülönítéséhez, amelyek esetünkben a *B. amyloliquefacies*, *B. atrophaeus*, *B. cereus*, *B. endophyticus*, *B. licheniformis*, *B. megaterium*, *B. pumilus*, *B. simplex*, B. *subtilis*, és *B. velezensis* csoportokba tartoztak. Az identifikáló rendszer által rendelkezésre bocsátott RTSBA6 könyvtár azonban összesen 40 *Bacillus* fajt tartalmazott, így voltak olyan fajok, melyek ebben az alap könyvtárban nem voltak elérhetők. Munkánk során előállítottunk egy új könyvtárat, melyben az alap *Bacillus* könyvtárhoz új elemeket rendeltünk hozzá. Megerősítő analízisként elvégeztük a kérdéses törzsek *gyrA* és *rpoB* parciális szekvenciáján alapuló meghatározásait, hogy megerősítsük a vizsgált fajok taxonómiai helyzetét. Ennek segítségével a korábban a Sherlock rendszerrel nem azonosított *B. endophyticus* és *B. velezensis* törzseket is sikerült meghatározni. A nemzettségbe tartozó törzseket magas hasonlósági indexszel (SI, SI > 0,5) és a fajokat jó SI elhatárolással (> 0,1) azonosítottuk, ami megerősítette az izolátumok taxonómiai pozícióját. Továbbá az FA biomarkerekkel sikerült megkülönböztetni a közeli

rokon fajokat tartalmazó, ún. „*B. amyloliquefaciens* operatív csoport” tagjait, a más taxonómiai módszerekkel nehezen elkülöníthető *B. velezensis* és a *B. amyloliquefaciens* fajokat.

A *C. auris* élesztő faj képviselői, egyre gyakrabban előforduló, multirezisztens kórokozók, melyeket az antibiotikum rezisztencia alapján 4 kládba, taxonómiai kategóriába sorol a szakirodalom. A faj az invazív candidiazis és egyéb egészségügyi problémák okozója világszerte, véráramfertőzéseket, valamint egyéb invazív és felületi fertőzéseket is okoz, viszonylag magas halálozási aránnyal. Ennek egyik oka, hogy a *C. auris* téves diagnosztizálása meglehetősen gyakori, mivel a klinikai és közegészségügyi laboratóriumokban elérhető diagnosztikai platformok referencia-adatbázisában a faj adatai sok esetben hiányoznak. Nagy szükség van ezért olyan hatékonyan alkalmazható új és gyors diagnosztikai módszerekre, amelyek elősegítik a fertőzések elleni védekezést, megkönnyítik a hatékony betegkezelést és végső soron csökkentik a *C. auris* transzmissziójának lehetőségét. Ezért kutatásaink során megvizsgáltuk a Sherlock Mikrobiológiai Identifikáló Rendszer alkalmazásának lehetőségét a *C. auris* faj azonosításában is. A mérések alapján a faj képviselői jellemzően a 16:0, 18:0, 18:1, 18:2 FA-kat tartalmazták, ahol a 16:0, 18:2 cis 9,12/18:0a, valamint a 18:1 cis 9 (ω9) és 18:1 (ω8) FA-kat tartalmazó ún. származtatott tulajdonság domináltak. A kapott FAME-profilok klaszteranalízise és főkomponens-analízise a vizsgált 12 *C. auris* törzset három GC alcsoportra osztotta. A GC-A alcsoportba tartozott az I. klád törzseinek egy csoportja (klád I. – GC-A alcsoport) (B11109 és B8441 törzsek), II. klád (B11220 törzs), III. klád (B11221 és B11222 törzsek) és III. klád (B11244 és B11245 törzsek) képviselői. A GC-B alcsoportba tartozott az I. klád másik csoportjába (klád I. – GC-B alcsoport) tartozó törzsek (B11098, B11203, AR0390 és MMC-1). Továbbá a GC C alcsoportba tartozott az MMC-2 törzs. Az I. kládban tapasztalt két klaszter jól megfeleltethető a kládon belüli két eltérő antifungális érzékenységgel jellemezhető csoportnak. A munkánk során felépítettünk egy könyvtárat (CAN1) a Sherlock rendszerben, amely a 3 alcsoport FA komponenseit tartalmazta, és egy másikat (CAN2), amely a 12 *C. auris* törzs FA komponenseit tartalmazta. Az új könyvtárak tesztelése során megállapítható, hogy minden vizsgált izolátum jó egyezést mutatott a könyvtári *C. auris* mintázattal (SI > 0,7) és félrehatározás nem történt. Ezenkívül a *C. auris* és más könyvtári fajok közötti SI különbségek (> 0,1) is alátámasztották, hogy a módszer nagy biztonsággal alkalmazható. Téves meghatározás csak az izolátumok klád szintű azonosításánál fordult elő. Az FA-alapú meghatározás során a *C. auris* jól elkülöníthető volt a más meghatározások során nehezen megkülönböztethető a *C. famata, C. guilliermondii, C. lusitaniae, C. parapsilosis, C. intermedia, C. catenulata, C. haemulonii, C. sake* és *S. kluyver* fajoktól vagy a filogenetikailag rokon fajoktól, mint a *C. catenulate, C. ethanolica, C. glabrata, C. guilliermondii, C.*

haemulonii, *C. inconspicua*, *C. intermedia*, *C. krusei*, *C. lusitaniae*, *C. parapsilosis*, *C. rugosa* és *C. tropicalis*. A vizsgálataink összeségében azt mutatták, hogy a kifejlesztett FA-alapú azonosítási módszer jól alkalmazható a *C. auris* fajba tartozó izolátumok azonosítására.

Az *Armillaria* (Basidiomycota, Agaricales, Physalacriaceae) fajok az erdőkben, a fák gyökerén, a kéreg alatt megtalálható, világszerte elterjedt kórokozók. A nemzetség tagjai elsősorban fás szárú, kétszikű gazdaszervezetek széles körének kórokozójaként ismertek. Az *Armillaria* fajok okozta gyökérrothadás, amely a fás szárú növényeken a fehérrothadás jelenti, nagy gazdasági veszteségekkel járó hatalmas erdőkárokat okozhat. A patogenitáson túl a nemzetség egyes képviselői a *Galeola* és a *Gastrodia* orchideák szimbiontáiként is ismertek. Az *Armillaria* fajok az ehető gombák csoportját gyarapítják. Ilyen ehető gomba az *A. mellea* (gyűrűs tuskógomba), amely szénhidrátban, zsírban, fehérjében és szerves savakban is nagyon gazdag. Főként az okozott erdőpusztulások és gazdasági károk miatt fontos a nemzetség vizsgálata, melynek részét képezik a rendszertani vizsgálatok is. A nemzetség tagjait eredetileg a Sherlock rendszer nem tartalmazta, ezért az azonosítási módszer kidolgozása során a teljes mintaelőkészítési, elválasztástechnikai folyamatot is optimalizálni kellett. Az előkészítés során optimalizáltuk a rendelkezésre álló *Armillaria* fajok tenyésztési körülményeit, valamint beállítottuk az extrakciós és az elszappanosítási paramétereket. Emellett a meghatározáshoz készült egy új kromatográfiás módszer (ARMI) és egy új könyvtár (ARMI) is. A vizsgálatok igazolták, hogy a FA profilok az *Armillaria* fajok között szignifikáns eltéréseket mutatnak, melyekben a páros szénatomszámú FA-k játszák a főszerepet. A legintenzívebb csúcsot a linolsav (18:2 ω6c) adta a mintázatokban, amely 59,5% volt az *A. cepistipes* és 56,4% az *A. gallica* izolátumokban, illetve 53,4% az *A. mellea* és 59,8% az *A. ostoyae* törzsekben. Nemzetség szinten nagy mennyiségben fordult elő a palmitinsav (16:0) 16,7-20,4% és a laurinsav (12:0) 4,0-12,0% is. Más FA-kat azonban csak alacsony szinten (<3%) lehetett detektálni. Figyelemre méltó, hogy a zsírsav-csoportok tekintetében a többszörösen telítetlen zsírsavak (ΣPUFA) fordultak elő a legmagasabb százalékban, ezt követte a telített zsírsavak (ΣSFA) és az egyszeresen telített zsírsavak (ΣMUFA) mennyisége. A telítettlen zsírsavak (UFA) mennyisége minden vizsgált fajban túlsúlyban volt a telített zsírsavakkal (SFA) szemben a linolsav nagymértékű hozzájárulása miatt. Az UFA/SFA arány körülbelül 1,93 volt az *A. cepistipes*, 1,72 az *A. gallica*, 1,64 az *A. mellea* és 2,36 volt az *A. ostoyae* esetében. Az újonnan létrehozott könyvtár segítségével a négy *Armillaria* faj FA-profilja megkülönböztethető volt, de esetenként előfordultak téves azonosítások is. Az *A. cepistipes* izolátumoknál az SI értéke 0,284-0,935, *A. gallica* esetében 0,594-0,941, *A. mellea* törzseknél 0,431-0,859, míg a és *A. ostoyae* faj képviselőinél 0,301-0,905 között volt.

Mint minden rutinban alkalmazható módszernél, a Sherlock Mikrobiológiai Identifikáló Rendszer esetében is fontos szerepet játszanak a költségtényezők, a technikai háttér komplexitása, valamint az egy minta analizálásához szükséges idő. Az alkalmazott módszert tekintve, egy technikus átlagosan 60 perc alatt tudja elvégezni egy 10 egységből álló mintasorral a mintaelőkészítést, míg a GC futás időigénye 7 perc a *Bacillus,* 21 perc a *Candida* és 12 perc az *Armillaria* fajok esetében. Az általunk kifejlesztett módszerek lehetővé teszik az identifikáló rendszerhez már korábban leírt azonosítások mellett a fenti nemzetségbe tartozó fajok megbízható, gyors, és költséghatékony, valamint nagy áteresztőképességű meghatározását.

11. ACKNOWLEDGEMENTS

I am greatly thankful to my supervisors - Dr. András Szekeres, Dr. György Sipos and the Head of Department of Microbiology - Prof. Dr. Csaba Vágvölgyi for their scientific and kindly support.

In addition, I express my heartfelt gratitude to all colleagues from Department of Microbiology, Faculty of Science and Informatics, University of Szeged for helping and being friend during my Ph.D. journey.

I am thankful to the Stipendium Hungaricum scholarship for pursuing my Ph.D. in Hungary.

This work was supported by the Hungarian Government and the European Union within the frames of the Széchenyi 2020 Programme through grant GINOP-2.3.2-15-2016-00012 and by the grant OTKA K-128659 from the Hungarian Scientific Research Fund. The infrastructural background was established with the support of GINOP-2.3.3-15-2016-00006 grant.

12. REFERENCES

An, S. *et al.* (2017) "Pharmacological basis for use of *Armillaria mellea* polysaccharides in Alzheimer's disease: Antiapoptosis and antioxidation," *Oxidative Medicine and Cellular Longevity*, 2017, p. 4184562. doi: 10.1155/2017/4184562.

Bajerski, F., Wagner, D. and Mangelsdorf, K. (2017) "Cell membrane fatty acid composition of *Chryseobacterium frigidisoli* PB4T, isolated from Antarctic Glacier Forefield soils, in response to changing temperature and pH conditions," *Frontiers in Microbiology*, 8, p. 677. doi: 10.3389/fmicb.2017.00677.

Baumgartner, K., Coetzee, M. P. A. and Hoffmeister, D. (2011) "Secrets of the subterranean pathosystem of *Armillaria*," *Molecular Plant Pathology*, 12(6), pp. 515–534. doi: 10.1111/j.1364-3703.2010.00693.x.

Beld, J. *et al.* (2016) "Probing fatty acid metabolism in bacteria, cyanobacteria, green microalgae and diatoms with natural and unnatural fatty acids," *Molecular BioSystems*, 12(4), pp. 1299–1312. doi: 10.1039/c5mb00804b.

Bentivenga, S. P. and Morton, J. B. (1994) "Stability and heritability of fatty acid methyl ester profiles of glomalean endomycorrhizal fungi," *Mycological Research*, 98(12), pp. 1419–1426. doi: 10.1016/S0953-7562(09)81073-3.

Berezhnaya, A. V. *et al.* (2019) "Molecular genetic and functional analysis of the genome of bacteria *Bacillus velezensis* BIM B-439D," *Applied Biochemistry and Microbiology*, 55(4), pp. 386–396. doi: https://doi.org/10.1134/S0003683819040033.

Bhandari, V. *et al.* (2013) "Molecular signatures for *Bacillus* species: Demarcation of the *Bacillus subtilis* and *Bacillus cereus* clades in molecular terms and proposal to limit the placement of new species into the genus *Bacillus*," *International Journal of Systematic and Evolutionary Microbiology*, 63(Pt_7), pp. 2712–2726. doi: 10.1099/ijs.0.048488-0.

Borriss, R. *et al.* (2011) "Relationship of *Bacillus amyloliquefaciens* clades associated with strains DSM 7^T and FZB42^T: A proposal for *Bacillus amyloliquefaciens* subsp. *amyloliquefaciens* subsp. nov. and *Bacillus amyloliquefaciens* subsp. *plantarum* subsp. nov. based on complete genome sequence comparisons," *International Journal of Systematic and Evolutionary Microbiology*, 61(8), pp. 1786–1801. doi: https://doi.org/10.1099/ijs.0.023267-0.

Borriss, R. *et al.* (2018) "*Bacillus subtilis*, the model Gram-positive bacterium: 20 years of annotation refinement," *Microbial Biotechnology*, 11(1), pp. 3–17. doi: https://doi.org/10.1111/1751-7915.13043.

Brondz, I., Høiland, K. and Ekeberg, D. (2004) "Multivariate analysis of fatty acids in spores of higher basidiomycetes: a new method for chemotaxonomical classification of fungi," *Journal of Chromatography B*, 800(1–2), pp. 303–307. doi: 10.1016/j.jchromb.2003.07.003.

Caceres, D. H. *et al.* (2019) "*Candida auris*: A review of recommendations for detection and control in healthcare settings," *Journal of Fungi*, 5(4), p. 111. doi: 10.3390/jof5040111.

Cao, L. *et al.* (2019) "Interaction of a novel *Bacillus velezensis* (BvL03) against *Aeromonas hydrophila in vitro* and *in vivo* in grass carp," *Applied Microbiology and Biotechnology*, 103, pp. 8987–8999. doi: https://doi.org/10.1007/s00253-019-10096-7.

De Carvalho, C. C. C. R. and Caramujo, M. J. (2014) "Fatty acids as a tool to understand microbial diversity and their role in food webs of mediterranean temporary ponds," *Molecules*, 19(5), pp. 5570–5598. doi: 10.3390/molecules19055570.

De Carvalho, C. C. C. R. and Caramujo, M. J. (2018) "The various roles of fatty acids," *Molecules*, 23(10), p. 2583. doi: 10.3390/molecules23102583.

Çayan, F. *et al.* (2017) "Comparative study of fatty acids profile of wild mushroom species from turkey," *Eurasian Journal of Analytical Chemistry*, 12(3), pp. 257–263. doi: 10.12973/ejac.2017.00168a.

Centers for Disease Control and Prevention (2019) *General information about Candida auris*, *Available online*. Available at: https://www.cdc.gov/fungal/candida-auris/candida-auris-qanda.html (Accessed: September 22, 2021).

Centers for Disease Control and Prevention (2020a) *Antifungal susceptibility testing and interpretation*, *Available online*. Available at: https://www.cdc.gov/fungal/candida-auris/c-auris-antifungal.html (Accessed: September 22, 2021).

Centers for Disease Control and Prevention (2020b) *Identification of Candida auris*, *Available online*. Available at: https://www.cdc.gov/fungal/candida-auris/identification.html?CDC_AA_refVal=https%3A%2F%2Fwww.cdc.gov%2Ffungal%2Fcandida-auris%2Frecommendations.html (Accessed: September 21, 2021).

Centers for Disease Control and Prevention (2021) *Candida auris*, *Available online*. Available at: https://wwwn.cdc.gov/ARIsolateBank/Panel/PanelDetail?ID=2 (Accessed: September 24, 2021).

Chen, L. *et al.* (2019) "Towards the biological control of devastating forest pathogens from the genus *Armillaria*," *Forests*, 10(11), pp. 1–22. doi: 10.3390/f10111013.

Chen, Y. J., Chen, C. C. and Huang, H. L. (2016) "Induction of apoptosis by *Armillaria mellea* constituent armillarikin in human hepatocellular carcinoma," *OncoTargets and Therapy*, 9, pp. 4773–4783. doi: 10.2147/OTT.S103940.

Choi, J., Nam, J. and Seo, M.-H. (2021) "Complete genome sequence of *Bacillus velezensis* NST6 and comparison with the species belonging to operational group *B. amyloliquefaciens*," *Genomics*, 113(1), pp. 380–386. doi: https://doi.org/10.1016/j.ygeno.2020.12.011.

Chow, N. A. *et al.* (2019) "Potential fifth clade of *Candida auris*, Iran, 2018," *Emerging Infectious Diseases*, 25(9), pp. 1780–1781. doi: 10.3201/eid2509.190686.

Coetzee, M. P. A. *et al.* (2011) "Paleogene radiation of a plant pathogenic mushroom," *PLoS ONE*, 6(12), p. e28545. doi: 10.1371/journal.pone.0028545.

da Costa, M. S. *et al.* (2011) "The identification of fatty acids in bacteria," in *Methods in Microbiology*. Elsevier Ltd, pp. 183–196. doi: 10.1016/B978-0-12-387730-7.00008-5.

Cox, K. D., Scherm, H. and Riley, M. B. (2006) "Characterization of *Armillaria* spp. from peach orchards in the southeastern United States using fatty acid methyl ester profiling," *Mycological Research*, 110(Pt 4), pp. 414–422. doi: 10.1016/j.mycres.2005.12.004.

Cronan, J. E. and Thomas, J. (2009) "Bacterial fatty acid synthesis and its relationships with polyketide synthetic pathways," in *Methods in Enzymology*. 1st ed. Elsevier Inc., pp. 395–433. doi: 10.1016/S0076-6879(09)04617-5.

Dahl, M. K. (1999) "*Bacillus*," in *Encyclopedia of Food Microbiology*. 1st ed. Germany: Elsevier, pp. 135–141. doi: 10.1006/rwfm.1999.0120.

Diomandé, S. E. *et al.* (2015) "Role of fatty acids in *Bacillus* environmental adaptation," *Frontiers in Microbiology*, 6, p. 813. doi: https://doi.org/10.3389/fmicb.2015.00813.

Drakulic, J. *et al.* (2017) "Associations between *Armillaria* species and host plants in U.K.

gardens," *Plant Disease*, 101(11), pp. 1903–1909. doi: 10.1094/PDIS-04-17-0472-RE.

Dunlap, C. A. *et al.* (2015) "Phylogenomic analysis shows that *Bacillus amyloliquefaciens* subsp. *plantarum* is a later heterotypic synonym of *Bacillus methylotrophicus*," *International Journal of Systematic and Evolutionary Microbiology*, 65(Pt_7), pp. 2104–2109. doi: https://doi.org/10.1099/ijs.0.000226.

Dunlap, C. A. *et al.* (2016) "*Bacillus velezensis* is not a later heterotypic synonym of *Bacillus amyloliquefaciens*; *Bacillus methylotrophicus*, *Bacillus amyloliquefaciens* subsp. *plantarum* and '*Bacillus oryzicola*' are later heterotypic synonyms of *Bacillus velezensis* based on phylogenomics," *International Journal of Systematic and Evolutionary Microbiology*, 66(3), pp. 1212–1217. doi: https://doi.org/10.1099/ijsem.0.000858.

Ehling-Schulz, M., Lereclus, D. and Koehler, T. M. (2019) "The *Bacillus cereus* group: *Bacillus* species with pathogenic potential," in *Gram-Positive Pathogens*. Washington, DC, USA: ASM Press, pp. 875–902. doi: 10.1128/9781683670131.ch55.

Emam, A. M. and Dunlap, C. A. (2020) "Genomic and phenotypic characterization of *Bacillus velezensis* AMB-y1; a potential probiotic to control pathogens in aquaculture," *Antonie van Leeuwenhoek*, 113, pp. 2041–2052. doi: https://doi.org/10.1007/s10482-020-01476-5.

Engels, B. *et al.* (2021) "Isolation of a gene cluster from *Armillaria gallica* for the synthesis of armillyl orsellinate–type sesquiterpenoids," *Applied Microbiology and Biotechnology*, 105(1), pp. 211–224. doi: 10.1007/s00253-020-11006-y.

Fan, B. *et al.* (2017) "*Bacillus amyloliquefaciens*, *Bacillus velezensis*, and *Bacillus siamensis* form an 'Operational Group *B. amyloliquefaciens*' within the *B. subtilis* species complex," *Frontiers in Microbiology*, 8, p. 22. doi: https://doi.org/10.3389/fmicb.2017.00022.

Fan, B. *et al.* (2018) "*Bacillus velezensis* FZB42 in 2018: The Gram-positive model strain for plant growth promotion and biocontrol," *Frontiers in Microbiology*, 9, p. 2491. doi: https://doi.org/10.3389/fmicb.2018.02491.

Fukumoto, J. (1943) "Studies on the production of bacterial amylase. I. Isolation of bacteria secreting potent amylases and their distribution," *Journal of the agricultural chemical society of Japan*, 19(7), pp. 487–503. doi: https://doi.org/10.1271/nogeikagaku1924.19.7_487.

Geiger, O. (2019) *Biogenesis of fatty acids, lipids and membranes*. 1st ed. Edited by K. N. Timmis et al. Springer International Publishing. doi: 10.1007/978-3-319-50430-8.

Geng, W. *et al.* (2011) "Complete genome sequence of *Bacillus amyloliquefaciens* LL3, which exhibits glutamic acid-independent production of poly-γ-glutamic acid," *Journal of Bacteriology*, 193(13), pp. 3393–3394. doi: https://doi.org/10.1128/JB.05058-11.

Grady, E. N. *et al.* (2019) "Characterization and complete genome analysis of the surfactin-producing, plant-protecting bacterium *Bacillus velezensis* 9D-6," *BMC Microbiology*, 19, p. 5. doi: https://doi.org/10.1186/s12866-018-1380-8.

Heleno, S. A. *et al.* (2009) "Study and characterization of selected nutrients in wild mushrooms from Portugal by gas chromatography and high performance liquid chromatography," *Microchemical Journal*, 93(2), pp. 195–199. doi: 10.1016/j.microc.2009.07.002.

Herbst, D. A., Townsend, C. A. and Maier, T. (2018) "The architectures of iterative type I PKS and FAS," *Natural Product Reports*, 35(10), pp. 1046–1069. doi: 10.1039/c8np00039e.

Hussain, S. A. *et al.* (2020) "Increased accumulation of medium-chain fatty acids by dynamic degradation of long-chain fatty acids in *Mucor circinelloides*," *Genes*, 11(8), p. 890. doi: 10.3390/genes11080890.

Huynh, T. *et al.* (2022) "Discrimination between the Two Closely Related Species of the Operational Group *B. amyloliquefaciens* Based on Whole-Cell Fatty Acid Profiling," *Microorganisms*, 10(2). doi: 10.3390/microorganisms10020418.

Iguchi, S. *et al.* (2019) "*Candida auris*: A pathogen difficult to identify, treat, and eradicate and its characteristics in Japanese strains," *Journal of Infection and Chemotherapy*, 25(10), pp. 743–749. doi: 10.1016/j.jiac.2019.05.034.

Jagtap, S. S. *et al.* (2014) "Characterization of a novel endo-β-1,4-glucanase from *Armillaria gemina* and its application in biomass hydrolysis," *Applied Microbiology and Biotechnology*, 98(2), pp. 661–669. doi: 10.1007/s00253-013-4894-x.

Jeffery-Smith, A. *et al.* (2018) "*Candida auris*: A review of the literature," *Clinical Microbiology Reviews*, 31(1), pp. 1–18. doi: 10.1128/CMR.00029-17.

Jenson, I. (2014) "*Bacillus*| Introduction," in Batt, C. A. and Tortorello, M. Lou (eds.) *Encyclopedia of Food Microbiology*. 2nd ed. Academic Press, pp. 111–117. doi: 10.1016/B978-0-12-384730-0.00018-5.

Jing, N. *et al.* (2012) "Determination of fatty acids from mushrooms using high performance liquid chromatography with fluorescence detection and online mass spectrometry," *Food Research International*, 48(1), pp. 155–163. doi: 10.1016/j.foodres.2012.02.014.

Kavishree, S. *et al.* (2008) "Fat and fatty acids of Indian edible mushrooms," *Food Chemistry*, 106(2), pp. 597–602. doi: 10.1016/j.foodchem.2007.06.018.

Keighley, C. *et al.* (2021) "*Candida auris*: Diagnostic challenges and emerging opportunities for the clinical microbiology laboratory," *Current Fungal Infection Reports*, 15(3), pp. 116–126. doi: 10.1007/s12281-021-00420-y.

de Kluijver, A. *et al.* (2021) "Bacterial precursors and unsaturated long-chain fatty acids are biomarkers of North-Atlantic deep-sea demosponges," *PLoS ONE*, 16(1), p. e0241095. doi: 10.1371/journal.pone.0241095.

Koch, R. A. *et al.* (2017) "Resolved phylogeny and biogeography of the root pathogen *Armillaria* and its gasteroid relative, *Guyanagaster*," *BMC Evolutionary Biology*, 17(1), p. 33. doi: 10.1186/s12862-017-0877-3.

Kordalewska, M. and Perlin, D. S. (2019) "Identification of drug resistant *Candida auris*," *Frontiers in Microbiology*, 10, p. 1918. doi: 10.3389/fmicb.2019.01918.

Kostić, M. *et al.* (2017) "Chemical, nutritive composition and a wide range of bioactive properties of honey mushroom: *Armillaria mellea* (Vahl: Fr.) Kummer," *Food and Function*, 8(9), pp. 3239–3249. doi: 10.1039/c7fo00887b.

Kubiak, K. *et al.* (2017) "*Armillaria* pathogenesis under climate changes," *Forests*, 8(100), pp. 1–15. doi: 10.3390/f8040100.

Kumar S., Stecher G., Li M., Knyaz C., and T. K. (2018) "MEGA X: Molecular Evolutionary Genetics Analysis across computing platforms," *Molecular Biology and Evolution*, 35, pp. 1547–1549. doi: https://doi.org/10.1093/molbev/msy096.

Kunitsky, C., Gerard, O. and Sasser, M. (2006) "Identification of microorganisms using fatty acid methyl ester (FAME) analysis and the MIDI Sherlock Microbial Identification System," *Encyclopedia of Rapid Microbiological Methods*, pp. 1–18.

Kwon, Y. J. *et al.* (2019) "*Candida auris* clinical isolates from South Korea: Identification, Antifungal Susceptibility, and Genotyping," *Journal of Clinical Microbiology Microbiol*, 57,

pp. e01624-18. doi: https://doi.org/10.1128/JCM.01624-18.

Li, Yanyan *et al.* (2010) "Differentiation of bacteria using fatty acid profiles from gas chromatography-tandem mass spectrometry," *Journal of the Science of Food and Agriculture*, 90(8), pp. 1380–1383. doi: 10.1002/jsfa.3931.

Lim, S. B. Y. *et al.* (2018) "Genome sequence of *Bacillus velezensis* SGAir0473, isolated from tropical air collected in Singapore," *Genome Announcements*, 6(27), pp. e00642-18. doi: https://doi.org/10.1128/genomeA.00642-18.

Lockhart, S. R. *et al.* (2017) "Simultaneous emergence of multidrug-resistant *Candida auris* on 3 continents confirmed by whole-genome sequencing and epidemiological analyses," *Clinical Infectious Diseases*, 64(2), pp. 134–140. doi: 10.1093/cid/ciw691.

Lu, Y. J., Zhang, Y. M. and Rock, C. O. (2004) "Product diversity and regulation of type II fatty acid synthases," *Biochemistry and Cell Biology*, 82(1), pp. 145–155. doi: 10.1139/o03-076.

McIntyre, A. B. R. *et al.* (2019) "Single-molecule sequencing detection of N6-methyladenine in microbial reference materials," *Nature Communications*, 10(1), pp. 1–11. doi: https://doi.org/10.1038/s41467-019-08289-9.

MIDI Inc. (2017) *Microbial identification using automated fatty acid methyl ester (FAME) analysis on a Shimadzu GC-2010/2030*.

MIDI Inc. (2018) *The Sherlock Chromatographic Analysis System Operating Manual*. 6th ed. Newark, DE, USA: MIDI, Inc.

Mukhopadhyay, K. *et al.* (2004) "Membrane Sphingolipid-Ergosterol interactions are important determinants of multidrug resistance in *Candida albicans*," *Antimicrobial Agents and Chemotherapy*, 48(5), pp. 1778–1787. doi: 10.1128/AAC.48.5.1778-1787.2004.

Mukhopadhyay, K., Kohli, A. and Prasad, R. (2002) "Drug susceptibilities of yeast cells are affected by membrane lipid composition," *Antimicrobial Agents and Chemotherapy*, 46(12), pp. 3695–3705. doi: 10.1128/AAC.46.12.3695-3705.2002.

Muñoz, J. F. *et al.* (2018) "Genomic insights into multidrug-resistance, mating and virulence in *Candida auris* and related emerging species," *Nature Communications*, 9, p. 5346. doi: 10.1038/s41467-018-07779-6.

Muñoz, J. F. *et al.* (2021) "Clade-specific chromosomal rearrangements and loss of subtelomeric adhesins in *Candida auris*," *Genetics*, 218(1), p. iyab029. doi: 10.1093/genetics/iyab029.

Nasrin, S., Hossain, M. J. and Liles, M. R. (2016) "Draft genome sequence of *Bacillus amyloliquefaciens* AP183 with antibacterial activity against methicillin-resistant *Staphylococcus aureus*," *Genome Announcements*, 3(2), pp. e00162-15. doi: https://doi.org/10.1128/genomeA.00162-15.

O'Leary, W. M. (1962) "The fatty acids of bacteria," *Bacteriological Reviews*, 26(4), pp. 421–447. doi: 10.1128/mmbr.26.4.421-447.1962.

Pan, J., Hu, C. and Yu, J. H. (2018) "Lipid biosynthesis as an antifungal target," *Journal of Fungi*, 4(2), p. 50. doi: 10.3390/jof4020050.

Patel, M. J., Tipre, D. R. and Dave, S. R. (2009) "Isolation and identification of a *Candida digboiensis* strain from an extreme acid mine drainage of the Lignite Mine, Gujarat," *Journal of Basic Microbiology*, 49(6), pp. 564–571. doi: 10.1002/jobm.200900084.

Peltroche-llacsahuanga, H. *et al.* (2000) "Differentiation between *Candida dubliniensis* and *Candida albicans* by Fatty Acid Methyl Ester analysis using Gas-Liquid Chromatography," *Journal of Clinical Microbiology*, 38(10), pp. 3696–3704. doi: 10.1128/JCM.38.10.3696-3704.2000.

Peltroche-Llacsahuanga, H. *et al.* (2000) "Discriminative power of fatty acid methyl ester (FAME) analysis using the Microbial Identification System (MIS) for *Candida* (*Torulopsis*) glabrata and Saccharomyces cerevisiae," *Diagnostic Microbiology and Infectious Disease*, 38(4), pp. 213–221. doi: 10.1016/S0732-8893(00)00205-4.

Perez, K. J. *et al.* (2017) "*Bacillus* spp. isolated from puba as a source of biosurfactants and antimicrobial lipopeptides," *Frontiers in Microbiology*, 8, p. 61. doi: https://doi.org/10.3389/fmicb.2017.00061.

Priest, F. G. *et al.* (1987) "*Bacillus amyloliquefaciens* sp. nov., nom. rev.," *International Journal of Systematic Bacteriology*, 37(1), pp. 69–71. doi: https://doi.org/10.1099/00207713-37-1-69.

Rabbee, M. *et al.* (2019) "*Bacillus velezensis*: A valuable member of bioactive molecules within plant microbiomes," *Molecules*, 24(6), p. 1046. doi: 10.3390/molecules24061046.

Rabbee, M. F. *et al.* (2019) "*Bacillus velezensis*: A valuable member of bioactive molecules within plant microbiomes," *Molecules*, 24(6), p. 1046. doi: https://doi.org/10.3390/molecules24061046.

Reva, O. N. *et al.* (2004) "Taxonomic characterization and plant colonizing abilities of some bacteria related to *Bacillus amyloliquefaciens* and *Bacillus subtilis*," *FEMS Microbiology Ecology*, 48(2), pp. 249–259. doi: https://doi.org/10.1016/j.femsec.2004.02.003.

Reva, O. N. *et al.* (2019) "Genetic, epigenetic and phenotypic diversity of four *Bacillus velezensis* strains used for plant protection or as probiotics," *Frontiers in Microbiology*, 10, p. 2610. doi: https://doi.org/10.3389/fmicb.2019.02610.

Roberts, M. S., Nakamura, L. K. and Cohan, F. M. (1994) "*Bacillus mojavensis* sp. nov., distinguishable from *Bacillus subtilis* by sexual isolation, divergence in DNA sequence, and differences in fatty acid composition," *International Journal of Systematic Bacteriology*, 44(2), pp. 256–264. doi: https://doi.org/10.1099/00207713-44-2-256.

Rock, C. O. (2008) "Fatty acid and phospholipid metabolism in prokaryotes," in *Biochemistry of Lipids, Lipoproteins and Membranes*. 5th ed. Elsevier Inc., pp. 60–96. doi: 10.1016/B978-0-444-63438-2.00003-1.

Rock, C. O. and Jackowski, S. (2002) "Forty years of bacterial fatty acid synthesis," *Biochemical and Biophysical Research Communications*, 292(5), pp. 1155–1166. doi: 10.1006/bbrc.2001.2022.

Ruiz-García, C. *et al.* (2005) "*Bacillus velezensis* sp. nov., a surfactant-producing bacterium isolated from the river Vélez in Málaga, southern Spain," *International Journal of Systematic and Evolutionary Microbiology*, 55(1), pp. 191–195. doi: https://doi.org/10.1099/ijs.0.63310-0.

Saitou N. and Nei M. (1987) "The neighbor-joining method: A new method for reconstructing phylogenetic trees," *Molecular Biology and Evolution*, 4, pp. 406–425. doi: https://doi.org/10.1093/oxfordjournals.molbev.a040454.

Satoh, K. *et al.* (2009) "*Candida auris* sp. nov., a novel ascomycetous yeast isolated from the external ear canal of an inpatient in a Japanese hospital," *Microbiology and Immunology*, 53(1),

pp. 41–44. doi: 10.1111/j.1348-0421.2008.00083.x.

Schujman, G. E. and de Mendoza, D. (2008) "Regulation of type II fatty acid synthase in Gram-positive bacteria," *Current Opinion in Microbiology*, 11(2), pp. 148–152. doi: 10.1016/j.mib.2008.02.002.

Schweizer, E. and Hofmann, J. (2004) "Microbial type I fatty acid synthases (FAS): major players in a network of cellular FAS systems," *Microbiology and Molecular Biology Reviews*, 68(3), pp. 501–517. doi: 10.1128/MMBR.68.3.501.

Shimadzu (2020) *Basics & Fundamentals: Gas Chromatography, Shimadzu Corporation*. Shimadzu. Available at: www.shimadzu.com.

Sibponkrung, S. *et al.* (2017) "Genome sequence of *Bacillus velezensis* S141, a new strain of plant growth-promoting rhizobacterium isolated from soybean rhizosphere," *Genome Announcements*, 5(48), pp. e01312-17. doi: https://doi.org/10.1128/genomeA.01312-17.

Sinanoglou, V. J. *et al.* (2015) "Lipid and fatty acid profile of the edible fungus *Laetiporus sulphurous*. Antifungal and antibacterial properties," *Journal of Food Science and Technology*, 52(6), pp. 3264–3272. doi: 10.1007/s13197-014-1377-8.

Singh, K. *et al.* (2020) "Discovery of a regulatory subunit of the yeast fatty acid synthase," *Cell Press*, 180(6), pp. 1130–1143. doi: 10.1016/j.cell.2020.02.034.

Sipos, G., Anderson, J. B. and Nagy, L. G. (2018) "*Armillaria*," *Current Biology*, pp. R297–R298. doi: 10.1016/j.cub.2018.01.026.

Spivak, E. S. and Hanson, K. E. (2018) "*Candida auris*: An emerging fungal pathogen," *Journal of Clinical Microbiology*, 56(2), pp. 1–10. doi: 10.1128/JCM.01588-17.

Stefanic, P. and Mandic-Mulec, I. (2009) "Social interactions and distribution of *Bacillus subtilis* pherotypes at microscale," *Journal of Bacteriology*, 191(6), pp. 1756–1764. doi: https://doi.org/10.1128/JB.01290-08.

Stillwell, W. (2013) "Membrane lipids: fatty acids," in *An Introduction to Biological Membranes*. Elsevier Inc., pp. 43–56. doi: 10.1016/B978-0-444-52153-8.00004-0.

Sugita, K. and Sato, H. (2021) "Sample introduction method in Gas Chromatography," *Analytical Sciences*, 37(1), pp. 159–165. doi: 10.2116/ANALSCI.20SAR19.

Taipale, S. *et al.* (2013) "Fatty acid composition as biomarkers of freshwater microalgae: Analysis of 37 strains of microalgae in 22 genera and in seven classes," *Aquatic Microbial Ecology*, 71(2), pp. 165–178. doi: 10.3354/ame01671.

Tamura K. and Nei M. (1993) "Estimation of the number of nucleotide substitutions in the control region of mitochondrial DNA in humans and chimpanzees," *Molecular Biology and Evolution*, 10, pp. 512–526. doi: https://doi.org/10.1093/oxfordjournals.molbev.a040023.

Tang, B. and Row, K. H. (2013) "Development of gas chromatography analysis of fatty acids in marine organisms," *Journal of Chromatographic Science*, 51(7), pp. 599–607. doi: 10.1093/chromsci/bmt005.

Vágvölgyi, C. *et al.* (2013) "Isolation and characterization of antagonistic *Bacillus* strains capable to degrade ethylenethiourea," *Current Microbiology*, 66(3), pp. 243–250. doi: https://doi.org/10.1007/s00284-012-0263-8.

Váradi, O. A. *et al.* (2021) "Verification of tuberculosis infection among Vác mummies (18th century CE, Hungary) based on lipid biomarker profiling with a new HPLC-HESI-MS approach," *Tuberculosis*, 126. doi: 10.1016/j.tube.2020.102037.

Wang, J. *et al.* (2019) "Complete genome sequencing of *Bacillus velezensis* WRN014, and comparison with genome sequences of other *Bacillus velezensis* strains," *Journal of Microbiology and Biotechnology*, 29(5), pp. 794–808. doi: https://doi.org/10.4014/jmb.1901.01040.

Wang, L. T. *et al.* (2008) "*Bacillus velezensis* is a later heterotypic synonym of *Bacillus amyloliquefaciens*," *International Journal of Systematic and Evolutionary Microbiology*, 58(3), pp. 671–675. doi: https://doi.org/10.1099/ijs.0.65191-0.

Willers, C., Jansen van Rensburg, P. J. and Claassens, S. (2015) "Phospholipid fatty acid profiling of microbial communities-a review of interpretations and recent applications," *Journal of Applied Microbiology*, 119(5), pp. 1207–1218. doi: 10.1111/jam.12902.

Xu, D. and Côté, J. C. (2003) "Phylogenetic relationships between *Bacillus* species and related genera inferred from comparison of 3′ end 16S rDNA and 5′ end 16S-23S ITS nucleotide sequences," *International Journal of Systematic and Evolutionary Microbiology*, 53(Pt 3), pp. 695–704. doi: 10.1099/ijs.0.02346-0.

Yafetto, L., Davis, D. J. and Money, N. P. (2009) "Biomechanics of invasive growth by *Armillaria* rhizomorphs," *Fungal Genetics and Biology*, 46(9), pp. 688–694. doi: 10.1016/j.fgb.2009.04.005.

Yang, H. *et al.* (2011) "Complete genome sequence of *Bacillus amyloliquefaciens* XH7, which exhibits production of purine nucleosides," *Journal of Bacteriology*, 193(19), pp. 5593–5594. doi: https://doi.org/10.1128/JB.05880-11.

Zamith-Miranda, D. *et al.* (2019) "Multi-omics signature of *Candida auris*, an emerging and multidrug-resistant pathogen," *mSystems*, 4(4), pp. e00257-19. doi: https://doi.org/10.1128/mSystems.00257-19.

Zamith-Miranda, D. *et al.* (2021) "Comparative molecular and immunoregulatory analysis of extracellular vesicles from *Candida albicans* and *Candida auris*," *mSystems*, 6(4), pp. e00822-21. doi: 10.1128/msystems.00822-21.

Zhang, D. *et al.* (2019) "*Bacillus velezensis* LF01: *in vitro* antimicrobial activity against fish pathogens, growth performance enhancement, and disease resistance against streptococcosis in Nile tilapia (Oreochromis niloticus)," *Applied Microbiology and Biotechnology*, 103(21–22), pp. 9023–9035. doi: 10.1007/s00253-019-10176-8.

Zhang, G. *et al.* (2011) "Complete genome sequence of *Bacillus amyloliquefaciens* TA208, a strain for industrial production of guanosine and ribavirin," *Journal of Bacteriology*, 193(12), pp. 3142–3143. doi: https://doi.org/10.1128/JB.00440-11.

13. LIST OF PUBLICATIONS

13.1 Publications related to this thesis

Thu Huynh, Mónika Vörös, Orsolya Kedves, Adiyadolgor Turbat, György Sipos, Balázs Leitgeb, László Kredics, Csaba Vágvölgyi, András Szekeres, Discrimination between the two closely related species of the operational group *B. amyloliquefaciens* based on whole-cell fatty acid profiling, Microorganisms, 10(2), 418, 2022. **IF: 4.128**

Adiyadolgor Turbat, Dávid Rakk, Aruna Vigneshwari, Sándor Kocsubé, **Thu Huynh**, Ágnes Szepesi, László Bakacsy, Biljana D. Škrbic, Enkh-Amgalan Jigjiddorj, Csaba Vágvölgyi and András Szekeres, Characterization of the plant growth-promoting activities of endophytic fungi isolated from *Sophora flavescens*, Microorganisms, 8(5), 683, 2020. **IF: 4.128**

Thu Huynh, Mónika Vörös, Balázs Leitgeb, Csaba Vágvölgyi, András Szekeres, Discrimination between two *Bacillus* species based on whole-cell fatty acid profiles, Acta Microbiologica et Immunologica Hungarica, Volume 68: Issue Supplement-1, 2021.

András Szekeres, Attila Bartal, **Thu Huynh**, Mónika Vörös, Csaba Vágvölgyi, Surfactin production of *Bacillus* strains isolated from rhizosphere of various vegetables, Acta Microbiologica et Immunologica Hungarica, Volume 68: Issue Supplement-1, 2021

György Sipos, László Kredics, Liqiong Chen, Neha Sahu, Arun Prasanna, Simang Champramary, Orsolya Kedves, Boris Indic, Garima Raj, Bendegúz Richárd Nyikos, **Thu Huynh**, Sándor Kocsubé, Mónika Vörös, Tamás Marik, Viktor Dávid Nagy, András Szekeres, Martin Münsterkötter, Bettina Bencsik-Bóka, Attila Szűcs, Chetna Tyagi, Zsolt Merényi, Csaba Vágvölgyi, László Nagy, Az erdészeti kártevő *Armillaria* (tuskógomba) nemzetség patológiája és a biológiai védekezés lehetőségei. Sopron, Magyarország: Soproni Egyetem Kiadó (2021), 16 p.

Bettina Bencsik-Bóka, Neha Sahu, **Thu Huynh**, Orsolya Kedves, Zsolt Merényi, Gábor Kovác, Liqiong Chen, Simang Champramary, Zoltán Patocskai, Martin Münsterkötter, Csaba Vágvölgyi, László Nagy, György Sipos, László Kredics Classical and 'omics' approaches towards the biological control of devastating forest pathogens from the genus *Armillaria*. In: A Magyar Mikrobiológiai Társaság 2018. évi Nagygyűlése és a XIII. Fermentációs Kollokvium : Abstractbook (2018) 70 p. p. 6

László Kredics, Neha Sahu, **Thu Huynh**, Orsolya Kedves, Zsolt Merényi, Gábor Kovács, Liqiong Chen, Bettina Bóka, Zoltán Patocskai, Martin Münsterkötter, Csaba Vágvölgyi, László Nagy, György Sipos. Devastating forest pathogens from the genus *Armillaria*: from genomics to biocontrol. In: Grenni, P; Fernández-López, M; Mercado-Blanco, J Soil biodiversity and European woody agroecosystem Rome, Italy: Water Research institute, National Research Council of Italy (2018) pp. 48-49, 2 p.

Sum IF: 8.256

13.2. Other publications

Mounir Raji, Tam Minh Le, **Thu Huynh**, András Szekeres, István Zupkó, Zsolt Szakonyi, Divergent Synthesis, Antiproliferative and Antimicrobial Studies of 1,3-Aminoalcohol and 3-Amino-1,2-Diol Based Diaminopyrimidines. Chemistry & Biodiversity (1612-1872 1612-1880): 22 Paper e202200077., 2022. **IF: 2.408**

Tam Minh Le, **Thu Huynh**, Fatima Zahra Bamou , András Szekeres, Ferenc Fülöp and Zsolt

Szakonyi, Novel (+)-neoisopulegol-based O-benzyl Derivatives as antimicrobial agents, International Journal of Molecular Sciences, 22(11), 5626, 2021. **IF: 5.923**

Tam Minh Le, **Thu Huynh**, Gabor Endre, Andras Szekeres, Ferenc Fulop and Zsolt Szakonyi, Stereoselective synthesis and application of isopulegol-based bi- and trifunctional chiral compounds, RSC Advances, 10(63), 38468-38477, 2020. **IF**: **3.361**

Liqiong Chen, Bettina Bóka, Orsolya Kedves, Viktor Dávid Nagy, Attila Szucs, Simang Champramary, Róbert Roszik, Zoltán Patocskai, Martin Münsterkötter, **Thu Huynh**, Boris Indic, Csaba Vágvölgyi, György Sipos and László Kredics, Towards the biological control of devastating forest pathogens from the genus *Armillaria*, Forests, 10(11), 1013, 2019. **IF: 2.221**

Sum IF: 13.913

Cumulative IF: 22.169

14. APPENDICES

Table S1. Fatty acids used as biomarkers (Kunitsky, Gerard and Sasser, 2006; De Carvalho and Caramujo, 2014, 2018; Willers, Jansen van Rensburg and Claassens, 2015)

Fatty Acid	IUPAC Systematic Name	Other names	Category
Straight-chain saturated fatty acids			
14:0		Myristic acid	General bacterial marker
15:0			
16:0		Palmitic acid	
17:0			
18:0		Stearic acid	
Mono-unsaturated fatty acids (MUFA)			
14:1ω5c			Gram-negative bacteria
15:1			
15:1ω6c			
16:1ω7t			
16:1ω9c			
16:1ω11c			
16:1ω7c	(9Z)-9-Hexadecenoic acid	Palmitoleic acid	Gram-negative bacteria Bacillariophyceae (diatoms) Cyanophyceae (cyanobacteria) Prymnesiophyceae
16:1ω5c	(11Z)-11-Hexadecenoic acid	cis-11-Palmitoleic acid	Arbuscular mycorrhizal fungi
16:1ω5t			Type I methanotrophs (gamma-proteobacteria) Methylococcaceae
16:1ω8	(8Z)-8-Hexadecenoic acid	cis-8-Palmitoleic acid	
17:1	cis-10-Heptadecenoic acid	Heptadecenoic acid	Cyanobacteria
17:1ω5			Sulphate reducing bacteria
17:1ω6c	(11Z)-11-Heptadecenoic acid	--	
17:1ω8			
18:1ω5c			Gram-negative bacteria
18:1ω9c	(9Z)-9-Octadecenoic acid	Oleic acid	Chlorophyceae (green algae) Cyanophyceae Dinophyceae Prymnesiophyceae Gram-positive bacteria Fungi
18:1ω7c	(11Z)-11-Octadecenoic acid	cis-Vaccenic acid	Gram-negative bacteria Lactobacilli Bacillariophyceae Cryptophyceae Cyanophyceae Prymnesiophyceae
18:1ω7t	(11E)-11-octadecenoic acid	trans-vaccenic acid	Gram-negative bacteria
18:1ω8c	(10Z)-10-Octadecenoic acid	cis-10-Oleic acid	Type II methanotrophs (α-proteobacteria) Methylocystaceae Beijerinckiaceae
19:1ω9c			Gram-negative bacteria
19:1ω12c			
20:1ω9c			
20:1ω9t			
22:1ω9c			
22:1ω9t			

Fatty Acid	IUPAC Systematic Name	Other names	Category
Hydroxy substituted fatty acids			
2OH 12:0			Gram-negative bacteria
3OH 12:0			
2OH 14:0			
3OH 14:0			
2OH 16:0			
2OH 18:0			
Cyclopropyl saturated fatty acids			
cy17:0			Gram-negative bacteria Anaerobic bacteria Sulphate reducing bacteria
cy19:0			
	Iso- and anteiso-branched Fatty Acids		Gram-positive bacteria Sulphate reducing bacteria
	Terminally branched fatty acids		Gram-positive bacteria
	Methyl-branched Fatty Acids		Actinomycetales (Actinobacteria) Sulphate reducing bacteria Cyanobacteria
10Me16:0			Actinomycetales (Actinobacteria)
10Me17:0			
10Me18:0			
Furan fatty acids			Dehalococcoides
Polyunsaturated fatty acids (PUFA)			
16:2ω4	9,12-cis-hexadecadienoic acid	--	Bacillariophyceae Prasinophyceae Cyanobacteria Diatoms Green algae Fungi
16:2ω6	(2E,4E)-hexadeca-2,4-dienoic acid	Hexadecadienoic acid	Chlorophyta Cyanobacteria Diatoms Green algae
16:2ω7			Bacillariophyceae Cyanobacteria Diatoms Green algae
16:3ω3	hexadeca-2,4,6-trienoic acid	Hexadecatrienoic acid	Chlorophyta Cyanobacteria Diatoms Green algae
16:3ω4	6,9,12-hexadecatrienoic acid	--	Bacillariophyceae Cyanobacteria Diatoms Green algae
16:4ω1	6,9,12,15-hexadecatetraenoic acid	--	Cyanobacteria Diatoms Green algae
16:4ω3	(2E,4E,6E,8E)-hexadeca-2,4,6,8-tetraenoic acid	hexadecatetraenoic acid	Chlorophyceae Prasinophyceae Cyanobacteria Diatoms Green algae
18:2ω6	(9Z,12Z)-octadeca-9,12-dienoic acid	linoleic acid	Chlorophyta Cyanophyceae (freshwater) Dinophyceae Prymnesiophyceae Fungi Saprotrophic fungi

Fatty Acid	IUPAC Systematic Name	Other names	Category
18:2ω9c	6(Z),9(Z)-Octadecadienoic acid	6,9-linoleic acid	Saprotrophic fungi
18:3ω6	(6Z,9Z,12Z)-octadeca-6,9,12-trienoic acid	γ-linoleic acid	Cyanophyceae (freshwater) Saprophytic fungi
18:3ω3	(9Z,12Z,15Z)-octadeca-9,12,15-trienoic acid	α-linolenic acid	Chlorophyceae Crypophyceae Cyanophyceae Dinophyceae Prasinophyceae Prymnesiophyceae Fungi
18:4ω3	(6Z,9Z,12Z,15Z)-octadeca-6,9,12,15-tetraenoic acid	Stearidonic acid	Various algal groups (both marine and freshwater) Cyanobacteria Diatoms Green algae
18:5ω3	(3Z,6Z,9Z,12Z,15Z)-3,6,9,12,15-Octadecapentaenoic acid	Octadecapentaenoic acid	Dynophyceae Cyanobacteria Diatoms Green algae
20:4ω6	(5Z,8Z,11Z,14Z)-icosa-5,8,11,14-tetraenoic acid	Arachidonic acid	Bacillariophyceae Rhodophyceae Cyanobacteria Diatoms Green algae
20:5ω3	(5Z,8Z,11Z,14Z,17Z)-icosa-5,8,11,14,17-pentaenoic acid	Eicosapentaenoic acid	Bacillariophyceae Cryptophyceae Dinophyceae Pavlovophyceae Rhodophyceae Cyanobacteria Diatoms Green algae
22:5ω3	(7Z,10Z,13Z,16Z,19Z)-docosa-7,10,13,16,19-pentaenoic acid	Docosapentaenoic acid	Bacillariophyceae Cryptophyceae Prasinophyceae Cyanobacteria Diatoms Green algae
22:6ω3	(4Z,7Z,10Z,13Z,16Z,19Z)-docosa-4,7,10,13,16,19-hexaenoic acid	Docosahexaenoic acid	Bacillariophyceae Cryptophyceae Dinophyceae Haptophyta Cyanobacteria Diatoms Green algae

Table S2. *Bacillus* strains used in this study

SZMC	Source	SI	Identification
SZMC 26891	Zenta (Serbia), Maize rhizosphere	0.613	*B. megaterium* GC subgroup A
SZMC 26893	Zenta (Serbia), Maize rhizosphere	0.736	*B. cereus* GC subgroup A
SZMC 26895	Zenta (Serbia), Maize rhizosphere	0.941	*B. megaterium* GC subgroup A
SZMC 26896	Zenta (Serbia), Maize rhizosphere	0.775	*B. megaterium* GC subgroup A
SZMC 26897	Zenta (Serbia), Maize rhizosphere	0.738	*B. cereus* GC subgroup A
SZMC 25610	Vaszar (47.382785, 17.499215) maize rhizosphere	0.928	*B. velezensis*

SZMC	Source	SI	Identification
SZMC 25613	Vaszar (47.382785, 17.499215) maize rhizosphere	0.83	*B. megaterium* GC subgroup A
SZMC 25614	Vaszar (47.382785, 17.499215) maize rhizosphere	0.874	*B. megaterium* GC subgroup A
SZMC 25635	Madaras, Pea rhizosphere	0.954	*B. simplex*
SZMC 25636	Madaras, Pea rhizosphere	0.933	*B. megaterium* GC subgroup A
SZMC 25637	Madaras, Pea rhizosphere	0.855	*B. megaterium* GC subgroup A
SZMC 25638	Madaras, Pea rhizosphere	0.826	*B. atrophaeus*
SZMC 25639	Madaras, Pea rhizosphere	0.681	*B. megaterium* GC subgroup B
SZMC 25640	Madaras, Pea rhizosphere	0.802	*B. atrophaeus*
SZMC 25641	Madaras, Pea rhizosphere	0.945	*B. megaterium* GC subgroup A
SZMC 25643	Madaras, Pea rhizosphere	0.917	*B. megaterium* GC subgroup A
SZMC 25644	Madaras, Pea rhizosphere	0.808	*B. megaterium* GC subgroup A
SZMC 25645	Madaras, Pea rhizosphere	0.935	*B. megaterium* GC subgroup A
SZMC 25646	Madaras, Pea rhizosphere	0.934	*B. velezensis*
SZMC 25647	Madaras, Pea rhizosphere	0.849	*B. velezensis*
SZMC 25648	Madaras, Pea rhizosphere	0.847	*B. subtilis*
SZMC 24978	Totovo selo (SRB), soil sample, tomato	0.811	*B. atrophaeus*
SZMC 24979	Totovo selo (SRB), soil sample, tomato	0.809	*B. megaterium* GC subgroup A
SZMC 24980	Totovo selo (SRB), soil sample, pepper	0.949	*B. velezensis*
SZMC 24981	Totovo selo (SRB), soil sample, pepper	0.798	*B. velezensis*
SZMC 24982	Totovo selo (SRB), soil sample, pepper	0.950	*B. velezensis*
SZMC 24983	Totovo selo (SRB), soil sample, pepper	0.936	*B. velezensis*
SZMC 24984	Cantavir (SRB), soil sample, pepper	0.957	*B. velezensis*
SZMC 24985	Cantavir (SRB), soil sample, pepper	0.891	*B. velezensis*
SZMC 24986	Cantavir (SRB), soil sample, tomato	0.949	*B. velezensis*
SZMC 24987	Cantavir (SRB), soil sample, tomato	0.764	*B. pumilus* GC subgroup B
SZMC 24988	Cantavir (SRB), soil sample, tomato	0.824	*B. megaterium* GC subgroup A
SZMC 24989	Cantavir (SRB), soil sample, tomato	0.971	*B. endophyticus*
SZMC 24990	Cantavir (SRB), soil sample, tomato	0.919	*B. megaterium* GC subgroup A
SZMC 24991	Cantavir (SRB), soil sample, tomato	0.917	*B. pumilus* GC subgroup B
SZMC 24992	Cantavir (SRB), soil sample, pepper	0.865	*B. subtilis*
SZMC 24993	Cantavir (SRB), soil sample, pepper	0.862	*B. megaterium* GC subgroup A
SZMC 24994	Cantavir (SRB), soil sample, tomato	0.655	*B. cereus* GC subgroup A
SZMC 24995	Cantavir (SRB), soil sample, tomato	0.911	*B. velezensis*
SZMC 24997	Székkutas (HU), soil sample, carrot	0.897	*B. megaterium* GC subgroup A
SZMC 24998	Madaras (HU), soil sample, carrot	0.865	*B. megaterium* GC subgroup A
SZMC 24999	Madaras (HU), soil sample, carrot	0.946	*B. subtilis*
SZMC 25000	Madaras (HU), soil sample, paprika	0.823	*B. megaterium* GC subgroup A
SZMC 25001	Madaras (HU), soil sample, pepper	0.78	*B. megaterium* GC subgroup A
SZMC 25002	Madaras (HU), soil sample, paprika	0.795	*B. megaterium* GC subgroup A
SZMC 25003	Madaras (HU), soil sample, paprika	0.603	*B. cereus* GC subgroup A
SZMC 25004	Ásotthalom (HU), soil sample, sweet potato	0.932	B. *megaterium* GC subgroup A
SZMC 25007	Cenej (SRB), soil sample, carrot	0.959	*B. subtilis*
SZMC 25008	Glozan (SRB), soil sample, carrot	0.886	*B. megaterium* GC subgroup A
SZMC 25009	Glozan (SRB), soil sample, carrot	0.693	*B. cereus* GC subgroup A
SZMC 25010	Temerin (SRB), soil sample, sweet potato	0.85	*B. megaterium* GC subgroup A

SZMC	Source	SI	Identification
SZMC 25011	Temerin (SRB), soil sample, sweet potato	0.81	*B. simplex*
SZMC 25012	SRB, soil sample, pepper	0.722	*B. cereus* GC subgroup A
SZMC 25013	SRB, soil sample, pepper	0.759	*B. megaterium* GC subgroup A
SZMC 25015	Cenej (SRB), soil sample, pepper	0.758	*B. megaterium* GC subgroup A
SZMC 25016	Cenej (SRB), soil sample, pepper	0.786	*B. megaterium* GC subgroup B
SZMC 25017	Cenej (SRB), soil sample, pepper	0.919	*B. megaterium* GC subgroup A
SZMC 25018	Cenej (SRB), soil sample, tomato	0.959	*B. subtilis*
SZMC 25019	Cenej (SRB), soil sample, tomato	0.875	*B. pumilus* GC subgroup B
SZMC 25020	Cenej (SRB), soil sample, tomato	0.941	*B. velezensis*
SZMC 25021	Cenej (SRB), soil sample, tomato	0.886	*B. simplex*
SZMC 25022	SRB, soil sample, tomato	0.861	*B. megaterium* GC subgroup A
SZMC 25024	Szentes (HU), soil sample	0.906	*B. megaterium* GC subgroup A
SZMC 25025	Szentes (HU), soil sample	0.913	*B. megaterium* GC subgroup A
SZMC 25026	Szentes (HU), soil sample	0.768	*B. megaterium* GC subgroup A
SZMC 25027	Szentes (HU), soil sample	0.875	*B. megaterium* GC subgroup A
SZMC 26571	SRB, soil sample	0.872	*B. megaterium* GC subgroup A
SZMC 26572	SRB, soil sample	0.791	*B. megaterium* GC subgroup A
SZMC 26573	SRB, soil sample	0.943	*B. subtilis*
SZMC 26574	SRB, soil sample	0.791	B. *megaterium* GC subgroup A
SZMC 26575	SRB, soil sample	0.884	*B. subtilis*
SZMC 26576	SRB, soil sample	0.942	*B. megaterium* GC subgroup A
SZMC 25286	mushroom compost	0.873	*B. simplex*
SZMC 25289	mushroom compost	0.857	*B. megaterium* GC subgroup A
SZMC 25293	mushroom compost	0.855	*B. simplex*
SZMC 25317	mushroom compost	0.952	*B. subtilis*
SZMC 25318	mushroom compost	0.799	*B. amyloliquefaciens*
SZMC 25320	mushroom compost	0.94	*B. licheniformis*
SZMC 25328	mushroom compost	0.802	*B. licheniformis*
SZMC 25329	mushroom compost	0.87	*B. licheniformis*
SZMC 25330	mushroom compost	0.898	*B. licheniformis*
SZMC 25336	mushroom compost	0.834	*B. subtilis*
SZMC 25337	mushroom compost	0.896	*B. subtilis*
SZMC 25338	mushroom compost	0.86	*B. subtilis*
SZMC 25339	mushroom compost	0.831	*B. subtilis*
SZMC 25340	mushroom compost	0.537	*B. atrophaeus*
SZMC 25367	mushroom compost	0.56	*B. velezensis*
SZMC 25370	mushroom compost	0.645	*B. licheniformis*
SZMC 25372	mushroom compost	0.528	*B. licheniformis*
SZMC 25388	mushroom compost	0.632	*B. pumilus* GC subgroup A
SZMC 25389	mushroom compost	0.781	*B. subtilis*
SZMC 25390	mushroom compost	0.85	*B. subtilis*
SZMC 25399	mushroom compost	0.698	*B. licheniformis*
SZMC 25400	mushroom compost	0.861	*B. licheniformis*
SZMC 25428	mushroom compost	0.674	*B. licheniformis*
SZMC 25429	mushroom compost	0.707	*B. licheniformis*

SZMC	Source	SI	Identification
SZMC 25430	mushroom compost	0.618	*B. subtilis*
SZMC 25431	mushroom compost	0.686	*B. velezensis*
SZMC 25434	mushroom compost	0.868	*B. licheniformis*
SZMC 25437	mushroom compost	0.711	*B. licheniformis*
SZMC 25438	mushroom compost	0.707	*B. licheniformis*
SZMC 25439	mushroom compost	0.718	*B. licheniformis*
SZMC 25440	mushroom compost	0.652	*B. licheniformis*
SZMC 25441	mushroom compost	0.741	*B. licheniformis*
SZMC 25442	mushroom compost	0.848	*B. velezensis*
SZMC 25443	mushroom compost	0.79	*B. subtilis*
SZMC 25444	mushroom compost	0.744	*B. licheniformis*
SZMC 25445	mushroom compost	0.777	*B. licheniformis*
SZMC 25446	mushroom compost	0.854	*B. licheniformis*
SZMC 25447	mushroom compost	0.959	*B. licheniformis*
SZMC 25449	mushroom compost	0.73	*B. subtilis*
SZMC 25450	mushroom compost	0.695	*B. megaterium* GC subgroup B
SZMC 25451	mushroom compost	0.809	*B. licheniformis*
SZMC 25453	mushroom compost	0.732	*B. licheniformis*
SZMC 25454	mushroom compost	0.716	*B. licheniformis*
SZMC 25457	mushroom compost	0.889	*B. licheniformis*
SZMC 25460	mushroom compost	0.831	*B. licheniformis*
SZMC 25462	mushroom compost	0.63	*B. licheniformis*
SZMC 25463	mushroom compost	0.84	*B. licheniformis*
SZMC 16093B	-	0.886	*B. velezensis*
SZMC 6387J	tomato rhizosphere, Mo, Hungary	0.934	*B. velezensis*
SZMC 6046		0.928	*B. velezensis*
SZMC 6235J		0.884	*B. velezensis*
SZMC 6027	soil and industrial amylase fermentations *B. amyloliquefaciens* DSM 7, ATCC 23350	0.87	*B. amyloliquefaciens*
SZMC 6222	unknown origin *B. amyloliquefaciens* DSM 1061, IAM 1523	0.812	*B. amyloliquefaciens*
SZMC 27497	beet rhizosphere, Berlin, Germany *B. velezensis* DSM 23117, BGSC 10A6, FZB42, LMG 26770	0.915	*B. velezensis*
SZMC 27565	*B. velezensis* LMG 22478	0.762	*B. velezensis*
	B. subtilis ATCC 6633	0.842	*B. subtilis*

* ATCC- American Type Culture Collection; BGSC- Bacillus Genetic Stock Center, The Ohio State University, USA; DSMZ- German Collection of Microorganisms and Cell Cultures; FZB- FZB Biotechnik GmbH/ ABiTEP, Berlin, LMG- Belgian Coordinated Collections of Microorganisms / LMG Bacteria Collection, Laboratorium voor Microbiologie, Universiteit Gent, Belgium; SZMC - Szeged Microbiological Collection

Table S3. *C. auris* strains using for this study

# AR Bank/CDC	Strain	Clade	Clade name	Isolation site	Source
0381	B11220	II	East Asia	auditory canal	CDC
0382	B11109	I	South Asia	burn wound	CDC
0383	B11221	III	Africa	blood	CDC
0384	B11222	III	Africa	blood	CDC
0385	B11244	IV	South America	blood	CDC
0386	B11245	IV	South America	blood	CDC
0387	B8441	I	South Asia	blood	CDC
0388	B11098	I	South Asia	blood	CDC
0389	B11203	I	South Asia	bronchoalveolar lavage	CDC
0390	AR0390	I	South Asia	Unknown	CDC
nd	MMC1	I	South Asia	blood	MMC
nd	MMC-2	nd	nd	nd	MMC

nd: not determined

Table S4. *Armillaria* strains used for the study

Species	Strain	Location	GPS-N	GPS-E
A. cepistipes	RF1	Rosalia	47° 41.649	16° 17.940
	RF2	Rosalia	47° 41.640	16° 17.937
	RF8	Rosalia	47° 41.654	16° 18.096
	RF9	Rosalia	47° 41.622	16° 17.922
	RF13	Rosalia	47° 41.655	16° 18.096
	RF14	Rosalia	47° 41.640	16° 17.949
	HF34	Hidegvízvölgy	47° 39.891	16° 26.454
	SZMC 23077	nd	nd	nd
	SZMC 23078	nd	nd	nd
A. gallica	KF15	Keszthely	46° 48.738	17° 16.956
	KF33	Keszthely	46° 48.733	17° 16.997
	KF37	Keszthely	46° 48.693	17° 16.991
	KF40	Keszthely	*46° 48.719*	*17° 16.957*
	KR12	Keszthely	46° 48.728	17° 16.992
	KR15	Keszthely	46° 48.702	17° 16.987
	VTF6	Vértes	47° 26.730	18° 25.918
	BF3	Budai hegys	47° 29.100	18° 58.040
	VF1	Várhely	47° 39.885	16° 35.072
	VF2	Várhely	47° 39.741	16° 33.250
	SzF1	nd	nd	nd
	KoF1	Horvátzsidány, Alsóerdő	47° 23.741	16° 36.018
	KoF6	Velem	47° 20.457	16° 30.169
A. mellea	DF1	nd	47° 06.086	16° 26.765
	KF5	Keszthely	46° 48.712	17° 16.978
	KF7	Keszthely	46° 48.772	17° 16.992
	KF11	Keszthely	46° 48.749	17° 16.936
	KF18	Keszthely	46° 48.917	17° 17.062
	KF24	Keszthely	46° 47.953	17° 16.979
	KF46	Keszthely	46° 48.759	17° 16.944
	HF13	Hidegvízvölgy	47° 39.856	16° 26.471
	HF25	Hidegvízvölgy	47° 39.876	16° 26.559
	VTF1	Vértes	47° 24.721	18° 15.580
	VTF10	Vértes	nd	nd
A. ostoyae	RF3	Rosalia	47° 41.618	16° 17.873
	RF4	Rosalia	nd	nd
	RF5	Rosalia	47° 41.629	16° 17.964

Species	Strain	Location	GPS-N	GPS-E
	RF10	Rosalia	47° 41.662	16° 17.929
	HF24	Hidegvízvölgy	47° 39.844	16° 26.513
	HF31	Hidegvízvölgy	47° 39.880	16° 26.529
	HF39	Hidegvízvölgy	47° 40.840	16° 34.631
	SZMC 23080	nd	nd	nd
	SZMC 23082	nd	nd	nd
	SZMC 23083	nd	nd	nd

Table S5. SI values based on strains

Sample Name	Classified As (1st / 2nd)	SI
Candida-auris-B11220	Candida-auris-B11220	0.977
	Candida-auris-B11244	0.577
Candida-auris-B11220	Candida-auris-B11220	0.977
	Candida-auris-B11244	0.600
Candida-auris-B11220	Candida-auris-B11220	0.977
	Candida-auris-B11244	0.594
Candida-auris-B11220	Candida-auris-B11220	0.974
	Candida-auris-B11244	0.601
Candida-auris-B11220	Candida-auris-B11220	0.974
	Candida-auris-B11244	0.497
Candida-auris-B11220	Candida-auris-B11220	0.971
	Candida-auris-B11244	0.532
Candida-auris-B11220	Candida-auris-B11220	0.967
	Candida-auris-B11244	0.650
Candida-auris-B11220	Candida-auris-B11220	0.965
	Candida-auris-B11244	0.503
Candida-auris-B11220	Candida-auris-B11220	0.924
	Candida-auris-B11244	0.629
Candida-auris-B11220	Candida-auris-B11220	0.922
	Candida-auris-B11244	0.570
Candida-auris-B11109	Candida-auris-B11109	0.976
	Candida-auris-B8441	0.728
Candida-auris-B11109	Candida-auris-B11109	0.975
	Candida-auris-B8441	0.749
Candida-auris-B11109	Candida-auris-B11109	0.973
	Candida-auris-B8441	0.760
Candida-auris-B11109	Candida-auris-B11109	0.970
	Candida-auris-B8441	0.799
Candida-auris-B11109	Candida-auris-B11109	0.961
	Candida-auris-B8441	0.712
Candida-auris-B11109	Candida-auris-B11109	0.955
	Candida-auris-B8441	0.757
Candida-auris-B11109	Candida-auris-B11109	0.948
	Candida-auris-B8441	0.737
Candida-auris-B11109	Candida-auris-B11109	0.943
	Candida-auris-B11221	0.799
Candida-auris-B11109	Candida-auris-B11109	0.940

Sample Name	Classified As (1st / 2nd)	SI
	Candida-auris-B11221	0.773
Candida-auris-B11109	Candida-auris-B11109	0.928
	Candida-auris-B8441	0.713
Candida-auris-B11221	Candida-auris-B11221	0.977
	Candida-auris-B11222	0.952
Candida-auris-B11221	Candida-auris-B11221	0.972
	Candida-auris-B11222	0.938
Candida-auris-B11221	Candida-auris-B11221	0.966
	Candida-auris-B11222	0.934
Candida-auris-B11221	Candida-auris-B11221	0.959
	Candida-auris-B11222	0.953
Candida-auris-B11221	Candida-auris-B11221	0.950
	Candida-auris-B11222	0.867
Candida-auris-B11221	Candida-auris-B11221	0.943
	Candida-auris-B11222	0.881
Candida-auris-B11221	Candida-auris-B11221	0.931
	Candida-auris-B11222	0.832
Candida-auris-B11221	Candida-auris-B11222	0.974
	Candida-auris-B11221	0.948
Candida-auris-B11221	Candida-auris-B11222	0.973
	Candida-auris-B11221	0.972
Candida-auris-B11221	Candida-auris-B11222	0.972
	Candida-auris-B11221	0.968
Candida-auris-B11222	Candida-auris-B11222	0.991
	Candida-auris-B11221	0.940
Candida-auris-B11222	Candida-auris-B11222	0.982
	Candida-auris-B11221	0.930
Candida-auris-B11222	Candida-auris-B11222	0.981
	Candida-auris-B11221	0.911
Candida-auris-B11222	Candida-auris-B11222	0.979
	Candida-auris-B11221	0.934
Candida-auris-B11222	Candida-auris-B11222	0.978
	Candida-auris-B11221	0.918
Candida-auris-B11222	Candida-auris-B11222	0.973
	Candida-auris-B11221	0.942
Candida-auris-B11222	Candida-auris-B11222	0.972
	Candida-auris-B11221	0.947
Candida-auris-B11222	Candida-auris-B11222	0.970
	Candida-auris-B11221	0.941
Candida-auris-B11222	Candida-auris-B11222	0.969
	Candida-auris-B11221	0.954
Candida-auris-B11222	Candida-auris-B11222	0.964
	Candida-auris-B11221	0.939
Candida-auris-B11244	Candida-auris-B11244	0.983
	Candida-auris-B11245	0.792
Candida-auris-B11244	Candida-auris-B11244	0.976
	Candida-auris-B11245	0.796
Candida-auris-B11244	Candida-auris-B11244	0.976
	Candida-auris-B11245	0.822

Sample Name	Classified As (1st / 2nd)	SI
Candida-auris-B11244	Candida-auris-B11244	0.972
	Candida-auris-B11245	0.719
Candida-auris-B11244	Candida-auris-B11244	0.970
	Candida-auris-B11245	0.687
Candida-auris-B11244	Candida-auris-B11244	0.962
	Candida-auris-B11245	0.667
Candida-auris-B11244	Candida-auris-B11244	0.949
	Candida-auris-B11245	0.646
Candida-auris-B11244	Candida-auris-B11244	0.939
	Candida-auris-B11245	0.782
Candida-auris-B11244	Candida-auris-B11244	0.913
	Candida-auris-B11245	0.878
Candida-auris-B11244	Candida-auris-B11245	0.931
	Candida-auris-B11244	0.927
Candida-auris-B11245	Candida-auris-B11245	0.993
	Candida-auris-B11244	0.832
Candida-auris-B11245	Candida-auris-B11245	0.984
	Candida-auris-B11244	0.861
Candida-auris-B11245	Candida-auris-B11245	0.978
	Candida-auris-B11244	0.752
Candida-auris-B11245	Candida-auris-B11245	0.978
	Candida-auris-B11244	0.850
Candida-auris-B11245	Candida-auris-B11245	0.975
	Candida-auris-B11244	0.741
Candida-auris-B11245	Candida-auris-B11245	0.970
	Candida-auris-B11244	0.875
Candida-auris-B11245	Candida-auris-B11245	0.959
	Candida-auris-B11244	0.877
Candida-auris-B11245	Candida-auris-B11245	0.956
	Candida-auris-B11244	0.871
Candida-auris-B11245	Candida-auris-B11245	0.953
	Candida-auris-B11244	0.736
Candida-auris-B11245	Candida-auris-B11245	0.949
	Candida-auris-B11222	0.784
Candida-auris-B8441	Candida-auris-B8441	0.987
	Candida-auris-B11109	0.776
Candida-auris-B8441	Candida-auris-B8441	0.962
	Candida-auris-B11109	0.760
Candida-auris-B8441	Candida-auris-B8441	0.961
	Candida-auris-B11109	0.745
Candida-auris-B8441	Candida-auris-B8441	0.952
	Candida-auris-B11109	0.674
Candida-auris-B8441	Candida-auris-B8441	0.947
	Candida-auris-B11109	0.797
Candida-auris-B8441	Candida-auris-B8441	0.947
	Candida-auris-B11109	0.640
Candida-auris-B8441	Candida-auris-B8441	0.943
	Candida-auris-B11109	0.617
Candida-auris-B8441	Candida-auris-B8441	0.915

Sample Name	Classified As (1st / 2nd)	SI
	Candida-auris-B11109	0.674
Candida-auris-B8441	Candida-auris-B8441	0.849
	Candida-auris-B11109	0.661
Candida-auris-B8441	Candida-auris-B8441	0.781
	Candida-auris-B11109	0.679
Candida-auris-B11098	Candida-auris-B11098	0.969
	Candida-auris-MMC-1	0.783
Candida-auris-B11098	Candida-auris-B11098	0.961
	Candida-auris-MMC-1	0.863
Candida-auris-B11098	Candida-auris-B11098	0.955
	Candida-auris-MMC-1	0.779
Candida-auris-B11098	Candida-auris-B11098	0.951
	Candida-auris-MMC-1	0.878
Candida-auris-B11098	Candida-auris-B11098	0.951
	Candida-auris-MMC-1	0.899
Candida-auris-B11098	Candida-auris-B11098	0.940
	Candida-auris-MMC-1	0.840
Candida-auris-B11098	Candida-auris-B11098	0.928
	Candida-auris-MMC-1	0.700
Candida-auris-B11098	Candida-auris-B11098	0.914
	Candida-auris-MMC-1	0.679
Candida-auris-B11098	Candida-auris-B11098	0.906
	Candida-auris-MMC-1	0.633
Candida-auris-B11098	Candida-auris-B11098	0.849
	Candida-auris-MMC-1	0.526
Candida-auris-B11203	Candida-auris-B11203	0.986
	Candida-auris-MMC-1	0.741
Candida-auris-B11203	Candida-auris-B11203	0.983
	Candida-auris-MMC-1	0.739
Candida-auris-B11203	Candida-auris-B11203	0.973
	Candida-auris-MMC-1	0.696
Candida-auris-B11203	Candida-auris-B11203	0.963
	Candida-auris-MMC-1	0.637
Candida-auris-B11203	Candida-auris-B11203	0.948
	Candida-auris-MMC-1	0.892
Candida-auris-B11203	Candida-auris-B11203	0.947
	Candida-auris-MMC-1	0.703
Candida-auris-B11203	Candida-auris-B11203	0.921
	Candida-auris-MMC-1	0.820
Candida-auris-B11203	Candida-auris-B11203	0.832
	Candida-auris-MMC-1	0.712
Candida-auris-B11203	Candida-auris-B11203	0.744
	Candida-auris-MMC-1	0.501
Candida-auris-B11203	Candida-auris-MMC-1	0.925
	Candida-auris-B11203	0.874
Candida-auris-AR0390	Candida-auris-AR0390	0.994
	Candida-auris-MMC-1	0.723
Candida-auris-AR0390	Candida-auris-AR0390	0.983
	Candida-auris-MMC-1	0.770

Sample Name	Classified As (1st / 2nd)	SI
Candida-auris-AR0390	Candida-auris-AR0390	0.951
	Candida-auris-B11098	0.527
Candida-auris-AR0390	Candida-auris-AR0390	0.942
	Candida-auris-MMC-1	0.623
Candida-auris-AR0390	Candida-auris-AR0390	0.930
	Candida-auris-MMC-1	0.854
Candida-auris-AR0390	Candida-auris-AR0390	0.917
	Candida-auris-MMC-1	0.909
Candida-auris-AR0390	Candida-auris-AR0390	0.900
	Candida-auris-MMC-1	0.364
Candida-auris-AR0390	Candida-auris-AR0390	0.896
	Candida-auris-MMC-1	0.543
Candida-auris-AR0390	Candida-auris-AR0390	0.754
	Candida-auris-MMC-1	0.560
Candida-auris-AR0390	Candida-auris-MMC-1	0.956
	Candida-auris-AR0390	0.886
Candida-auris-MMC1	Candida-auris-MMC-1	0.970
	Candida-auris-AR0390	0.812
Candida-auris-MMC1	Candida-auris-MMC-1	0.946
	Candida-auris-AR0390	0.897
Candida-auris-MMC1	Candida-auris-MMC-1	0.945
	Candida-auris-B11203	0.873
Candida-auris-MMC1	Candida-auris-MMC-1	0.940
	Candida-auris-AR0390	0.726
Candida-auris-MMC1	Candida-auris-MMC-1	0.929
	Candida-auris-B11203	0.916
Candida-auris-MMC1	Candida-auris-MMC-1	0.926
	Candida-auris-AR0390	0.757
Candida-auris-MMC1	Candida-auris-MMC-1	0.914
	Candida-auris-AR0390	0.828
Candida-auris-MMC1	Candida-auris-MMC-1	0.900
	Candida-auris-AR0390	0.753
Candida-auris-MMC1	Candida-auris-MMC-1	0.817
	Candida-auris-B11098	0.778
Candida-auris-MMC1	Candida-auris-MMC-1	0.732
	Candida-auris-AR0390	0.628
Candida-auris-MMC2	Candida-auris-MMC-2	0.995
	Candida-auris-MMC-1	0.096
Candida-auris-MMC2	Candida-auris-MMC-2	0.990
	Candida-auris-MMC-1	0.095
Candida-auris-MMC2	Candida-auris-MMC-2	0.976
	Candida-auris-MMC-1	0.074
Candida-auris-MMC2	Candida-auris-MMC-2	0.971
	Candida-auris-MMC-1	0.119
Candida-auris-MMC2	Candida-auris-MMC-2	0.971
	Candida-auris-MMC-1	0.112
Candida-auris-MMC2	Candida-auris-MMC-2	0.966
	Candida-auris-MMC-1	0.085
Candida-auris-MMC2	Candida-auris-MMC-2	0.952

Sample Name	Classified As (1st / 2nd)	SI
	Candida-auris-MMC-1	0.098
Candida-auris-MMC2	Candida-auris-MMC-2	0.950
	Candida-auris-MMC-1	0.053
Candida-auris-MMC2	Candida-auris-MMC-2	0.949
	Candida-auris-MMC-1	0.048
Candida-auris-MMC2	Candida-auris-MMC-2	0.835
	Candida-auris-B11098	0.028

Table S6. SI values based on GC subgroups of *C. auris*

Sample Name	Classified As (1st / 2nd)	SI
Candida-auris-B11245	Candida-auris-GC subgroup A	0.973
	Candida-auris-GC subgroup B	0.201
Candida-auris-B11245	Candida-auris-GC subgroup A	0.965
	Candida-auris-GC subgroup B	0.191
Candida-auris-B11245	Candida-auris-GC subgroup A	0.961
	Candida-auris-GC subgroup B	0.252
Candida-auris-B11222	Candida-auris-GC subgroup A	0.956
	Candida-auris-GC subgroup B	0.286
Candida-auris-B11245	Candida-auris-GC subgroup A	0.956
	Candida-auris-GC subgroup B	0.190
Candida-auris-B11245	Candida-auris-GC subgroup A	0.955
	Candida-auris-GC subgroup B	0.173
Candida-auris-B11222	Candida-auris-GC subgroup A	0.954
	Candida-auris-GC subgroup B	0.303
Candida-auris-B11244	Candida-auris-GC subgroup A	0.953
	Candida-auris-GC subgroup B	0.174
Candida-auris-B11221	Candida-auris-GC subgroup A	0.950
	Candida-auris-GC subgroup B	0.336
Candida-auris-B11245	Candida-auris-GC subgroup A	0.949
	Candida-auris-GC subgroup B	0.215
Candida-auris-B11245	Candida-auris-GC subgroup A	0.948
	Candida-auris-GC subgroup B	0.175
Candida-auris-B11245	Candida-auris-GC subgroup A	0.944
	Candida-auris-GC subgroup B	0.215
Candida-auris-B11109	Candida-auris-GC subgroup A	0.941
	Candida-auris-GC subgroup B	0.258
Candida-auris-B11222	Candida-auris-GC subgroup A	0.938
	Candida-auris-GC subgroup B	0.293
Candida-auris-B11221	Candida-auris-GC subgroup A	0.932
	Candida-auris-GC subgroup B	0.369
Candida-auris-B11109	Candida-auris-GC subgroup A	0.932
	Candida-auris-GC subgroup B	0.272
Candida-auris-B11221	Candida-auris-GC subgroup A	0.931
	Candida-auris-GC subgroup B	0.339
Candida-auris-B11222	Candida-auris-GC subgroup A	0.930
	Candida-auris-GC subgroup B	0.317

Sample Name	Classified As (1st / 2nd)	SI
Candida-auris-B11221	Candida-auris-GC subgroup A	0.926
	Candida-auris-GC subgroup B	0.305
Candida-auris-B11221	Candida-auris-GC subgroup A	0.925
	Candida-auris-GC subgroup B	0.303
Candida-auris-B11222	Candida-auris-GC subgroup A	0.924
	Candida-auris-GC subgroup B	0.348
Candida-auris-B11221	Candida-auris-GC subgroup A	0.922
	Candida-auris-GC subgroup B	0.402
Candida-auris-B11244	Candida-auris-GC subgroup A	0.921
	Candida-auris-GC subgroup B	0.175
Candida-auris-B11221	Candida-auris-GC subgroup A	0.918
	Candida-auris-GC subgroup B	0.391
Candida-auris-B11221	Candida-auris-GC subgroup A	0.917
	Candida-auris-GC subgroup B	0.349
Candida-auris-B11222	Candida-auris-GC subgroup A	0.915
	Candida-auris-GC subgroup B	0.384
Candida-auris-B11221	Candida-auris-GC subgroup A	0.915
	Candida-auris-GC subgroup B	0.377
Candida-auris-B11109	Candida-auris-GC subgroup A	0.914
	Candida-auris-GC subgroup B	0.234
Candida-auris-B11245	Candida-auris-GC subgroup A	0.912
	Candida-auris-GC subgroup B	0.132
Candida-auris-B11222	Candida-auris-GC subgroup A	0.908
	Candida-auris-GC subgroup B	0.336
Candida-auris-B11109	Candida-auris-GC subgroup A	0.907
	Candida-auris-GC subgroup B	0.291
Candida-auris-B11245	Candida-auris-GC subgroup A	0.906
	Candida-auris-GC subgroup B	0.135
Candida-auris-B11222	Candida-auris-GC subgroup A	0.906
	Candida-auris-GC subgroup B	0.395
Candida-auris-B11109	Candida-auris-GC subgroup A	0.905
	Candida-auris-GC subgroup B	0.291
Candida-auris-B11222	Candida-auris-GC subgroup A	0.895
	Candida-auris-GC subgroup B	0.374
Candida-auris-B11222	Candida-auris-GC subgroup A	0.894
	Candida-auris-GC subgroup B	0.365
Candida-auris-B11109	Candida-auris-GC subgroup A	0.889
	Candida-auris-GC subgroup B	0.344
Candida-auris-B11244	Candida-auris-GC subgroup A	0.888
	Candida-auris-GC subgroup B	0.121
Candida-auris-B11109	Candida-auris-GC subgroup A	0.885
	Candida-auris-GC subgroup B	0.335
Candida-auris-B11244	Candida-auris-GC subgroup A	0.878
	Candida-auris-GC subgroup B	0.107
Candida-auris-B8441	Candida-auris-GC subgroup A	0.878
	Candida-auris-GC subgroup B	0.283
Candida-auris-B11109	Candida-auris-GC subgroup A	0.870
	Candida-auris-GC subgroup B	0.315
Candida-auris-B8441	Candida-auris-GC subgroup A	0.869

Sample Name	Classified As (1st / 2nd)	SI
	Candida-auris-GC subgroup B	0.292
Candida-auris-B11221	Candida-auris-GC subgroup A	0.868
	Candida-auris-GC subgroup B	0.385
Candida-auris-B11109	Candida-auris-GC subgroup A	0.863
	Candida-auris-GC subgroup B	0.289
Candida-auris-B8441	Candida-auris-GC subgroup A	0.861
	Candida-auris-GC subgroup B	0.263
Candida-auris-B11244	Candida-auris-GC subgroup A	0.861
	Candida-auris-GC subgroup B	0.103
Candida-auris-B11244	Candida-auris-GC subgroup A	0.855
	Candida-auris-GC subgroup B	0.082
Candida-auris-B11244	Candida-auris-GC subgroup A	0.853
	Candida-auris-GC subgroup B	0.084
Candida-auris-B11244	Candida-auris-GC subgroup A	0.853
	Candida-auris-GC subgroup B	0.078
Candida-auris-B11244	Candida-auris-GC subgroup A	0.852
	Candida-auris-GC subgroup B	0.094
Candida-auris-B8441	Candida-auris-GC subgroup A	0.850
	Candida-auris-GC subgroup B	0.261
Candida-auris-B11220	Candida-auris-GC subgroup A	0.845
	Candida-auris-GC subgroup B	0.147
Candida-auris-B11220	Candida-auris-GC subgroup A	0.842
	Candida-auris-GC subgroup B	0.142
Candida-auris-B11220	Candida-auris-GC subgroup A	0.841
	Candida-auris-GC subgroup B	0.151
Candida-auris-B11220	Candida-auris-GC subgroup A	0.837
	Candida-auris-GC subgroup B	0.113
Candida-auris-B11220	Candida-auris-GC subgroup A	0.836
	Candida-auris-GC subgroup B	0.109
Candida-auris-B11220	Candida-auris-GC subgroup A	0.833
	Candida-auris-GC subgroup B	0.144
Candida-auris-B11220	Candida-auris-GC subgroup A	0.822
	Candida-auris-GC subgroup B	0.160
Candida-auris-B8441	Candida-auris-GC subgroup A	0.821
	Candida-auris-GC subgroup B	0.199
Candida-auris-B8441	Candida-auris-GC subgroup A	0.821
	Candida-auris-GC subgroup B	0.292
Candida-auris-B11109	Candida-auris-GC subgroup A	0.819
	Candida-auris-GC subgroup B	0.307
Candida-auris-B11244	Candida-auris-GC subgroup A	0.818
	Candida-auris-GC subgroup B	0.067
Candida-auris-B11220	Candida-auris-GC subgroup A	0.809
	Candida-auris-GC subgroup B	0.120
Candida-auris-B8441	Candida-auris-GC subgroup A	0.802
	Candida-auris-GC subgroup B	0.216
Candida-auris-B11220	Candida-auris-GC subgroup A	0.798
	Candida-auris-GC subgroup B	0.127
Candida-auris-B11220	Candida-auris-GC subgroup A	0.794
	Candida-auris-GC subgroup B	0.110

Sample Name	Classified As (1st / 2nd)	SI
Candida-auris-B8441	Candida-auris-GC subgroup A	0.783
	Candida-auris-GC subgroup B	0.201
Candida-auris-B8441	Candida-auris-GC subgroup A	0.757
	Candida-auris-GC subgroup B	0.250
Candida-auris-B8441	Candida-auris-GC subgroup A	0.728
	Candida-auris-GC subgroup B	0.230
Candida-auris-MMC1	Candida-auris-GC subgroup B	0.975
	Candida-auris-GC subgroup A	0.205
Candida-auris-AR0390	Candida-auris-GC subgroup B	0.970
	Candida-auris-GC subgroup A	0.254
Candida-auris-MMC1	Candida-auris-GC subgroup B	0.968
	Candida-auris-GC subgroup A	0.133
Candida-auris-AR0390	Candida-auris-GC subgroup B	0.957
	Candida-auris-GC subgroup A	0.145
Candida-auris-MMC1	Candida-auris-GC subgroup B	0.952
	Candida-auris-GC subgroup A	0.165
Candida-auris-B11203	Candida-auris-GC subgroup B	0.947
	Candida-auris-GC subgroup A	0.121
Candida-auris-B11098	Candida-auris-GC subgroup B	0.939
	Candida-auris-GC subgroup A	0.234
Candida-auris-MMC1	Candida-auris-GC subgroup B	0.936
	Candida-auris-GC subgroup A	0.163
Candida-auris-B11098	Candida-auris-GC subgroup B	0.934
	Candida-auris-GC subgroup A	0.212
Candida-auris-AR0390	Candida-auris-GC subgroup B	0.932
	Candida-auris-GC subgroup A	0.252
Candida-auris-B11203	Candida-auris-GC subgroup B	0.932
	Candida-auris-GC subgroup A	0.080
Candida-auris-B11098	Candida-auris-GC subgroup B	0.931
	Candida-auris-GC subgroup A	0.256
Candida-auris-AR0390	Candida-auris-GC subgroup B	0.930
	Candida-auris-GC subgroup A	0.170
Candida-auris-B11203	Candida-auris-GC subgroup B	0.930
	Candida-auris-GC subgroup A	0.135
Candida-auris-AR0390	Candida-auris-GC subgroup B	0.929
	Candida-auris-GC subgroup A	0.246
Candida-auris-B11098	Candida-auris-GC subgroup B	0.918
	Candida-auris-GC subgroup A	0.286
Candida-auris-B11098	Candida-auris-GC subgroup B	0.914
	Candida-auris-GC subgroup A	0.306
Candida-auris-MMC1	Candida-auris-GC subgroup B	0.913
	Candida-auris-GC subgroup A	0.163
Candida-auris-B11098	Candida-auris-GC subgroup B	0.909
	Candida-auris-GC subgroup A	0.314
Candida-auris-B11203	Candida-auris-GC subgroup B	0.906
	Candida-auris-GC subgroup A	0.062
Candida-auris-B11203	Candida-auris-GC subgroup B	0.905
	Candida-auris-GC subgroup A	0.063
Candida-auris-B11203	Candida-auris-GC subgroup B	0.892

Sample Name	Classified As (1st / 2nd)	SI
	Candida-auris-GC subgroup A	0.055
Candida-auris-MMC1	Candida-auris-GC subgroup B	0.878
	Candida-auris-GC subgroup A	0.119
Candida-auris-B11203	Candida-auris-GC subgroup B	0.868
	Candida-auris-GC subgroup A	0.061
Candida-auris-B11203	Candida-auris-GC subgroup B	0.867
	Candida-auris-GC subgroup A	0.045
Candida-auris-AR0390	Candida-auris-GC subgroup B	0.866
	Candida-auris-GC subgroup A	0.188
Candida-auris-MMC1	Candida-auris-GC subgroup B	0.863
	Candida-auris-GC subgroup A	0.160
Candida-auris-AR0390	Candida-auris-GC subgroup B	0.849
	Candida-auris-GC subgroup A	0.264
Candida-auris-MMC1	Candida-auris-GC subgroup B	0.846
	Candida-auris-GC subgroup A	0.155
Candida-auris-B11098	Candida-auris-GC subgroup B	0.842
	Candida-auris-GC subgroup A	0.354
Candida-auris-B11098	Candida-auris-GC subgroup B	0.841
	Candida-auris-GC subgroup A	0.241
Candida-auris-AR0390	Candida-auris-GC subgroup B	0.827
	Candida-auris-GC subgroup A	0.386
Candida-auris-MMC1	Candida-auris-GC subgroup B	0.823
	Candida-auris-GC subgroup A	0.168
Candida-auris-B11098	Candida-auris-GC subgroup B	0.812
	Candida-auris-GC subgroup A	0.208
Candida-auris-B11203	Candida-auris-GC subgroup B	0.789
	Candida-auris-GC subgroup A	0.070
Candida-auris-AR0390	Candida-auris-GC subgroup B	0.777
	Candida-auris-GC subgroup A	0.196
Candida-auris-B11098	Candida-auris-GC subgroup B	0.762
	Candida-auris-GC subgroup A	0.161
Candida-auris-B11203	Candida-auris-GC subgroup B	0.751
	Candida-auris-GC subgroup A	0.028
Candida-auris-MMC1	Candida-auris-GC subgroup B	0.713
	Candida-auris-GC subgroup A	0.129
Candida-auris-AR0390	Candida-auris-GC subgroup B	0.705
	Candida-auris-GC subgroup A	0.203
Candida-auris-MMC2	Candida-auris-GC subgroup C	0.995
	Candida-auris-GC subgroup A	0.135
Candida-auris-MMC2	Candida-auris-GC subgroup C	0.990
	Candida-auris-GC subgroup A	0.135
Candida-auris-MMC2	Candida-auris-GC subgroup C	0.976
	Candida-auris-GC subgroup A	0.105
Candida-auris-MMC2	Candida-auris-GC subgroup C	0.971
	Candida-auris-GC subgroup A	0.138
Candida-auris-MMC2	Candida-auris-GC subgroup C	0.971
	Candida-auris-GC subgroup A	0.159
Candida-auris-MMC2	Candida-auris-GC subgroup C	0.966
	Candida-auris-GC subgroup A	0.111

Sample Name	Classified As (1st / 2nd)	SI
Candida-auris-MMC2	Candida-auris-GC subgroup C	0.952
	Candida-auris-GC subgroup A	0.112
Candida-auris-MMC2	Candida-auris-GC subgroup C	0.950
	Candida-auris-GC subgroup A	0.149
Candida-auris-MMC2	Candida-auris-GC subgroup C	0.949
	Candida-auris-GC subgroup A	0.149
Candida-auris-MMC2	Candida-auris-GC subgroup C	0.835
	Candida-auris-GC subgroup A	0.139

Table S7. SI values based on *A. cepistipes* FAME profiles

Sample Name	Classified As (1st / 2nd)	SI
Armillaria-cepistipes-RF2	Armillaria-cepistipes	0.935
	Armillaria-gallica	0.804
Armillaria-cepistipes-RF14	Armillaria-cepistipes	0.917
	Armillaria-ostoyae	0.765
Armillaria-cepistipes-RF14	Armillaria-cepistipes	0.910
	Armillaria-ostoyae	0.788
Armillaria-cepistipes-RF2	Armillaria-cepistipes	0.907
	Armillaria-ostoyae	0.756
Armillaria-cepistipes-RF2	Armillaria-cepistipes	0.887
	Armillaria-ostoyae	0.746
Armillaria-cepistipes-RF2	Armillaria-cepistipes	0.882
	Armillaria-ostoyae	0.752
Armillaria-cepistipes-RF2	Armillaria-cepistipes	0.880
	Armillaria-gallica	0.737
Armillaria-cepistipes-RF14	Armillaria-cepistipes	0.876
	Armillaria-ostoyae	0.845
Armillaria-cepistipes-RF8	Armillaria-cepistipes	0.875
	Armillaria-gallica	0.820
Armillaria-cepistipes-RF14	Armillaria-cepistipes	0.870
	Armillaria-gallica	0.757
Armillaria-cepistipes-RF14	Armillaria-cepistipes	0.869
	Armillaria-ostoyae	0.837
Armillaria-cepistipes-RF14	Armillaria-cepistipes	0.864
	Armillaria-ostoyae	0.654
Armillaria-cepistipes-RF2	Armillaria-cepistipes	0.864
	Armillaria-gallica	0.625
Armillaria-cepistipes-RF9	Armillaria-cepistipes	0.861
	Armillaria-ostoyae	0.730
Armillaria-cepistipes-RF14	Armillaria-cepistipes	0.856
	Armillaria-ostoyae	0.745
Armillaria-cepistipes-RF8	Armillaria-cepistipes	0.854
	Armillaria-gallica	0.704
Armillaria-cepistipes-RF14	Armillaria-cepistipes	0.852
	Armillaria-ostoyae	0.720
Armillaria-cepistipes-RF2	Armillaria-cepistipes	0.851
	Armillaria-gallica	0.622
Armillaria-cepistipes-SZMC 23077	Armillaria-cepistipes	0.845
	Armillaria-mellea	0.692
Armillaria-cepistipes-RF8	Armillaria-cepistipes	0.842
	Armillaria-ostoyae	0.800
Armillaria-cepistipes-RF13	Armillaria-cepistipes	0.838
	Armillaria-mellea	0.611
Armillaria-cepistipes-RF9	Armillaria-cepistipes	0.837
	Armillaria-ostoyae	0.759
Armillaria-cepistipes-RF1	Armillaria-cepistipes	0.836
	Armillaria-ostoyae	0.796
Armillaria-cepistipes-RF14	Armillaria-cepistipes	0.834
	Armillaria-ostoyae	0.767
Armillaria-cepistipes-RF8	Armillaria-cepistipes	0.831

Sample Name	Classified As (1st / 2nd)	SI
	Armillaria-gallica	0.621
Armillaria-cepistipes-RF9	Armillaria-cepistipes	0.831
	Armillaria-ostoyae	0.681
Armillaria-cepistipes-RF8	Armillaria-cepistipes	0.815
	Armillaria-ostoyae	0.762
Armillaria-cepistipes-RF8	Armillaria-cepistipes	0.810
	Armillaria-gallica	0.600
Armillaria-cepistipes-23078	Armillaria-cepistipes	0.808
	Armillaria-ostoyae	0.671
Armillaria-cepistipes-RF14	Armillaria-cepistipes	0.806
	Armillaria-gallica	0.805
Armillaria-cepistipes-RF9	Armillaria-cepistipes	0.805
	Armillaria-ostoyae	0.691
Armillaria-cepistipes-RF9	Armillaria-cepistipes	0.805
	Armillaria-ostoyae	0.756
Armillaria-cepistipes-RF2	Armillaria-cepistipes	0.801
	Armillaria-mellea	0.584
Armillaria-cepistipes-SZMC 23078	Armillaria-cepistipes	0.800
	Armillaria-mellea	0.624
Armillaria-cepistipes-RF14	Armillaria-cepistipes	0.791
	Armillaria-gallica	0.737
Armillaria-cepistipes-RF2	Armillaria-cepistipes	0.785
	Armillaria-mellea	0.676
Armillaria-cepistipes-RF1	Armillaria-cepistipes	0.766
	Armillaria-mellea	0.739
Armillaria-cepistipes-SZMC 23078	Armillaria-cepistipes	0.766
	Armillaria-mellea	0.655
Armillaria-cepistipes-SZMC 23077	Armillaria-cepistipes	0.764
	Armillaria-mellea	0.727
Armillaria-cepistipes-RF9	Armillaria-cepistipes	0.760
	Armillaria-ostoyae	0.647
Armillaria-cepistipes-RF13	Armillaria-cepistipes	0.759
	Armillaria-gallica	0.644
Armillaria-cepistipes-SZMC 23077	Armillaria-cepistipes	0.756
	Armillaria-mellea	0.570
Armillaria-cepistipes-RF8	Armillaria-cepistipes	0.752
	Armillaria-gallica	0.675
Armillaria-cepistipes-RF8	Armillaria-cepistipes	0.749
	Armillaria-gallica	0.604
Armillaria-cepistipes-23078	Armillaria-cepistipes	0.748
	Armillaria-gallica	0.681
Armillaria-cepistipes-RF14	Armillaria-cepistipes	0.745
	Armillaria-gallica	0.728
Armillaria-cepistipes-RF8	Armillaria-cepistipes	0.724
	Armillaria-gallica	0.496
Armillaria-cepistipes-RF13	Armillaria-cepistipes	0.716
	Armillaria-mellea	0.463
Armillaria-cepistipes-RF13	Armillaria-cepistipes	0.699
	Armillaria-mellea	0.551
Armillaria-cepistipes-RF13	Armillaria-cepistipes	0.696
	Armillaria-mellea	0.564
Armillaria-cepistipes-RF2	Armillaria-cepistipes	0.695
	Armillaria-gallica	0.666
Armillaria-cepistipes-RF14	Armillaria-cepistipes	0.670
	Armillaria-ostoyae	0.596
Armillaria-cepistipes-RF13	Armillaria-cepistipes	0.663
	Armillaria-mellea	0.500
Armillaria-cepistipes-SZMC 23077	Armillaria-cepistipes	0.631
	Armillaria-mellea	0.546
Armillaria-cepistipes-SZMC 23077	Armillaria-cepistipes	0.587
	Armillaria-mellea	0.408
Armillaria-cepistipes-HF34	Armillaria-cepistipes	0.553
	Armillaria-gallica	0.300
Armillaria-cepistipes-HF34	Armillaria-cepistipes	0.532
	Armillaria-mellea	0.430
Armillaria-cepistipes-RF1	Armillaria-cepistipes	0.500
	Armillaria-mellea	0.369
Armillaria-cepistipes-SZMC 23077	Armillaria-cepistipes	0.492

Sample Name	Classified As (1st / 2nd)	SI
	Armillaria-gallica	0.297
Armillaria-cepistipes-RF13	Armillaria-cepistipes	0.445
	Armillaria-mellea	0.380
Armillaria-cepistipes-RF14	Armillaria-cepistipes	0.365
	Armillaria-mellea	0.166
Armillaria-cepistipes-HF34	Armillaria-cepistipes	0.347
	Armillaria-gallica	0.313
Armillaria-cepistipes-SZMC 23078	Armillaria-cepistipes	0.284
	Armillaria-mellea	0.199
Armillaria-cepistipes-HF34	Armillaria-gallica	0.856
	Armillaria-cepistipes	0.838
Armillaria-cepistipes-RF2	Armillaria-gallica	0.842
	Armillaria-cepistipes	0.832
Armillaria-cepistipes-HF34	Armillaria-gallica	0.831
	Armillaria-cepistipes	0.795
Armillaria-cepistipes-HF34	Armillaria-gallica	0.822
	Armillaria-cepistipes	0.806
Armillaria-cepistipes-RF1	Armillaria-mellea	0.769
	Armillaria-cepistipes	0.724
Armillaria-cepistipes-HF34	Armillaria-mellea	0.342
	Armillaria-cepistipes	0.338
Armillaria-cepistipes-HF34	Armillaria-gallica	0.251
	Armillaria-cepistipes	0.237

Table S8. SI values based on *A. gallica* FAME profiles

Sample Name	Classified As (1st / 2nd)	SI
Armillaria-gallica-VTF6	Armillaria-gallica	0.941
	Armillaria-cepistipes	0.809
Armillaria-gallica-BF3	Armillaria-gallica	0.936
	Armillaria-cepistipes	0.855
Armillaria-gallica-VF1	Armillaria-gallica	0.927
	Armillaria-cepistipes	0.883
Armillaria-gallica-SzF1	Armillaria-gallica	0.924
	Armillaria-cepistipes	0.921
Armillaria-gallica-KR12	Armillaria-gallica	0.922
	Armillaria-cepistipes	0.835
Armillaria-gallica-KR12	Armillaria-gallica	0.921
	Armillaria-cepistipes	0.891
Armillaria-gallica-KR12	Armillaria-gallica	0.915
	Armillaria-cepistipes	0.879
Armillaria-gallica-KF15	Armillaria-gallica	0.912
	Armillaria-cepistipes	0.817
Armillaria-gallica-KR12	Armillaria-gallica	0.911
	Armillaria-cepistipes	0.806
Armillaria-gallica-KR12	Armillaria-gallica	0.909
	Armillaria-cepistipes	0.867
Armillaria-gallica-KoF6	Armillaria-gallica	0.906
	Armillaria-cepistipes	0.874
Armillaria-gallica-SzF1	Armillaria-gallica	0.901
	Armillaria-cepistipes	0.808
Armillaria-gallica-VF1	Armillaria-gallica	0.897
	Armillaria-cepistipes	0.845
Armillaria-gallica-KR12	Armillaria-gallica	0.893
	Armillaria-cepistipes	0.752
Armillaria-gallica-KR15	Armillaria-gallica	0.889
	Armillaria-cepistipes	0.841
Armillaria-gallica-VF1	Armillaria-gallica	0.884
	Armillaria-cepistipes	0.823
Armillaria-gallica-KoF6	Armillaria-gallica	0.881
	Armillaria-cepistipes	0.816
Armillaria-gallica-KR12	Armillaria-gallica	0.874
	Armillaria-cepistipes	0.592
Armillaria-gallica-KR15	Armillaria-gallica	0.874

Sample Name	Classified As (1st / 2nd)	SI
	Armillaria-cepistipes	0.855
Armillaria-gallica-BF3	Armillaria-gallica	0.869
	Armillaria-cepistipes	0.780
Armillaria-gallica-KR12	Armillaria-gallica	0.866
	Armillaria-mellea	0.711
Armillaria-gallica-KF15	Armillaria-gallica	0.864
	Armillaria-cepistipes	0.768
Armillaria-gallica-KF40	Armillaria-gallica	0.859
	Armillaria-cepistipes	0.777
Armillaria-gallica-VF1	Armillaria-gallica	0.858
	Armillaria-mellea	0.747
Armillaria-gallica-KF33	Armillaria-gallica	0.858
	Armillaria-cepistipes	0.542
Armillaria-gallica-KoF1	Armillaria-gallica	0.857
	Armillaria-cepistipes	0.822
Armillaria-gallica-VF1	Armillaria-gallica	0.855
	Armillaria-cepistipes	0.750
Armillaria-gallica-VTF6	Armillaria-gallica	0.845
	Armillaria-cepistipes	0.738
Armillaria-gallica-VTF6	Armillaria-gallica	0.841
	Armillaria-cepistipes	0.680
Armillaria-gallica-KR15	Armillaria-gallica	0.829
	Armillaria-cepistipes	0.523
Armillaria-gallica-SzF1	Armillaria-gallica	0.821
	Armillaria-cepistipes	0.732
Armillaria-gallica-SzF1	Armillaria-gallica	0.819
	Armillaria-cepistipes	0.792
Armillaria-gallica-KF15	Armillaria-gallica	0.817
	Armillaria-cepistipes	0.744
Armillaria-gallica-VTF6	Armillaria-gallica	0.811
	Armillaria-cepistipes	0.702
Armillaria-gallica-KF40	Armillaria-gallica	0.809
	Armillaria-cepistipes	0.802
Armillaria-gallica-VTF6	Armillaria-gallica	0.807
	Armillaria-cepistipes	0.742
Armillaria-gallica-KF33	Armillaria-gallica	0.807
	Armillaria-cepistipes	0.321
Armillaria-gallica-KF33	Armillaria-gallica	0.806
	Armillaria-cepistipes	0.388
Armillaria-gallica-VTF6	Armillaria-gallica	0.800
	Armillaria-cepistipes	0.757
Armillaria-gallica-KF33	Armillaria-gallica	0.793
	Armillaria-cepistipes	0.490
Armillaria-gallica-KF40	Armillaria-gallica	0.793
	Armillaria-ostoyae	0.755
Armillaria-gallica-KoF1	Armillaria-gallica	0.790
	Armillaria-cepistipes	0.319
Armillaria-gallica-KR15	Armillaria-gallica	0.789
	Armillaria-cepistipes	0.388
Armillaria-gallica-KoF1	Armillaria-gallica	0.781
	Armillaria-cepistipes	0.679
Armillaria-gallica-KF15	Armillaria-gallica	0.781
	Armillaria-cepistipes	0.662
Armillaria-gallica-KF33	Armillaria-gallica	0.777
	Armillaria-cepistipes	0.747
Armillaria-gallica-VF2	Armillaria-gallica	0.768
	Armillaria-mellea	0.748
Armillaria-gallica-KF33	Armillaria-gallica	0.765
	Armillaria-cepistipes	0.472
Armillaria-gallica-KF33	Armillaria-gallica	0.757
	Armillaria-cepistipes	0.263
Armillaria-gallica-KF40	Armillaria-gallica	0.744
	Armillaria-cepistipes	0.737
Armillaria-gallica-VF1	Armillaria-gallica	0.721
	Armillaria-cepistipes	0.668
Armillaria-gallica-KF15	Armillaria-gallica	0.717
	Armillaria-ostoyae	0.547
Armillaria-gallica-KF15	Armillaria-gallica	0.705

Sample Name	Classified As (1st / 2nd)	SI
	Armillaria-mellea	0.678
Armillaria-gallica-KoF1	Armillaria-gallica	0.695
	Armillaria-cepistipes	0.171
Armillaria-gallica-KF33	Armillaria-gallica	0.687
	Armillaria-cepistipes	0.503
Armillaria-gallica-KR15	Armillaria-gallica	0.685
	Armillaria-cepistipes	0.385
Armillaria-gallica-KR15	Armillaria-gallica	0.685
	Armillaria-cepistipes	0.289
Armillaria-gallica-KF15	Armillaria-gallica	0.665
	Armillaria-cepistipes	0.606
Armillaria-gallica-KF15	Armillaria-gallica	0.660
	Armillaria-cepistipes	0.562
Armillaria-gallica-KF15	Armillaria-gallica	0.654
	Armillaria-cepistipes	0.581
Armillaria-gallica-KR15	Armillaria-gallica	0.631
	Armillaria-cepistipes	0.627
Armillaria-gallica-KoF1	Armillaria-gallica	0.616
	Armillaria-cepistipes	0.139
Armillaria-gallica-KF33	Armillaria-gallica	0.594
	Armillaria-cepistipes	0.351
Armillaria-gallica-BF3	Armillaria-cepistipes	0.862
	Armillaria-gallica	0.828
Armillaria-gallica-BF3	Armillaria-cepistipes	0.853
	Armillaria-gallica	0.832
Armillaria-gallica-KoF6	Armillaria-cepistipes	0.840
	Armillaria-gallica	0.797
Armillaria-gallica-KF40	Armillaria-cepistipes	0.783
	Armillaria-gallica	0.751
Armillaria-gallica-KR15	Armillaria-cepistipes	0.744
	Armillaria-mellea	0.660
	Armillaria-gallica	0.658
Armillaria-gallica-KoF1	Armillaria-cepistipes	0.743
	Armillaria-gallica	0.728
Armillaria-gallica-KF37	Armillaria-mellea	0.739
	Armillaria-gallica	0.711
Armillaria-gallica-KF40	Armillaria-cepistipes	0.608
	Armillaria-gallica	0.588

Table S9. SI values based on *A. mellea* FAME profiles

Sample Name	Classified As (1st / 2nd)	SI
Armillaria-mellea-DF1	Armillaria-mellea	0.859
	Armillaria-cepistipes	0.677
Armillaria-mellea-VTF10	Armillaria-mellea	0.857
	Armillaria-cepistipes	0.653
Armillaria-mellea-KF7	Armillaria-mellea	0.854
	Armillaria-cepistipes	0.506
Armillaria-mellea-DF1	Armillaria-mellea	0.848
	Armillaria-cepistipes	0.417
Armillaria-mellea-VTF10	Armillaria-mellea	0.847
	Armillaria-cepistipes	0.658
Armillaria-mellea-VTF10	Armillaria-mellea	0.840
	Armillaria-cepistipes	0.473
Armillaria-mellea-HF13	Armillaria-mellea	0.840
	Armillaria-cepistipes	0.592
Armillaria-mellea-VTF1	Armillaria-mellea	0.836
	Armillaria-cepistipes	0.782
Armillaria-mellea-HF25	Armillaria-mellea	0.836
	Armillaria-cepistipes	0.408
Armillaria-mellea-KF11	Armillaria-mellea	0.828
	Armillaria-cepistipes	0.474
Armillaria-mellea-DF1	Armillaria-mellea	0.823
	Armillaria-cepistipes	0.510
Armillaria-mellea-KF46	Armillaria-mellea	0.819
	Armillaria-cepistipes	0.535
Armillaria-mellea-KF7	Armillaria-mellea	0.818

Sample Name	Classified As (1st / 2nd)	SI
	Armillaria-cepistipes	0.728
Armillaria-mellea-HF25	Armillaria-mellea	0.817
	Armillaria-cepistipes	0.585
Armillaria-mellea-VTF10	Armillaria-mellea	0.808
	Armillaria-cepistipes	0.701
Armillaria-mellea-HF13	Armillaria-mellea	0.803
	Armillaria-gallica	0.757
Armillaria-mellea-VTF1	Armillaria-mellea	0.803
	Armillaria-ostoyae	0.364
Armillaria-mellea-KF7	Armillaria-mellea	0.801
	Armillaria-gallica	0.799
Armillaria-mellea-KF18	Armillaria-mellea	0.798
	Armillaria-cepistipes	0.358
Armillaria-mellea-DF1	Armillaria-mellea	0.794
	Armillaria-cepistipes	0.580
Armillaria-mellea-KF18	Armillaria-mellea	0.792
	Armillaria-cepistipes	0.629
Armillaria-mellea-KF46	Armillaria-mellea	0.791
	Armillaria-gallica	0.633
Armillaria-mellea-KF5	Armillaria-mellea	0.789
	Armillaria-cepistipes	0.763
Armillaria-mellea-HF25	Armillaria-mellea	0.786
	Armillaria-ostoyae	0.384
Armillaria-mellea-KF46	Armillaria-mellea	0.785
	Armillaria-cepistipes	0.546
Armillaria-mellea-KF18	Armillaria-mellea	0.783
	Armillaria-cepistipes	0.553
Armillaria-mellea-KF18	Armillaria-mellea	0.781
	Armillaria-cepistipes	0.419
Armillaria-mellea-DF1	Armillaria-mellea	0.779
	Armillaria-cepistipes	0.690
Armillaria-mellea-KF11	Armillaria-mellea	0.774
	Armillaria-cepistipes	0.555
Armillaria-mellea-HF13	Armillaria-mellea	0.772
	Armillaria-gallica	0.660
Armillaria-mellea-VTF10	Armillaria-mellea	0.762
	Armillaria-cepistipes	0.511
Armillaria-mellea-HF13	Armillaria-mellea	0.757
	Armillaria-gallica	0.671
Armillaria-mellea-VTF1	Armillaria-mellea	0.756
	Armillaria-cepistipes	0.453
Armillaria-mellea-KF18	Armillaria-mellea	0.749
	Armillaria-cepistipes	0.530
Armillaria-mellea-DF1	Armillaria-mellea	0.747
	Armillaria-cepistipes	0.378
Armillaria-mellea-KF46	Armillaria-mellea	0.745
	Armillaria-gallica	0.524
Armillaria-mellea-HF25	Armillaria-mellea	0.738
	Armillaria-cepistipes	0.616
Armillaria-mellea-KF18	Armillaria-mellea	0.734
	Armillaria-cepistipes	0.554
Armillaria-mellea-DF1	Armillaria-mellea	0.734
	Armillaria-cepistipes	0.331
Armillaria-mellea-HF13	Armillaria-mellea	0.725
	Armillaria-gallica	0.472
Armillaria-mellea-DF1	Armillaria-mellea	0.723
	Armillaria-cepistipes	0.375
Armillaria-mellea-KF11	Armillaria-mellea	0.715
	Armillaria-cepistipes	0.199
Armillaria-mellea-HF25	Armillaria-mellea	0.712
	Armillaria-cepistipes	0.160
Armillaria-mellea-DF1	Armillaria-mellea	0.710
	Armillaria-cepistipes	0.244
Armillaria-mellea-KF7	Armillaria-mellea	0.707
	Armillaria-cepistipes	0.670
Armillaria-mellea-KF18	Armillaria-mellea	0.705
	Armillaria-cepistipes	0.225
Armillaria-mellea-KF46	Armillaria-mellea	0.702

Sample Name	Classified As (1st / 2nd)	SI
	Armillaria-gallica	0.603
Armillaria-mellea-KF18	Armillaria-mellea	0.702
	Armillaria-cepistipes	0.698
Armillaria-mellea-KF5	Armillaria-mellea	0.701
	Armillaria-cepistipes	0.505
Armillaria-mellea-VTF10	Armillaria-mellea	0.699
	Armillaria-cepistipes	0.502
Armillaria-mellea-HF25	Armillaria-mellea	0.692
	Armillaria-cepistipes	0.342
Armillaria-mellea-HF25	Armillaria-mellea	0.688
	Armillaria-cepistipes	0.421
Armillaria-mellea-KF5	Armillaria-mellea	0.682
	Armillaria-cepistipes	0.589
Armillaria-mellea-KF46	Armillaria-mellea	0.679
	Armillaria-gallica	0.655
Armillaria-mellea-VTF10	Armillaria-mellea	0.676
	Armillaria-gallica	0.669
Armillaria-mellea-HF25	Armillaria-mellea	0.650
	Armillaria-cepistipes	0.098
Armillaria-mellea-KF46	Armillaria-mellea	0.621
	Armillaria-gallica	0.325
Armillaria-mellea-KF11	Armillaria-mellea	0.618
	Armillaria-cepistipes	0.195
Armillaria-mellea-KF24	Armillaria-mellea	0.615
	Armillaria-cepistipes	0.129
Armillaria-mellea-KF24	Armillaria-mellea	0.596
	Armillaria-cepistipes	0.124
Armillaria-mellea-KF24	Armillaria-mellea	0.583
	Armillaria-cepistipes	0.104
Armillaria-mellea-KF7	Armillaria-mellea	0.541
	Armillaria-cepistipes	0.218
Armillaria-mellea-KF11	Armillaria-mellea	0.539
	Armillaria-cepistipes	0.245
Armillaria-mellea-KF24	Armillaria-mellea	0.489
	Armillaria-cepistipes	0.056
Armillaria-mellea-KF24	Armillaria-mellea	0.482
	Armillaria-cepistipes	0.041
Armillaria-mellea-KF46	Armillaria-mellea	0.481
	Armillaria-cepistipes	0.471
Armillaria-mellea-KF11	Armillaria-mellea	0.454
	Armillaria-cepistipes	0.186
Armillaria-mellea-KF18	Armillaria-mellea	0.448
	Armillaria-cepistipes	0.274
Armillaria-mellea-HF13	Armillaria-mellea	0.442
	Armillaria-cepistipes	0.109
Armillaria-mellea-KF5	Armillaria-mellea	0.441
	Armillaria-cepistipes	0.103
Armillaria-mellea-KF18	Armillaria-mellea	0.433
	Armillaria-cepistipes	0.152
Armillaria-mellea-VTF10	Armillaria-mellea	0.431
	Armillaria-gallica	0.159

Table S10. SI values based on *A. ostoyae* FAME profiles

Sample Name	Classified As (1st / 2nd)	SI
Armillaria-ostoyae-RF5	Armillaria-ostoyae	0.905
	Armillaria-cepistipes	0.781
Armillaria-ostoyae-RF3	Armillaria-ostoyae	0.899
	Armillaria-cepistipes	0.636
Armillaria-ostoyae-RF4	Armillaria-ostoyae	0.891
	Armillaria-cepistipes	0.748
Armillaria-ostoyae-RF3	Armillaria-ostoyae	0.888
	Armillaria-cepistipes	0.618
Armillaria-ostoyae-RF3	Armillaria-ostoyae	0.883
	Armillaria-cepistipes	0.776
Armillaria-ostoyae-RF5	Armillaria-ostoyae	0.880
	Armillaria-cepistipes	0.814

Sample Name	Classified As (1st / 2nd)	SI
Armillaria-ostoyae-RF5	Armillaria-ostoyae	0.878
	Armillaria-cepistipes	0.579
Armillaria-ostoyae-HF39	Armillaria-ostoyae	0.875
	Armillaria-gallica	0.485
Armillaria-ostoyae-HF31	Armillaria-ostoyae	0.874
	Armillaria-cepistipes	0.539
Armillaria-ostoyae-SZMC 23080	Armillaria-ostoyae	0.862
	Armillaria-cepistipes	0.762
Armillaria-ostoyae-RF4	Armillaria-ostoyae	0.860
	Armillaria-gallica	0.747
Armillaria-ostoyae-RF5	Armillaria-ostoyae	0.857
	Armillaria-cepistipes	0.567
Armillaria-ostoyae-RF10	Armillaria-ostoyae	0.852
	Armillaria-gallica	0.407
Armillaria-ostoyae-SZMC 23080	Armillaria-ostoyae	0.847
	Armillaria-cepistipes	0.501
Armillaria-ostoyae-RF5	Armillaria-ostoyae	0.837
	Armillaria-cepistipes	0.619
Armillaria-ostoyae-RF5	Armillaria-ostoyae	0.832
	Armillaria-cepistipes	0.762
Armillaria-ostoyae-SZMC 23080	Armillaria-ostoyae	0.830
	Armillaria-cepistipes	0.592
Armillaria-ostoyae-RF3	Armillaria-ostoyae	0.830
	Armillaria-cepistipes	0.572
Armillaria-ostoyae-HF24	Armillaria-ostoyae	0.823
	Armillaria-cepistipes	0.660
Armillaria-ostoyae-HF24	Armillaria-ostoyae	0.822
	Armillaria-cepistipes	0.536
Armillaria-ostoyae-RF10	Armillaria-ostoyae	0.818
	Armillaria-cepistipes	0.258
Armillaria-ostoyae-HF31	Armillaria-ostoyae	0.817
	Armillaria-cepistipes	0.753
Armillaria-ostoyae-RF3	Armillaria-ostoyae	0.807
	Armillaria-cepistipes	0.426
Armillaria-ostoyae-HF31	Armillaria-ostoyae	0.807
	Armillaria-gallica	0.516
Armillaria-ostoyae-SZMC 23082	Armillaria-ostoyae	0.799
	Armillaria-mellea	0.460
Armillaria-ostoyae-RF5	Armillaria-ostoyae	0.793
	Armillaria-cepistipes	0.771
Armillaria-ostoyae-HF39	Armillaria-ostoyae	0.791
	Armillaria-cepistipes	0.322
Armillaria-ostoyae-HF39	Armillaria-ostoyae	0.791
	Armillaria-cepistipes	0.733
Armillaria-ostoyae-RF3	Armillaria-ostoyae	0.789
	Armillaria-cepistipes	0.783
Armillaria-ostoyae-HF24	Armillaria-ostoyae	0.787
	Armillaria-cepistipes	0.781
Armillaria-ostoyae-RF3	Armillaria-ostoyae	0.784
	Armillaria-cepistipes	0.410
Armillaria-ostoyae-HF39	Armillaria-ostoyae	0.777
	Armillaria-cepistipes	0.596
Armillaria-ostoyae-HF31	Armillaria-ostoyae	0.776
	Armillaria-cepistipes	0.748
Armillaria-ostoyae-RF3	Armillaria-ostoyae	0.773
	Armillaria-cepistipes	0.707
Armillaria-ostoyae-HF24	Armillaria-ostoyae	0.770
	Armillaria-cepistipes	0.704
Armillaria-ostoyae-RF3	Armillaria-ostoyae	0.769
	Armillaria-gallica	0.190
Armillaria-ostoyae-SZMC 23082	Armillaria-ostoyae	0.762
	Armillaria-mellea	0.522
Armillaria-ostoyae-SZMC 23082	Armillaria-ostoyae	0.757
	Armillaria-cepistipes	0.430
Armillaria-ostoyae-HF24	Armillaria-ostoyae	0.754
	Armillaria-gallica	0.232
Armillaria-ostoyae-RF10	Armillaria-ostoyae	0.745
	Armillaria-mellea	0.084

Sample Name	Classified As (1st / 2nd)	SI
Armillaria-ostoyae-SZMC 23082	Armillaria-ostoyae	0.735
	Armillaria-mellea	0.109
Armillaria-ostoyae-RF4	Armillaria-ostoyae	0.730
	Armillaria-gallica	0.436
Armillaria-ostoyae-SZMC 23082	Armillaria-ostoyae	0.724
	Armillaria-cepistipes	0.414
Armillaria-ostoyae-SZMC 23082	Armillaria-ostoyae	0.722
	Armillaria-cepistipes	0.542
Armillaria-ostoyae-SZMC 23083	Armillaria-ostoyae	0.717
	Armillaria-mellea	0.212
Armillaria-ostoyae-HF39	Armillaria-ostoyae	0.716
	Armillaria-mellea	0.150
Armillaria-ostoyae-SZMC 23083	Armillaria-ostoyae	0.712
	Armillaria-mellea	0.089
Armillaria-ostoyae-RF10	Armillaria-ostoyae	0.711
	Armillaria-mellea	0.296
Armillaria-ostoyae-SZMC 23083	Armillaria-ostoyae	0.709
	Armillaria-mellea	0.554
Armillaria-ostoyae-HF39	Armillaria-ostoyae	0.699
	Armillaria-gallica	0.563
Armillaria-ostoyae-HF31	Armillaria-ostoyae	0.694
	Armillaria-mellea	0.387
Armillaria-ostoyae-SZMC 23083	Armillaria-ostoyae	0.681
	Armillaria-mellea	0.296
Armillaria-ostoyae-RF4	Armillaria-ostoyae	0.675
	Armillaria-gallica	0.666
Armillaria-ostoyae-RF10	Armillaria-ostoyae	0.642
	Armillaria-mellea	0.195
Armillaria-ostoyae-SZMC 23083	Armillaria-ostoyae	0.603
	Armillaria-gallica	0.508
Armillaria-ostoyae-SZMC 23082	Armillaria-ostoyae	0.601
	Armillaria-cepistipes	0.316
Armillaria-ostoyae-HF24	Armillaria-ostoyae	0.599
	Armillaria-cepistipes	0.241
Armillaria-ostoyae-RF5	Armillaria-ostoyae	0.598
	Armillaria-mellea	0.051
Armillaria-ostoyae-SZMC 23082	Armillaria-ostoyae	0.595
	Armillaria-mellea	0.331
Armillaria-ostoyae-SZMC 23083	Armillaria-ostoyae	0.576
	Armillaria-mellea	0.120
Armillaria-ostoyae-SZMC 23080	Armillaria-ostoyae	0.559
	Armillaria-mellea	0.547
Armillaria-ostoyae-SZMC 23080	Armillaria-ostoyae	0.551
	Armillaria-mellea	0.326
Armillaria-ostoyae-SZMC 23083	Armillaria-ostoyae	0.549
	Armillaria-mellea	0.281
Armillaria-ostoyae-RF4	Armillaria-ostoyae	0.495
	Armillaria-mellea	0.005
Armillaria-ostoyae-SZMC 23080	Armillaria-ostoyae	0.487
	Armillaria-cepistipes	0.361
Armillaria-ostoyae-SZMC 23083	Armillaria-ostoyae	0.414
	Armillaria-mellea	0.130
Armillaria-ostoyae-RF4	Armillaria-ostoyae	0.397
	Armillaria-mellea	0.001
Armillaria-ostoyae-RF5	Armillaria-ostoyae	0.395
	Armillaria-cepistipes	0.309
Armillaria-ostoyae-SZMC 23080	Armillaria-ostoyae	0.350
	Armillaria-mellea	0.011
Armillaria-ostoyae-SZMC 23080	Armillaria-ostoyae	0.335
	Armillaria-mellea	0.002
Armillaria-ostoyae-SZMC 23082	Armillaria-ostoyae	0.323
	Armillaria-mellea	0.000
Armillaria-ostoyae-HF31	Armillaria-ostoyae	0.301
	Armillaria-mellea	0.221

Table S11: Reference *Bacillus* species and their sequence data using in phylogenetic construction

Strain number	GenBank accession number	length (bp)	positions (bp)	length (bp)	positions (bp)	Reference	Origin
			gyrA		*rpoB*		
B. amyloliquefaciens							
LL3	NC_017190.1	937	7107 to 8043	743	117089 to 117831	(Geng *et al.*, 2011)	isolated from fermented food (Korean bibimbap), China
TA208	NC_017188.1	937	7107 to 8043	743	112280 to 113022	(Zhang *et al.*, 2011)	industrial production of guanosine and synthesis of ribavirin, China
XH7	CP002927.1	937	7107 to 8043	743	112278 to 113020	(Yang *et al.*, 2011)	industrial production of purine nucleoside inosine, China
B. velezensis							
AP183	CP029296.1	937	7136 to 8072	744	116972 to 117715	(Nasrin, Hossain and Liles, 2016)	isolated from a cotton plant rhizosphere, USA
AS43.3	CP003838.1	945	7099 to 8043	744	122589 to 123332	(Dunlap *et al.*, 2015)	Not provided
At1	CP041145.1	948	7133 to 8080	743	122719 to 123461	(Reva *et al.*, 2004)	isolated from *Arabidopsis thaliana* seedling from surface sterilized seed, Uppsala, Sweden
BIM B-439D	CP032144.1	943	7097 to 8039	742	122917 to 123658	(Berezhnaya *et al.*, 2019)	isolated from the sample of soddy, ash-grey soil obtained on the territory of the Minsk region, Vileyka, Belarus
BvL03	CP041192.1	948	6608 to 7555	742	129097 to 129838	(Cao *et al.*, 2019)	isolated from the sediment samples of fish pond, Wangcheng, Changsha, China

Strain number	GenBank accession number	length (bp)	positions (bp)	length (bp)	positions (bp)	Reference	Origin
			gyrA		*rpoB*		
LF01	CP058216.1	937	2094067 to 2095003	742	2209767 to 2210508	(Zhang *et al.*, 2019)	isolated from tilapia, Guangzhou, China
QST713	CP025079.1	937	7100 to 8036	741	116750 to 117490	(Borriss *et al.*, 2011)	isolated from the commercial product Serenade (Bayer), France
S141	AP018402.1	945	7100 to 8044	742	122957 to 123698	(Sibponkrung *et al.*, 2017)	isolated from soybean (Glycine max) rhizosphere, Thailand
SGAir0473	CP027868.1	956	2217071 to 2218026	743	2333101 to 2333843	(Lim *et al.*, 2018)	isolated from tropical air, Singapore
SQR9	CP006890.1	937	7100 to 8036	742	117092 to 117833	(Dunlap *et al.*, 2015)	isolated from the plant rhizosphere soil, China
WRN014	CP041361.1	948	6790 to 7737	742	122609 to 123350	(Wang *et al.*, 2019)	isolated from soil of banana root in fields, Hainan, China
B. subtilis							
ATCC 6633	CP039755.1	2466	3779374 to 3781839	743	3894578 to 3895320	(McIntyre *et al.*, 2019)	Japan

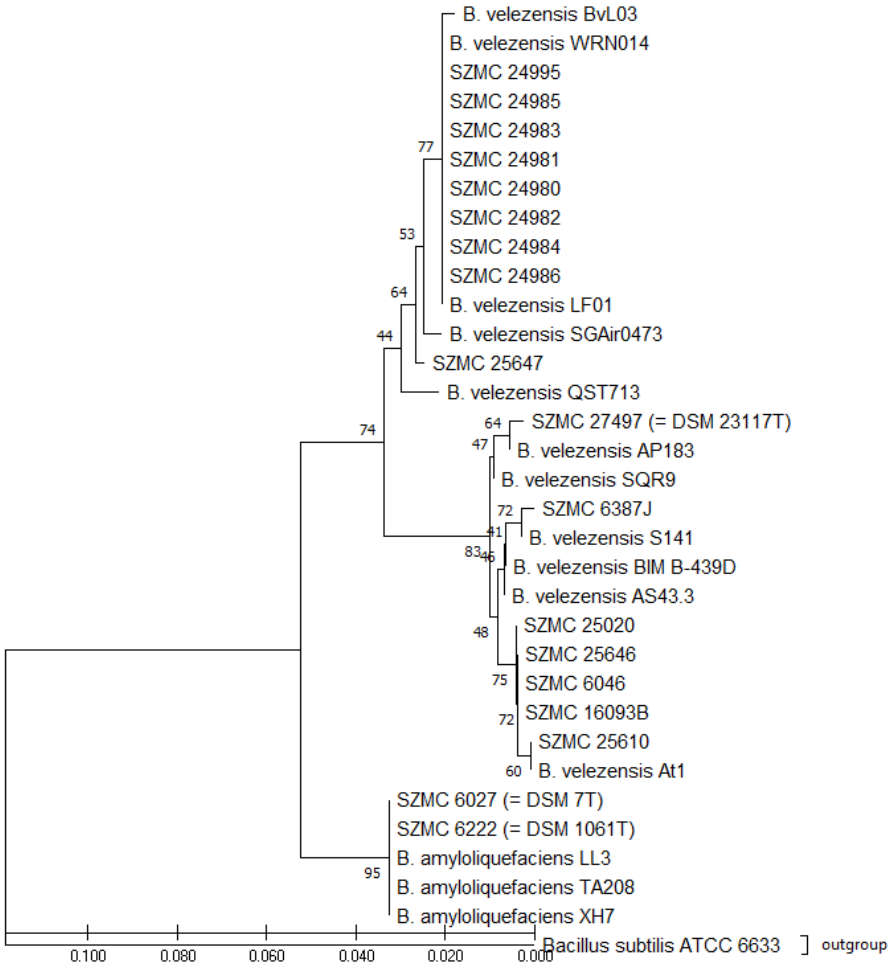

Fig S1. The Neighbor-Joining phylogenetic tree based on *gyrA* gene sequences. Evolutionary distances were computed by the Tamura-Nei method. Bars, 0.020 substitutions per nucleotide position.

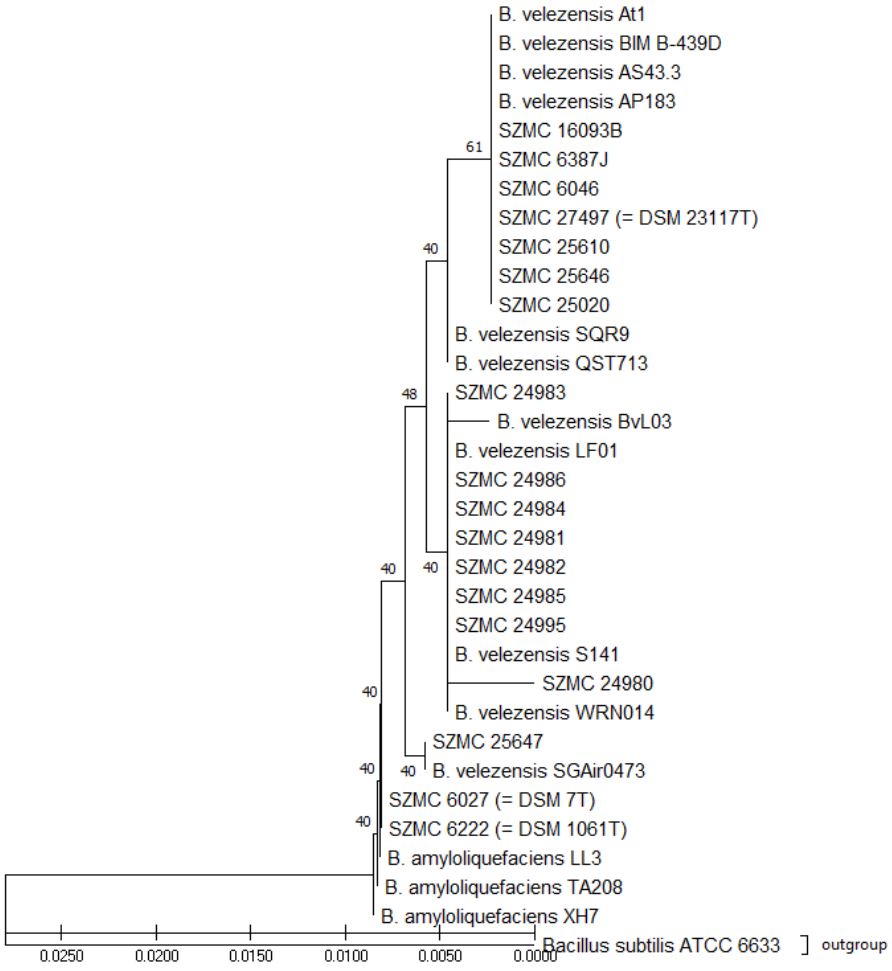

Fig S2. The Neighbor-Joining phylogenetic tree based on *rpoB* gene sequences. Evolutionary distances were computed by the Tamura-Nei method. Bars, 0.0050 substitutions per nucleotide position.